REAL TIME OPTIMIZATION AND AUTOMATIC MANIPULATION OF MACHINING PARAMETERS THROUGH ADAPTIVE CONTROL METHODS

Thesis

Submitted in

Fulfillment of the requirement of

DOCTOR OF PHILOSOPHY

in

Department of Mechanical Engineering

By

NARENDRAKUMAR AMRUTLAL PATEL

(149997119015)

Under the Supervision of

DR. JEETENDRA A. VADHER

GUJARAT TECHNOLOGICAL UNIVERSITY,

CHANDKHEDA, AHMEDABAD

DECEMBER – 2021

REAL TIME OPTIMIZATION AND AUTOMATIC MANIPULATION OF MACHINING PARAMETERS THROUGH ADAPTIVE CONTROL METHODS

Thesis

Submitted in

Fulfillment of the requirement of

DOCTOR OF PHILOSOPHY

in

Department of Mechanical Engineering

By

NARENDRAKUMAR AMRUTLAL PATEL

(149997119015)

Under the Supervision of

DR. JEETENDRA A. VADHER

GUJARAT TECHNOLOGICAL UNIVERSITY,

CHANDKHEDA, AHMEDABAD

DECEMBER – 2021

I dedicate my thesis to my family,

to my wife Kalpa and

to my adored kids Sonam and Stuti,

for their unwavering support and affection.

I love you all.

DECLARATION

I declare that the thesis entitled **"Real Time Optimization and Automatic Manipulation of Machining Parameters Through Adaptive Control Methods"** submitted by me for the degree of Doctor of Philosophy is the record of research work carried out by me during the period from January-2015 to February-2021 under the supervision of **Dr. Jeetendrakumar A. Vadher** and this has not formed the basis for the award of any degree, diploma, Associateship, fellowship, titles in this or any other University or other institution of higher learning.

I further declare that the material obtained from other sources has been duly acknowledged in the thesis. I shall be solely responsible for any plagiarism or other irregularities if noticed in the thesis.

Signature of the Research Scholar________________________Date: ___30/06/2021__

Name of Research Scholar: Narendrakumar Amrutlal Patel

Place: Palanpur

CERTIFICATE

I certify that the work incorporated in the thesis **"Real Time Optimization and Automatic Manipulation of Machining Parameters Through Adaptive Control Methods"** was submitted by Shri /Smt. /Kumari **Narendrakumar Amrutlal Patel** was carried out by the candidate under my supervision/guidance. To the best of my knowledge: (i) the candidate has not submitted the same research work to any other institution for any degree/ diploma, Associateship, Fellowship, or other similar titles (ii) the thesis submitted is a record of original research work done by the Research Scholar during the period of study under my supervision, and (iii) the thesis represents independent research work on the part of the Research Scholar.

Signature of Supervisor: ______________________________ **Date:** **30/06/2021**

Name of Supervisor: **Dr. Jeetendrakumar A. Vadher**

Prof. & Head of Mechanical Engg. Dept.,

Government Engineering College,

Palanpur.

Place: Palanpur

COURSE-WORK COMPLETION CERTIFICATE

This is to certify that Mr./Mrs./Ms. Narendrakumar Amrutlal Patel Enrolment No.149997119015 is a Ph.D. scholar enrolled for the Ph.D. program in the branch Mechanical Engineering of Gujarat Technological University, Ahmedabad.

(Please tick the relevant option(s))

☐ He/She has been exempted from the course-work (successfully completed during M.Phil Course)

☐ He/She has been exempted from Research Methodology Course only (successfully completed during M.Phil Course)

☑ He/She has successfully completed the Ph.D. course work for the partial requirement for the award of Ph.D. Degree. His/ Her performance in the course work is as follows-

Grade Obtained in Research Methodology (PH001)	Grade Obtained in Self Study Course (Core Subject) (PH002)
BB	AB

Supervisor’s Sign

(Dr. Jeetendrakumar A. Vadher)

ORIGINALITY REPORT CERTIFICATE

It is certified that the Ph.D. thesis titled **"Real Time Optimization and Automatic Manipulation of Machining Parameters Through Adaptive Control Methods"** by **Narendrakumar Amrutlal Patel** has been examined by us. We undertake the following:

a. Thesis has significant new work/knowledge as compared already published or are under consideration to be published elsewhere. No sentence, equation, diagram, table, paragraph, or section has been copied verbatim from previous work unless it is placed under quotation marks and duly referenced.

b. The work presented is original and the own work of the author (i.e. there is no plagiarism). No ideas, processes, results, or words of others have been presented as the Author's work.

c. There is no fabrication of data or results, which have been compiled/analyzed.

d. There is no falsification by manipulating research materials, equipment or processes, or changing or omitting data or results such that the research is not accurately represented in the research record.

e. The thesis has been checked using Plagiarism Checker**Turnitin** (copy of originality report attached) and found within limits as per GTU Plagiarism Policy and instructions issued from time to time (i.e. permitted similarity index <10%).

Signature of the Research Scholar________________________**Date: 30/06/2021**

Name of Research Scholar: NarendrakumarAmrutlal Patel

Place: Palanpur

Signature of Supervisor: ________________________________ **Date: 30/06/2021**

Name of Supervisor: Dr. Jeetendrakumar A. Vadher

Prof. & Head of Mechanical Engg. Dept.,

Government Engineering College, Palanpur.

Place: Palanpur

REAL TIME OPTIMIZATION AND AUTOMATIC MANIPULATION OF MACHINING PARAMETERS THROUGH ADAPTIVE CONTROL METHODS

ORIGINALITY REPORT

8%	7%	3%	3%
SIMILARITY INDEX	INTERNET SOURCES	PUBLICATIONS	STUDENT PAPERS

PRIMARY SOURCES

1	livrepository.liverpool.ac.uk Internet Source	1%
2	en.wikipedia.org Internet Source	1%
3	jcinfotr.com Internet Source	1%
4	www.keyence.com Internet Source	1%
5	Submitted to University of Rajshahi Student Paper	1%
6	www.ijream.org Internet Source	<1%
7	D. Broda, L. Pieczonka, V. Hiwarkar, W.J. Staszewski, V.V. Silberschmidt. "Generation of higher harmonics in longitudinal vibration of beams with breathing cracks", Journal of Sound and Vibration, 2016 Publication	<1%

PH.D. THESIS NON-EXCLUSIVE LICENSE TO GUJARAT TECHNOLOGICAL UNIVERSITY

In consideration of being a Ph.D. Research Scholar at GTU and in the interests of the facilitation of research at GTU and elsewhere, I, Narendrakumar Amrutlal Patel having (Enrollment No.). 149997119015 hereby grant a non-exclusive, royalty-free, and perpetual license to GTU on the following terms:

a) GTU is permitted to archive, reproduce and distribute my thesis, in whole or in part, and/or my abstract, in whole or in part (referred to collectively as the "Work") anywhere in the world, for non-commercial purposes, in all forms of media;

b) GTU is permitted to authorize, sub-lease, sub-contract, or procure any of the acts mentioned in paragraph (a);

c) GTU is authorized to submit the Work at any National / International Library, under the authority of their "Thesis Non-Exclusive License";

d) The Universal Copyright Notice (©) shall appear on all copies made under the authority of this license;

e) I undertake to submit my thesis, through my University, to any Library and Archives. Any abstract submitted with the thesis will be considered to form part of the thesis.

f) I represent that my thesis is my original work, does not infringe any rights of others, including privacy rights, and that I have the right to make the grant conferred by this non-exclusive license.

g) If third party copyrighted material was included in my thesis for which, under the terms of the Copyright Act, written permission from the copyright owners is required, I have obtained such permission from the copyright owners to do the acts mentioned in paragraph (a) above for the full term of copyright protection.

h) I retain copyright ownership and moral rights in my thesis and may deal with the copyright in my thesis, in any way consistent with rights granted by me to my University in this non-exclusive license.

i) I further promise to inform any person to whom I may hereafter assign or license my copyright in my thesis of the rights granted by me to my University in this non- exclusive license.

j) I am aware of and agree to accept the conditions and regulations of a PhD including all policy matters related to authorship and plagiarism.

Signature of the Research Scholar______________________**Date:** **30/06/2021**

Name of Research Scholar: Narendrakumar Amrutlal Patel

Place: Palanpur

Signature of Supervisor: ______________________________ **Date:** **30/06/2021**

Name of Supervisor:Dr. Jeetendrakumar A. Vadher

Prof.& Head of Mechanical Engg. Dept.,

Government Engineering College, Palanpur.

Place: Palanpur

Seal:

Professor & Head
(GES Class-I)
Mechanical Engineering Department
Government Engineering College
Palanpur-385001

Annexure-VII

Thesis Approval Form

The viva-voce of the PhD Thesis submitted by Shri/Smt./Kum. ....PATEL NARENDRAKUMAR AMRUTLAL.. (Enrollment No. ..149997119015...) entitled Real Time Optimization and Automatic Manipulation of Machining Parameters Through Adaptive Control Methods .... was conducted on ...16/12/2021...................... (day and date) at Gujarat Technological University.

(Please tick any one of the following option)

- [x] The performance of the candidate was satisfactory. We recommend that he/she be awarded the PhD degree.

- [ ] Any further modifications in research work recommended by the panel after 3 months from the date of first viva-voce upon request of the Supervisor or request of Independent Research Scholar after which viva-voce can be re-conducted by the same panel again.

(briefly specify the modifications suggested by the panel)

- [ ] The performance of the candidate was unsatisfactory. We recommend that he/she should not be awarded the PhD degree.

(The panel must give justifications for rejecting the research work)

16/12/21 Prof. J A Vadher — Name and Signature of Supervisor with Seal

ELANGO NATARAJAN — 1) (External Examiner 1) Name and Signature

16/12/21 (Dr Ramesh.S) — 2) (External Examiner 2) Name and Signature

3) (External Examiner 3) Name and Signature

ABSTRACT

This research work aims to provide an overview of the various methods for evaluating cutting tool efficiency specifically for the turning operation. The cutting operation variables like cutting speed, feed rate, and depth of cut have to be selected cautiously during the turning operation to increase profitability by increasing efficiency and lowering overall manufacturing costs for each part. High vibration causes poor surface finish, lower efficiency, and shorter tool life; as a result, this parameter should be kept under control.

The performance of the cutting tool while turning operation depends on the material strength, structural design, and attachment configuration. For different configurations such as simply supported and fixed (clamped) end, the structural strength of the tool varies along the length of the cutting tool. The present work encompasses the structural analysis of cutting tools in two different conditions of simply supported and fixed-end conations utilizing numerical simulation techniques. The analysis shows that the stress distribution of the simply supported condition from minimum to maximum variations along the length of the tool periodically; whereas the fixed/clamped scenario leads to the maximum value at the end of the tool other than the clamped one along with the distributions of the minimum to mid-range values along the length of the cutting tool.

The performance of the cutting tool subjected to vibration depends upon the operational parameters of the systems. Experimentation is the most reliable means of investigating the vibration behavior of the cutting tool during the turning operation on the workpiece. However, the empirical expressions developed based on the well-designed experimental observations give many reliable predictions. Hence, the core objective of the present study is to apply the design of experiment (DOE) approach on

the vibration study of cutting tool considering the four key variables: rotational speed (N) of the spindle i.e. work-piece, feed rate (f), depth of cut (DOC) (d_C) and the work-piece diameter (D). Based on the observations, the optimum parameter values identified are: N = 350 RPM, f = 0.15mm/rev, d_C = 0.3 mm and D = 40 mm. Regression analysis is a mathematical method of determining which of those factors has an effect. A set of statistical procedures for estimating relationships between a dependent variable and one or more independent variables is known as regression analysis. Moreover, the second-order polynomial equation with cross-terms has been identified as the more suitable regression expression than the second and third-order polynomial.

Using the regression equations, the adaptive control methodology has been applied and the input parameters are optimized for lower vibrations. Present research work is the implementation of adaptive control for machining process. It is another step towards automation, wherein the additional elements are added in decision-making process. When a component or an object is being manufactured, the important variables are measured, and then if needed, the certain variables are altered with programmed limits, to get an accurate finished part as possible. The constraint of the adaptive control in the present research is tool vibration. Adaptive Control Constraint is used to constrain the tool vibration and for finding the affected parameter. The outcomes of the regression analysis are validated concerning the experimental observations. This research work can further be used for the optimization of the affected parameter and can be fed in to the system for reconsideration.

ACKNOWLEDGMENT

Without the intimate relationships I have with others, the work detailed in this thesis would not have been possible. I would want to use this opportunity to express my heartfelt gratitude and thanks to everyone who contributed to the completion of this research work.

To begin, I want to express my heartfelt gratitude to Dr. Jeetendrakumar A. Vadher, my research supervisor, for exposing me to this interesting profession of engineering and for his unwavering support, advice, inspiration, encouragement, and ongoing assistance during my research. His passion, his logical approach to research, and his commitment to producing high-quality work have all left a lasting effect on me. I've learned a great deal from him over the years, including how to generate new possibilities, how to reframe the topic, how to approach an issue with methodical thinking, data-driven decision-making, and how to use serendipity.

I would also want to express my gratitude to Dr. Darshak Desai and Dr. Vinod Patel, members of my Doctoral Progress Committee (DPC), for their unwavering support, advice, collaboration, and encouragement. Their ongoing counsel, collaboration, inspiration, and encouragement have kept me moving forward. I owe them plenty of thanks for always being there for me, and I consider myself fortunate to have been involved with individuals like them throughout my life.

I would want to offer my sincerest thanks to the Balief Corporation's owner, and employees. Their assistance with the experimental setup, personal assistance, and polite demeanor has always put me at ease when I needed assistance through my research. The work I've done with them has taught me how an individual may succeed in attaining what initially appears to be impossible.

I owe my lifelong appreciation to Kalpa Patel, my better half, for his unflinching support and understanding of my ambitions and desires. Her encouragement has always been a source of strength for me. Her fortitude and selflessness will serve as an influence throughout my life. Without her assistance, I would not have been able to accomplish much of what I have accomplished or develop into who I am. I am grateful to my princesses Stuti and Sonam for their smiles and exquisite expressions that provide me joy and encouragement. My beloved girls, simply seeing you both smile reminds me how wonderful my life is. I adore you and am indebted to you. My particular thanks to my teachers, whose instruction at various stages of schooling enabled me to witness this day. I believe that it is because of their goodwill that I was able to reach the point where I could write this thesis.

As is customary, naming persons who inspired this research is difficult, but there are others whose spiritual assistance is much more essential. I am indebted to my family for being a part of my vision and teaching me the important things in life. Their unwavering love and support have always been a source of strength for me. Their fortitude and sacrifice will serve as an inspiration for the rest of my life. Additionally, I am indebted to my family for their continual inspiration and encouragement.

Above all, I am indebted to the Almighty God for bestowing this wonderful life onto me and for sticking with me through each stage of my life.

(Narendrakumar Amrutlal Patel)

TABLE OF CONTENT

DECLARATION II
CERTIFICATE III
COURSE-WORK COMPLETION CERTIFICATE IV
ORIGINALITY REPORT CERTIFICATE V
PH.D. THESIS NON-EXCLUSIVE LICENSE VII
ABSTRACT X
ACKNOWLEDGMENT XII
TABLE OF CONTENT XIV
LIST OF FIGURES XVII
LIST OF TABLES XX
NOMENCLATURE XXII
1. INTRODUCTION 1
1.1. Preamble 1
1.2. Brief description of the research topic 1
1.3. Machining process 2
1.4. Cutting tool 4
1.5. Machining vibrations 7
1.6. Adaptive Control 9
1.6.1. Adaptive Control with Optimization (ACO) 10
1.6.2. Adaptive Control with Constraints System (ACC) 10
1.6.3. Main Features of Adaptive Control for Machine Tool 13
1.6.4. Benefits of Adaptive Control in Machining 13
1.7. Thesis organization 14
2. LITERATURE REVIEW 15
2.1. Preamble 15
2.2. Introduction 15
2.3. Dynamic modeling for turning operations 17
2.4. Methods of numerical integration of vibration study 17
2.4.1. Frequency Response Analysis 19
2.4.2. Transient Response Analysis 20
2.4.3. Runge-Kutta Technique 20
2.5. Effect of vibration on machining 22
2.6. Experimental modal analysis 24
2.7. Optimization and Adaptive control for vibration applications 28

2.8. Adaptive Control Constraints (ACC) 34
2.9. Literature review Summary 39
2.10. Research gaps 41
2.11. Objectives of the research 42
2.12. Research Methodology 42
2.13. Scope and original contribution of the present work 43
2.14. Summary 43
3. CUTTING TOOL PERFORMANCE ASSESSMENT FOR CUTTING TOOL VIBRATION 45
3.1. Preamble 45
3.2. Mathematical Modeling for system parameters 45
3.3. Rotating Beam Moving Loads with Regenerative Chatter 48
3.3.1. Lateral Vibration of Beams 50
3.3.2. Initial Conditions 52
3.3.3. Free Vibration 52
3.3.4. Boundary Conditions 54
3.3.4.1. Case 1: simply supported 54
3.3.4.2. Case 2: fixed (clamped) end or Cantilever 55
3.4. Background for Experimental Investigation. 56
3.5. Methodology for Experimentation 59
3.6. Experimental Setup 59
3.6.1. Components/Equipment used in the experimental setup 60
3.6.1.1. Lathe Machine 60
3.6.1.2. Single Point Cutting tool (With Carbide brazed Insert) 62
3.6.1.3. Work Samples 63
3.6.1.4. Vibration Sensor 66
3.6.1.5. Arduino UNO (ATmega328P) 66
3.6.2. Experimental Setup 68
3.7. Selection of Parameters 69
3.8. Experimentation 69
3.8.1. Design of Experiments Introduction 71
3.8.1.1. DOE 71
3.8.1.2. Taguchi 71
3.8.1.3. ANOVA (Analysis of Variance) 71
3.8.2. Pilot Experiment 72
3.8.3. Final Experimentation (Actual Work) 74
3.8.3.1. Response table for 0-50 mm 85

3.8.3.2. ANOVA for 0-50 mm 86
3.8.3.3. Response table for 50-100 mm 88
3.8.3.4. ANOVA for 50-100 mm 89
3.8.3.5. Response table for 100-150 mm 91
3.8.3.6. ANNOVA for 100-150 mm 92
3.8.3.7. Response table for 150-200 mm 94
3.8.3.8. ANOVA for 150-200 mm 95
3.8.3.9. Response table for 0-200 mm 97
3.8.3.10. ANOVA for 0-200 mm 98
3.8.4. Percentage Contribution of Parameter for Tool Vibration 100
3.8.5. Root Mean Square (RMS) 102
3.8.6. Regression Analysis 102
3.8.6.1. Polynomial relation of order 2 105
3.8.6.2. Polynomial relation of order 3 107
3.8.6.3. Polynomial relation of order 2 with cross-terms 110
3.8.6.4. Overall outcome of regression analysis 112
3.9. Summary 116
4. ADAPTIVE CONTROL IMPLEMENTATION 117
4.1. Preamble 117
4.2. Introduction 117
4.3. Adaptive Control Constraints 119
4.4. Adaptive Control Constraints (ACC) Algorithm 120
4.4.1. Constraints 125
4.4.2. Strategies and selection of input parameters 125
4.5. Results Validation 127
4.6. Summary 132
5. CONCLUSION 133
5.1. FUTURE SCOPE 134
RESEARCH PUBLICATIONS 135
REFERENCES 136
APPENDIX A1: MATLAB CODE FOR ROTATING BEAM ANALYSIS 150
APPENDIX A2: ARDINO UNO CODE 154
APPENDIX A3: MATLAB CODE FORADAPTIVECONTROL SYSTEM 156

LIST OF FIGURES

Fig.1.1. Machining by cutting operation[2] 3
Fig 1.2. Different types of lathe cutting tools [3] 4
Fig.1.3. Single point cutting tool with nomenclature[4] 5
Fig.1.4. Single point cutting tool geometry[4] 6
Fig.2.1. Flow chart of the proposed methodology [21] 29
Fig.2.2. The relationship between the variables [21] 30
Fig.2.3. Aurdino UNO circuit with annotations[31] 30
Fig.2.4. ADXL345 Accelerometer[28]..31
Fig.2.5. Methodology of chatter vibration study[33] 31
Fig.2.6. Traditional block diagram of feedrate optimization using MRR[25] 32
Fig.2.7. Schematic depiction of experimental set-up for deflection measurement[25] 33
Fig.2.8. Overall procedure of vibration surveillance and generation of the spindle speed program[20] 34
Fig.2.9. Composition of an adaptive control constraint (ACC) [11] 35
Fig.2.10. Parameter adaptive control based ACC system[10] 36
Fig.2.11. The model reference adaptive control based ACC system[10] 36
Fig.2.12. Configuration of the proposed adaptive control constraint system[49] 37
Fig.2.13. Methodology in condition monitoring system with ACC system[49] 38
Fig.3.1. Lateral vibrations of beam 50
Fig.3.2. Lathe machine used for the experimental study 61
Fig.3.3. Cutting tool of material: tungsten-cobalt cemented carbide (*YG6*) 63
Fig. 3.4. Cutting tool and the work-piece mounted on the lathe machine used for the experimental study 63
Fig. 3.5. Experimental specimen of work-piece...65
Fig. 3.6 ADXL335 vibration sensor 66
Fig. 3.7 Arduino UNO...67
Fig. 3.8. Schematic representation of the experimental setup with Arduino UNO 68
Fig. 3.9. Experimental setup with dimensional depiction..68
Fig. 3.10 Experimental setup with Arduino UNO and ADXL335 70
Fig.3.11 Response values of the pilot study 73
Fig.3.12 Division of workpiece in 4 segments...75
Fig.3.13 Outcome of Experimental set 1 77
Fig.3.14 Outcome of Experimental set 2 77
Fig.3.15 Outcome of Experimental set 3 78

Fig.3.16 Outcome of Experimental set 4 78
Fig.3.17 Outcome of Experimental set 5 79
Fig.3.18 Outcome of Experimental set 6 79
Fig.3.19 Outcome of Experimental set 7 80
Fig.3.20 Outcome of Experimental set 8 80
Fig.3.21 Outcome of Experimental set 9 81
Fig.3.22 Outcome of Experimental set 10 81
Fig.3.23 Outcome of Experimental set 11 82
Fig.3.24 Outcome of Experimental set 12 82
Fig.3.25 Outcome of Experimental set 13 83
Fig.3.26 Outcome of Experimental set 14 83
Fig.3.27 Outcome of Experimental set 15 84
Fig.3.28 Outcome of Experimental set 16 84
Fig.3.29 Main effect plot (0-50 mm size from the free end) for (a) ΔX_{maxg}, (b) ΔY_{maxg}, and (c) ΔZ_{maxg} 87
Fig.3.30 S-N ratio (0-50 mm from the free end) 87
Fig.3.31 Main effect plot (50-100 mm size from the free end) for (a) ΔX_{maxg}, (b) ΔY_{maxg} and (c) ΔZ_{maxg} 90
Fig.3.32 S-N ratio (0-50 mm from the free end) 90
Fig.3.33 Main effect plot (100-150 mm size from the free end) for (a) ΔX_{maxg}, (b) ΔY_{maxg} and (c) ΔZ_{maxg} 93
Fig.3.34 S-N ratio (100-150 mm from the free end) 93
Fig.3.35 Main effect plot (150-200 mm size from the free end) for (a) ΔX_{maxg}, (b) ΔY_{maxg}, and (c) ΔZ_{maxg} 96
Fig.3.36 S-N ratio (150-200 mm from the free end) 96
Fig.3.37 Main effect plot (0-200 mm size from the free end) for (a) ΔX_{maxg}, (b) ΔY_{maxg}, and (c) ΔZ_{maxg} 99
Fig.3.38 S-N ratio (0-200 mm size from the free end) 99
Fig.3.39 Percentage contribution of parameter for tool vibration 101
Fig.3.40 Effect of work-piece diameter variation on vibration 114
Fig.3.41 Effect of depth of cut variation on vibration 114
Fig.3.42 Effect of feed variation on vibration 115
Fig.3.43 Effect of speed variation on vibration 115
Fig.4.1 Flowchart of ACC methodology 122
Fig.4.2 Block diagram of adaptive control system 122
Fig.4.3 Flowchart of ACC corrective action 123
Fig.4.4 RMS values for variable depth of cut 124

Fig.4.5 RMS values for variable feed rate 124
Fig.4.6 RMS values for variable rotation speed 125

LIST OF TABLES

Table 3.1 The values of specific cutting force for different work materials 46
Table 3.2Technical specifications of lathe machine 61
Table 3.3 Different applications of EN8 Material 64
Table 3.4 EN8 chemical composition 65
Table 3.5 EN8 mechanical properties 65
Table 3.6 Factors and levels for DOE 72
Table 3.7 L16 table of the pilot study 72
Table 3.8 L16 table of pilot study – Response table 73
Table 3.9 L16 Parameter Combination 74
Table 3.10 Calculated values of the system parameters for the L16 sets of experimentation based on the mathematical model 76
Table 3.11 DOE parameters for 0-50 mm size from the free end 85
Table 3.12 DOE parameters for 50-100 mm size from the free end 88
Table 3.13 DOE parameters for 100-150 mm size from the free end 91
Table 3.14 DOE parameters for 150-200 mm size from the free end 94
Table 3.15 DOE parameters for 0-200 mm size from the free end 97
Table 3.16 Optimum parameter values for different sets of analysis based on the distance from the free end 100
Table 3.17 Percentage contribution of parameter for tool vibration 101
Table 3.18 Statistics of regression fit (polynomial order 2) for ΔX_{maxg} 105
Table 3.19 Statistics of regression fit (polynomial order 2) for ΔY_{maxg} 106
Table 3.20 Statistics of regression fit (polynomial order 2) for ΔZ_{maxg} 106
Table 3.21 Statistics of regression fit (polynomial order 2) for *RMS* 107
Table 3.22 Statistics of regression fit (polynomial order 3) for ΔX_g 108
Table 3.23 Statistics of regression fit (polynomial order 3) for ΔY_{maxg} 108
Table 3.24 Statistics of regression fit (polynomial order 2) for ΔZ_{maxg} 109
Table 3.25 Statistics of regression fit (polynomial order 2) for *RMS* 109
Table 3.26 Statistics of regression fit (polynomial order 2 with cross-terms) for ΔX_{maxg} 110
Table 3.27 Statistics of regression fit (polynomial order 2 with cross-terms) for ΔY_{maxg} 111
Table 3.28 Statistics of regression fit (polynomial order 2 with cross-terms) for ΔZ_{maxg} 111
Table 3.29 Statistics of regression fit (polynomial order 2 with cross-terms) for *RMS* 112
Table 3.30 R-Square values for the considered three regression fits 113
Table 4.1 RMS values for the corresponding input parameters and vibration components 127
Table 4.2 Experimental recordings 128

Table 4.3 Regression findings..129
Table 4.4 Percentage difference between experimental and regression results 129
Table 4.5 Validation of regression outcomes with reference to the experimental observations 131

NOMENCLATURE

Abbreviations

ACC	Adaptive Control with Constraints
ACO	Adaptive Control with Optimization
ANNOVA	Analysis of variance
CAM	Computer-Assisted Manufacturing
CNC	Computer Numerical Control
DDE	Delay Differential Equation
DOC	Depth of cut
DOE	Design of Experiments
DOF	Degrees of freedom
EMA	Experimental modal analysis
FRF	Frequency reaction functions
HSS	High-speed steel
RK	Runge-Kutta
RMS	Root Mean Square
RSM	response surface method
WC	Tungsten carbide

Symbols

$A(x)$	Cross-sectional area
c	Damping constant
D	Workpiece diameter (mm)
d_C	Depth of cut (mm)
d_C	Depth of cut (mm)
E	Young’s modulus
f	Feed per revolution (mm/rev)
f	Feed per revolution (mm/rev)
f_n	Feed rate per revolution (mm).
h	Finished surface roughness (micron)

$I(x)$	Moment of inertia
k	Spring stiffness
K_C	Specific cutting force
l	Length of work-piece (mm)
l_C	Cutting length per minute (mm/min)
m	Mass
$M(x, t)$	Bending moment
MRR	Material Removal Rate (mm^3/min)
N	Number of time steps
n	Main axis spindle speed (min-1)
P_C	Actual cutting power (kW)
Q	Heat generation
r	radius of workpiece
RE	Corner radius
t	Time
T	Total time
T_C	Cutting time (min)
$V(x, t)$	Shear force
v, w	Cutting forces in y and z directions
V_C	Cutting speed (m/min)
$W(x)$	Normal mode or characteristic function
x, y, z	Cartesian Coordinates
Z	Measured mode shape
$\Delta X_{max\ g}, \Delta Y_{max\ g}, \Delta Z_{max\ g}$	Components of tool vibration
η	Machine coefficient
ρ	Mass density
ω	Natural Frequency (Hz)

1. INTRODUCTION

1.1. Preamble

The current chapter discusses the history of the field of study, the rationale for choosing the current research topic, and the format of the thesis.

1.2. Brief description of the research topic

The current research focuses on the performance of cutting tools that are subjected to vibration throughout various operations. In machining, a cutting tool used to remove material from a workpiece using shear deformation. Cutting can be accomplished with single-point or multipoint cutting tools. Single-point cutting tools are used for turning, shaping, planning, and comparable activities because they remove material by cutting edges. Tools for processing and drilling are usually multipoint cutting tools. It is a body with teeth or front lines. Additionally, crushing tools are multipoint cutting tools. Each grain of grating functions as a tiny single-point front line (despite its high adverse rake point) and shears a small chip.

Cutting tool materials should be more robust than the material being cut, and the tool should be capable of withstanding the heat and force generated during the metal-cutting contact. Additionally, the tool should have a unique calculation, with freedom points built in such a way that the frontend can make contact with the workpiece without the remainder of the device delaying the workpiece surface. The point of the cutting face is additionally significant, just like the flute width, the number of woodwinds or teeth, and edge size. To have a long working life, the entirety of the above should be enhanced, in addition to the velocities and feeds at which the tool is run.

1.3. Machining process

Machining is process in which excess material is continuously removed as chips from a required size and shape. Fig 1.1 illustrate the basic mechanism of turning process. A rigid, hard, wedge-shaped tool referred to as a cutting device is used to condense the work material and so shear the abundant layer of material. Thus, the purpose of the cutting tool (also known as a shaper) is to compact a particular layer of work material to shear it off. Following that, the tool should have a wedge form with a sharp edge for simply and effectively removing material with the least amount of force. Simultaneously, tool material should be sufficiently robust to withstand the intense scouring that occurs during machining. Along with the definition and model, the accompanying portions discuss the purposes, various highlights, assignments, materials, and characteristics of cutting devices [1].

When cutting is used to the machine, the tool is inserted into the work material to the depth of the cut [2]. Turning creates round and hollow pieces, molding, and processing create flat surfaces, and piercing creates apertures of varying widths. There is a certain number of known calculation foundations for each tool. Cutting eliminates the machining waste in the form of chips, which are visible to the unaided eye. When the cutting device has the completed form of the work-piece, the condition of the work-piece may be generated by shaping. Regardless of the device feed inside and out, an overall movement is required to convey the chip (principle movement). The precision of the surface profile is generally dependent on the structure cutting device's precision. Additionally, a surface can be generated through a series of movements that achieve the chip arrangement measure (principal movement) and the growth of the commitment mark along the surface (feed movement).

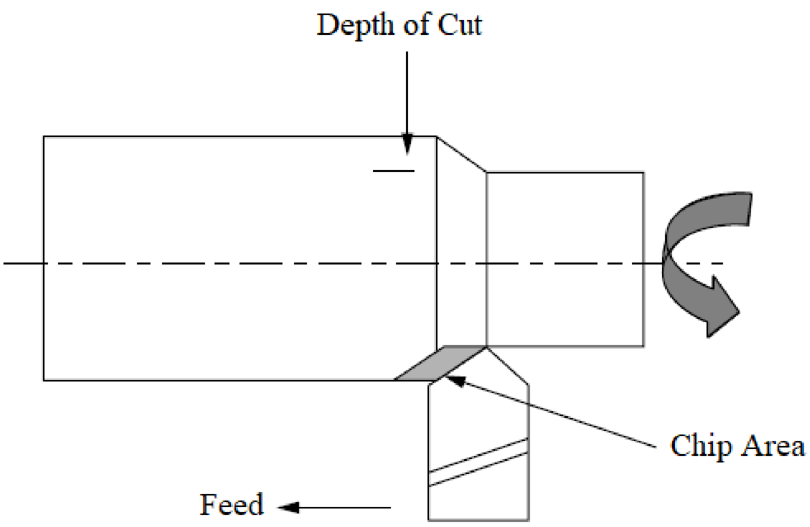

Fig.1.1. Machining by cutting operation[2]

Speed, feed, and depth of cut are the three essential parameters in any basic turning operation. While other parameters such as material type and tool type have a significant impact, these three are the ones that the operator may change directly at the machine by modifying the control.

The term "speed" is always used in reference to the spindle and the workpiece. The number of revolutions per minute (rpm) indicates their rotational speed. However, the critical parameter for any turning process is the surface speed or the rate at which the workpiece material moves past the cutting tool. It is calculated by multiplying the rotational speed by the circumference (in feet) of the workpiece prior to initiating the cut. It is measured in surface feet per minute and is specific to the workpiece. Each diameter of a workpiece has a varied cutting speed, even if the rotational speed remains constant.

The term "feed" is always used to refer to the cutting tool and is used to describe the rate at which the tool progresses along its cutting path. On the majority of power-fed lathes, the feed rate is proportional to the spindle speed and is given in inches (of tool advancement) per spindle revolution or in millimeters per revolution.

The term "Depth of Cut" is self-explanatory. It is the thickness of the layer being removed from the workpiece or the distance between the work's uncut and cut surfaces in inches. It is critical to notice, however, that the diameter of the workpiece is reduced by twice the depth of cut, as this layer is removed from both sides.

1.4. Cutting tool

The workpiece is held and secured in a sling on a center lathe machine. When fabricating a segment from a circular bar, the bar is passed through the empty axle of the headstock and the required length is pulled out and then engaged in the jaws of the throw, with the free end of the bar extending toward the tailstock end. Generally, the tool progresses from option to choose. This is referred to as right-handed work. In some instances, it becomes necessary to perform some tasks while moving equipment from left to right, i.e., left-handed work. Devices for right-handed machine tasks are quite distinct from tools for left-handed labor. Indeed, they are mirror images of one another[3].

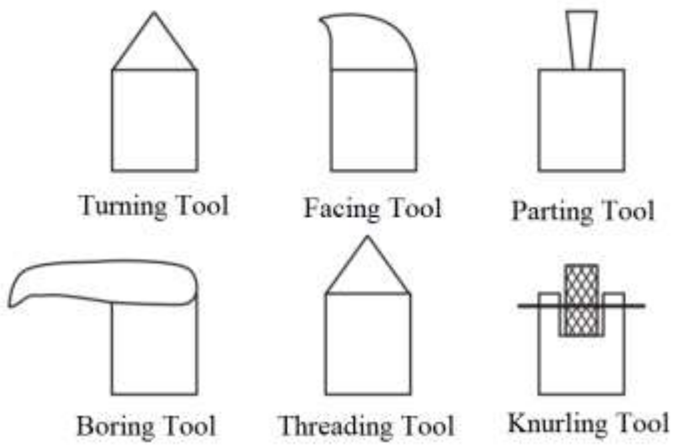

Fig 1.2. Different types of lathe cutting tools [3]

A cutting tool is a wedge-molded, sharp-edged that is utilized to shear away abundance material from a workpiece during machining to accomplish the ideal structure, size, and accuracy. Fig 1.2 shows various types of lathe cutting tools. It is unbendingly appended to the machine gadget. Additionally, distinct mechanical and cutting activity courses of action contribute to the overall speed between the workpiece and the cutting tool.

The tool is made up of two components: one is sharpened cutting edges and another is shank. The cutting point of the tool is defined by its face (along which chips slide as they are cut), its side flank or major flank, its end flank or minor flank, and its base. Tool geometry of single point cutting tool is illustrated in fig 1.3 and fig 1.4. As previously stated, we accomplish a variety of operations on the lathe (such as turning and facing) using a single-point cutting tool. This tool is extremely simple to design and fabricate. This tool can be manufactured at a significantly lower cost than other multipoint cutting tools[4]. This tool can be manufactured of a variety of materials, including high carbon steel, high-speed steel, ceramics, cemented carbide, cubic boron nitrite).

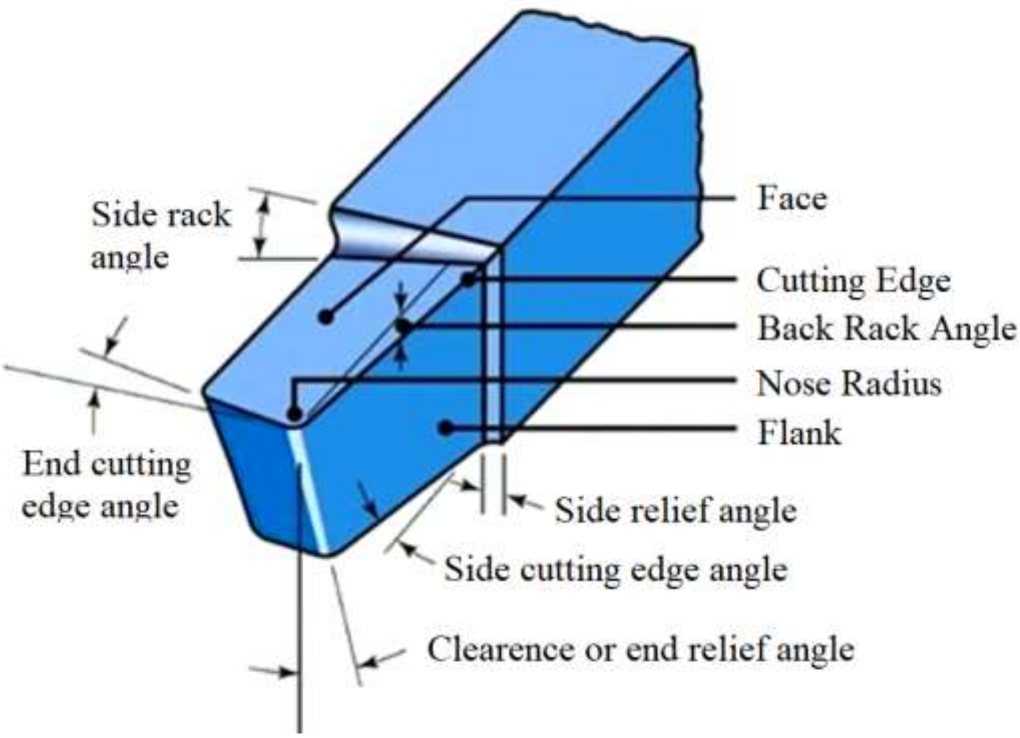

Fig.1.3. Single point cutting tool with nomenclature[4]

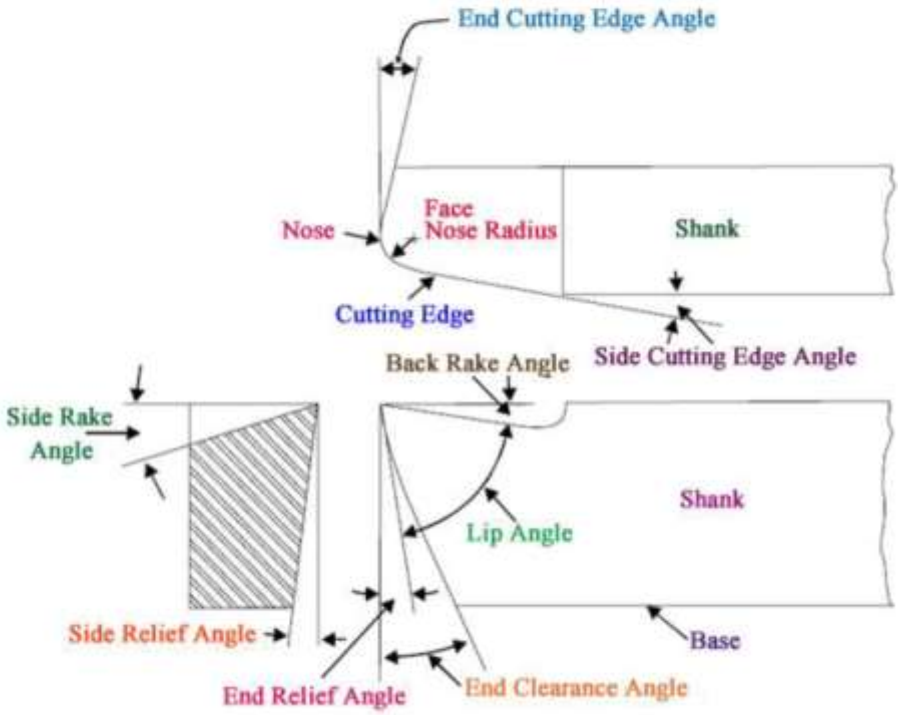

Fig.1.4. Single point cutting tool geometry[4]

Beside the application of single point cutting tools, there are a few disadvantages of single point cutting tools that are described below as compared to multipoint cutting tools.

- Little high tool wear rate
- Shorter tool life
- Low metal removal rate
- Low productive

The calculation of cutting tool takes into account the tendency and direction of the tool's various planes and front lines, as well as the nose span. The expression "tool task" alludes to the act of showing different parts of the cutting mechanical assembly in a notable however normalized way. There are a few mechanical assembly task systems, and everyone tends to such qualities unequivocally.

During machining, a segment of the cutting tool comes into real contact with the workpiece, presenting it to high cutting temperatures and relentless scouring. The cutting device's material should be fit for withstanding such high cutting temperatures and powers. Each tool material should show specific qualities, including high hardness, high hot hardness, high strength, a higher dissolving point, and compound idleness at raised cutting temperatures. As an overall rule, the tool material's hardness ought to be at any rate 1.5 occasions that of the workpiece to guarantee smooth cutting activity.

Also, an appropriate covering can be added to the tool to improve an assortment of wanted highlights. A covered tool, then again, doesn't consider fast re-honing by means of granulating when the edges become exhausted from broad use. These days, embed based tools are accessible, which consider the connection or clasping of little tradable additions to a major knife. These inserts have a cutting capacity and are in this way slowly exhausted. At the point when wear arrives at the adequate level, the additions can be supplanted, yet the knife can be reused. Coming up next are the absolute most often utilized device materials available today: High-Speed Steel (HSS), Tungsten carbide, Ceramics, Cubic Boron Nitride (CBN), and Diamond.

1.5. Machining vibrations

Machining vibrations, then again alluded to as gab, are brought about by the general development of the workpiece and the cutting device. On the machined surface, the vibrations produce waves. This is valid for both customary machining tasks like turning, processing, and boring and for uncommon machining methods like boring.The current research has been designed to study the impact described above on the performance of the cutting tool.

Chatter is a type of resonant vibration that occurs within a machine or workpiece. It is capable of becoming fairly aggressive and producing a distinctively loud noise. It is virtually never a good idea to keep the machine running in the presence of significant chatter–chatter in machining is extremely detrimental to tool life, impairs the accuracy of the machining operation, and shortens the life of the machine as well [5].

Chatter can self-feed, similar to how feedback on a loudspeaker system produces those obnoxious screaming noises. As a result, it is occasionally referred to as "regenerative chatter." Grasp how chatter operates requires an understanding of the regeneration phenomena. A vibration in the tool generates a wave in the workpiece, and continuous vibration generates a series of these waves [5].

Making a second run over a chatter-wavy surface–the pressures acting on cutting tool fluctuate according to the peaks and troughs of the waves that would amplify the vibrations. This is a feedback effect that amplifies noise by producing more waves of the same frequency on workpiece [5].

There are two kinds of chatter to be aware of–tool chatter and work-piece chatter. With tool chatter, your machine and tool are doing the vibrating, which is then transmitted to the work-piece. The tool chatter is the prime focus of the present study.

Techniques for avoiding the cutting tool vibration areas listed below.

- Make the apparatus and the machine as inflexible as could be expected.
- Choosing the device that will least energize vibrations (changing points, measurements, surface treatment, and so forth)
- Choosing the energizing frequencies that best breakpoint the vibrations of the machining framework (axle speed, number of teeth and relative positions, and so on)
- Choosing tools that consolidate vibration-damping innovation (with structure damping utilizing high damping material in the joint regions and

with mass dampers utilizing a neutralizing power to balance out the movement).

Uncontrolled vibration creates multiple problems in metal cutting operations. The machine tool is made of various parts and when vibrations are produced, they also start vibrating at the same frequency. If this frequency approaches the natural frequency of vibration of that part then the amplitude of vibrations will be very excessive and the part may break even. As the tool-life is a function of the cutting variables only, the tool-life is greatly affected by the presence of vibrations in machine tools. It is found out that the tool life is decreased of the normal value if vibrations are present. The adverse effects of cutting tool vibration are as given below.

- Surface roughness on the machining surface, i.e. poor surface finish
- Compromise in machining accuracy and dimensional precision
- Decreased productivity
- Excess wear and the possibility of tear (for cutting tool, work-piece, and machine fasteners)
- Lower tool life
- Lower possibility of machining with higher depth of cut or higher feed rate

1.6. Adaptive Control

Adaptive control is a step towards automation, wherein decision-making elements are added [6]. When a component is being manufactured, the important variables are measured, and then if needed be, certain variables are altered with programmed limits, to get as accurate a finished part as possible [7].It is the technique of automatically adjusting cutting parameters such as speeds, feeds and depth of cut, etc. to an optimum satisfaction level during the machining operation, and the maximum metal removal rate which will result in minimum machining cost.

Adaptive control is the ability of the framework to alter its own activity to accomplish the most ideal method of activity [8]. The overall meaning of adaptive control suggests that a versatile framework should be fit for playing out the accompanying capacities: giving nonstop data about the current situation with the framework or recognizing the cycle; contrasting present framework execution with the ideal or ideal exhibition and settling on a choice to change the framework to accomplish the characterized ideal presentation, and starting an appropriate adjustment to drive the control framework to the ideal [9].

The types of Adaptive Control systems are:

1) Adaptive Control with Optimization (ACO)
2) Adaptive Control with Constraints (ACC)

1.6.1. Adaptive Control with Optimization (ACO)

The performance of this system is optimized in accordance with the specified performance metric. Typically, the performance metric is an economic function, such as maximum production rate or lowest machining cost. It is the most delicate closed-loop control system available, automatically optimizing the operating conditions. Adaptive control optimization systems strive to maximize the ratio of work material removed to tool wear, which is referred to as a performance indicator.

1.6.2. Adaptive Control with Constraints System (ACC)

In this system, the machining conditions such as feed rate or/and speed are maximized within given limits of machine and tool constraints e.g. Maximum force, torque, or power.

The adaptive controllers are fed by signals of the following two sensors.

1. Tool Vibration sensor

   a. The vibration of the tool is measured by an accelerometer mounted on the machine spindle housing.

2. Spindle torque sensor
   a. The torque of the spindle is measured by a strain gauge mounted on the machine spindle.

Important Constraints for ACC system:

- Maximum and Minimum spindle speed
- Maximum allowed torque
- Maximum and Minimum allowed chip load
- The maximum permitted feed rate
- Impact chip load
- Maximum allowed vibration

Adaptive control constraint (ACC) is one of the machining cycle control types. The significant ACC of the systems can be viewed as dependent on the analysis control, limit versatile control/self-tuning control, model reference versatile control, variable development control/sliding mode control, neural organization control, and cushioned control [10]. ACC is one of the successful ways to deal with handling the above challenges of cutting apparatus vibration. ACC changes the machining boundaries to keep up the most extreme working conditions during the time-shifting machining measure. The early forms of boundary versatile control-based ACC frameworks were assembled using an essential online assessor for the interaction acquire and an indispensable technique to change the addition of a vital regulator. The issues of this procedure are that the elements of the cutting interaction were neglected and no hypothetical versatile plan philosophy was applied. The versatile regulator comprises of two capacities: (a) Online assessment of the boundaries of the cutting interaction and (b) Real-time control.

The ACC amplifies the feed rate under the condition that various estimated or assessed factors of the cutting cycle are kept beneath or at individual limitation limit esteems are extensively less difficult to foster the frameworks than the rest. Versatile control limitation has just been applied for practical frameworks [11]. The versatile control program creates the ideal feed rate as per the difference in the cutting cycle.

Regression analysis is a set of measurable cycles used in statistical modeling to assess the relationships between a dependent variable (also known as the ‘result variable') and at least one free factor (also known as 'indicators', 'covariates', or 'features'). [12]. The most widely recognized type of relapse investigation is direct relapse, in which one discovers the line (or a more intricate straight mix) that most intently fits the information as per a particular numerical measure [13]. For instance, the strategy for customary least squares figures the extraordinary line (or hyperplane) that limits the amount of squared contrasts between the genuine information and that line (or hyper plane) [14]. For explicit numerical reasons (see direct relapse), this permits the scientist to appraise the restrictive assumption (or populace normal worth) of the reliant variable when the free factors take on a given arrangement of qualities [15]. More uncommon types of relapse utilize somewhat various systems to gauge elective area boundaries (e.g., quantile relapse or Necessary Condition Analysis) or gauge the restrictive assumption across a more extensive assortment of non-straight models (e.g., nonparametric regression) [16].

1.6.3. Main Features of Adaptive Control for Machine Tool

- Real-time Feed Optimization
- Tool Breakage Protection
- Spindle Drive Protection
- Tool Overload Detection
- Automatic Feed Adjustment for Tool Wear Compensation
- Tool Wear Monitoring Tool Breakage Detection
- Process Monitoring & Tool Performance Statistics

1.6.4. Benefits of Adaptive Control in Machining

- **Increased tool life:** Along with increased production rates, adaptive control generally results in a more efficient and consistent usage of the cutter across the tool's life. Because feed rate changes are made to avoid over-loading the tool, fewer cutters will be broken.
- **Greater part protection:** Rather from establishing the cutter force constraint limit based on the maximum permitted cutter and spindle deflection, the force constraint limit might be based on the work size tolerance. This safeguards the part from an out-of-tolerance state and potential damage.
- **Less operator intervention:** With the introduction of adaptive control machining, control of the process has been transferred even further away from the operator and into the hands of management via the part programmer.
- **Easier part programming:** By and large, the programmer's role necessitates a far more cautious approach than that required for numerical control. It takes less time to create the tape for a job, and fewer tryouts are required.

1.7. Thesis organization

The current chapter (Introduction) provides concise overview of the field of current research, the reason for the current study, and a description of the thesis's structure.

Chapter 1: Introduction: This chapter provides a summary of the field of current research, the rationale for the current study, and an outline of the thesis's structure.

Chapter 2: Literature Review: The chapter offers a review of the literature on research conducted on various methods for evaluating the performance of cutting tools with an emphasis on the vibration-induced between the tool and the workpiece, followed by a discussion of the research gaps. Based on the findings of the literature review, research gaps are identified and objectives are defined accordingly along with research methodology.

Chapter 3: Cutting tool performance assessment for cutting tool vibration: The purpose of this chapter is to examine the mathematical modeling of the vibrations and stresses produced during cutting operations using the concept of lateral beam vibrations. The chapter details the experimental procedure used to determine tool performance under a variety of cutting parameter configurations.

Chapter 4: Adaptive control implementation: This chapter discusses adaptive control implementation in the machining process for minimization of cutting tool vibration. Adaptive Control Constraints are used to limit tool vibration and to locate the impacted parameter. In the current study, the adaptive control is constrained by tool vibration.

Chapter 5: Conclusion: This chapter encompasses the conclusion of the research work and future scope of the work.

2. LITERATURE REVIEW

2.1. Preamble

This chapter includes a review of the literature on research conducted on various methods for evaluating the performance of cutting tools with an emphasis on the vibration-induced between the tool and the workpiece. This chapter will discuss the numerous ways for measuring the efficiency of cutting tools used in the turning activity. Cutting operation factors such as cutting speed, feed rate, and depth of cut must be carefully selected during the turning operation to maximize profitability by boosting efficiency and minimizing overall production costs for each product. Vibration results in a poor surface finish decreased efficiency, and shortened tool life; as a result, this parameter should be kept within acceptable limits. This chapter summarizes the literature study that resulted in the identification of research gaps and the research objectives, as well as the thesis premise and overall design process.

2.2. Introduction

The industry's objective has always been to manufacture cost-effective, cutting tool inserts in a short period of time [17]. Contemporary businesses try to improve these characteristics. To attain great cutting efficiency, the industry must work closely to the optimal cutting parameters [18]. As a result, turning phase cutting settings such as feed rate, speed, and depth of cut must be carefully selected to maximize efficiency, reduce total manufacturing costs for each item, or match a preset criterion [19,20]. Due to the higher cost of digitally regulated machine tools compared to their conventional equivalents, they must be run efficiently to generate the required product [17].

Vibrations arise during the turning process as a result of the tool rubbing on the workpiece [8]. Chatter is a self-energized vibration that can happen during machining tasks and become a typical constraint to efficiency and part quality. As a result, it has been a source of contemporary and scholarly interest in the assembly field for a lengthy period of time. Since the late 1950s, extensive research has been conducted to resolve the gab issue. Analysts have concentrated how to distinguish, recognize, stay away from, forestall, lessen, control, or smother chat As a result, efficiency is strongly dependent on vibration-reducing techniques, with an ideal vibration-free environment [21]. Vibration monitoring [17] can be used to determine the rate of degradation and inaccuracy that increases with the operation of the machine tool. Coupling circumstances hypotheses have developed into popular vibration theories [22]. According to Wiercigroch and Budak [23], vibration in the movement orientation causes vibration in the cutting force directions and vice versa, resulting in a multidirectional route (in cutting thrust directions). Due to variation effects, Hamdan and Bayoumi [24] showed that increasing flank clearance and rake angle improves dynamic cutting stability [25]. Additionally, for an in-depth study of the cutting operation, a mathematical model consisting of a set of linear differential equations based on the appropriate operation variables for cutting speed variations, dynamic cutting process (regarding the friction force acting on the flank), and tool of the tool rake was developed [23]. Additionally, these variables had an effect on the initial friction power. There are numerous strategies and procedures available for assessing the vibration phenomena that occur during the tool's cutting process [26]. Majority work in this area is by mathematical techniques, preceding sections [27] have elaborated on these various methods and the techniques of validating them through experimentation, which is a major contribution of the current work. In section 2.3 dynamic modeling for turning is reviewed and discussed. In section 2.4. various method of numerical integration of vibration investigation described. Review of vibration effect on machining is discussed in section 2.5. The experimental investigation and Adaptive control related work is reviewed in section 2.6 and 2.7 respectively.

2.3. Dynamic modeling for turning operations

A powerful model is characterized as a period fluctuating cycle but instead that the condition of the interaction eventually to is reliant on the advancement on the condition of the interaction throughout the time span [0, t_0] [28]. Additionally, it is utilized to convey and explain the framework's long-term behavior. In this investigation, another numerical model for turning metal workpieces is created by combining ideas from two fundamental gatherings of specialists: primary dynamists and assembly engineers. The workpiece is viewed as an adaptable workpiece and the cutting devices as an adaptable cutting tool with regenerative jabber effects. Previously, the majority of investigations into dynamic models of turning activity assumed an unbending workpiece and so disregarded workpiece deformation [30]. In any case, the workpiece eventually twists as a consequence of an exterior force applied by the machining tool [31]. This deformity affects and alters the thickness of the chip [32]. There are currently no powerful models that consider the workpiece and cutting equipment to be adaptive, and so this investigation is necessary [33]. The subtleties of the advancement of numerical definition of this unique model [34] are altogether talked about and clarified in the accompanying themes.

2.4. Methods of numerical integration of vibration study

At the point when the differential condition of movement of a vibrating framework can't be coordinated into shut structure, a mathematical method is required [33,35]. For vibration problems, there are several numerical methods available: (1) Runge-Kutta method, (2) Houbolt method, (3) Wilson method, and (4) Newmark method. The current dislodging is expressed in terms of recently defined uprooting and speed esteems, and the future conditions are established in Runge-Kutta strategies to track down the current removal.

Then, direct mathematical incorporation of the unique 85 balance conditions is the broadest technique for settling the powerful reaction of primary frameworks. This entails attempting to achieve dynamic harmony at distinct points on the schedule after the arrangement is established at time zero. At *t*, *2t*, *3t........Nt*, the majority of methods make use of identical time spans. While a variety of distinct mathematical processes have been offered previously, all approaches can be classified as either unambiguous or understandable combination strategies. Unambiguous techniques do not require the arrangement of a series of straight conditions at each stage. Fundamentally, these solutions make use of the differential condition at time "*t*" to evaluate an answer at a time "*t* + *t*." To obtain a consistent response for the majority of actual structures with hardened components, modest progress is necessary. As a result, all express tactics are strictly constant in terms of time stage length. After determining the arrangement at a time "*t* – *t*", well-understood techniques anticipate satisfying the differential condition at time *t*. These solutions necessitate the arrangement of a series of straight conditions at every time interval; however, larger time intervals can be utilized. Implied procedures might be constant in a restricted or unrestrictive manner.

Mathematics procedures for instance Runge-Kutta (RK) and deferred differential approaches need a period stage. The time step size has a regular effect on the arrangement's precision. There are two primary aspects of mathematical coordinating schemes that stand out [36]. The first stage is to dependably satisfy the administering differential condition *t*, but only at discrete time stretches *t*. Second, an appropriate type of variety of uprooting *x*, speed *x*, and speed increase *x* is acknowledged within each time span *t*. At $t = 0$, the estimations of *x* and *x* are considered independently as x_0 and *x*

$_0$, and the issue should be addressed from $t = 0$ to $t = T$. The recurrence reaction and time area investigations are the two most often used techniques in mathematical coordination for vibrating frameworks [37].

2.4.1. Frequency Response Analysis

The framework's reaction properties when exposed to sinusoidal sources of information are investigated using recurrence reaction analysis [38]. The yield characteristics are modeled or transmitted as a component of the differentiated information recurrence [39]. The robustness and execution characteristics of a certain framework can be determined via recurrence reaction analysis [40].

By and large, empowering an actual gadget with a data signal, assessing both the data and yield time stories, and looking at the two utilizing a procedure, for example, the Fast Fourier Transform is utilized to gauge the intermittent response [12,17,41]. The repeat substance of the data signal should include the entire repeat scope of income all together for the outcomes to be precise for the bit of the repeat range that isn't covered [42].

Utilizing the exchange ability to address a recurring reaction in order to create a strong framework is advantageous in control hypothesis testing as well as vibration testing for estimating the unique reaction and framework. The exchange capacity can be determined tentatively by estimating the reaction or yield because of a known contribution for a gadget whose boundaries like mass (m), damping steady (c), and spring solidness (k) are obscure. Until the structure's dynamic properties are resolved, the trade work explains them totally.

In vibration testing, the determined vibration reaction (as a result of known information or driving capability) may be removal, speed, or, more frequently, speed increase. The ratio of where *F(s)* is the information's Laplace's Transform and $S^2X(s)$ is the speed increase's Laplace's Transform refers to the exchange work in comparison to the speed increase reaction.

2.4.2. Transient Response Analysis

Transient reaction study is the most commonly acknowledged technique for registering restricted unique reactions [43]. A transient reaction analysis is used to determine how a structure behaves when subjected to time-varying excitation/load. The transient excitation is easily determined in the time domain [44]. Suddenly, the entirety of the authorities enforcing the framework is identified. Examples of powers include applied powers and extra implemented advances. Transient evaluation frequently yields essential results such as lattice focus relocations, speeds, and speed rise, as well as powers and tensions in components.

For dynamic transient examination, two mathematical strategies might be utilized, contingent upon the construction and the plan of the stacking: immediate and modular[9]. On the total coupled condition of movement, the immediate methodology plays out a mathematical reconciliation. The modular methodology lessens and uncouples the condition of movement by utilizing the design's mode shapes; the arrangement is then gotten by adding the individual modular reactions [45]. The underlying reaction is processed by tackling a progression several conditions utilizing direct mathematical coordination in transient reaction. In an immediate transient reaction, starting uprooting or/and speeds should be applied.

2.4.3. Runge-Kutta Technique

At present, the Runge-Kutta strategy is by a long shot the frequently used technique in most designing applications. They were grown around 100 years prior (very later as far as numerical history, as Newton lived in the seventeenth century and Euler lived in the mid-eighteenth century), and are an augmentation of the number-crunching Euler created. Euler's work seemed to support the use of Taylor arrangement to a wide range of issues. Since it is a first request Taylor polynomial development, its exactness is restricted, and if the capacity's subordinates are bad, significant blunders will result.

The Runge-Kutta (RK) procedure consolidates an extra incline estimation in each time step and assesses the capacity utilizing a weighted normal of the qualities. This helps with lessening mistake as it advances through time steps, and can bring about some very exact results. These techniques are alluded to as RK2 (2nd order model) and are generally basic. They are indistinguishable from the Midpoint MATLAB's ODE45 work picks between a RK4 and a RK5 dependent on which delivers the best outcome, accordingly the name ODE45. The Runge-Kutta approach depends on playing out different assessments of an ODE at different places and afterward averaging the outcomes.:

$$k_{1,n} = h * f(t_n, y_n)$$

$$k_{2,n} = h * f\left(t_n + \frac{h}{2}, y_n + \frac{k_{1,n}}{2}\right)$$

$$y_{n+1} = y_n + \left(\frac{k_1 + k_2}{2}\right)$$

k_1 and k_2 are Euler's Method and by assessing the capacity at the midpoint, utilizing past estimation of y in k_1. Then, at that point, normal these qualities to get (more exact) assessment for y_n+1. The RK4 works precisely like the RK2 aside from two focuses, there are more k terms, and the normal is weighted generally in the center. Here is the iterative capacity when all is said in done:

$$k_1 = h * f(t_n, y_n)$$

$$k_2 = h * f\left(t_n + \frac{h}{2}, y_n + \frac{k_1}{2}\right)$$

$$k_3 = h * f\left(t_n + \frac{h}{2}, y_n + \frac{k_1}{2}\right)$$

$$k_4 = h * f(t_n + h\,, y_n + k_3)$$

$$y_{n+1} = y_n + \left(\frac{k_1 + 2k_2 + 2k_3 + k_4}{6}\right)$$

Notice that the initial two terms are equivalent to RK2. The third term k_3 is determined a similar route as k_2, however with $k_2$as y-esteem rather than k_1. This is only a refinement technique for k_2's worth. k_4 assesses y at $(t + h)$ utilizing k_3's estimate for y, and afterward the weighted normal is taken where the center qualities are more weighted than the finishes.

Runge-Kutta strategy is self-beginning and stable for multi-level of opportunity frameworks. Yet, it needs a worth of relocation, $x\ (t = 0)$ or speed, to figure the time step. Conversely, utilizing a Delay Differential Equation (DDE) will consequently perceive the time venture since it is a self-produced calculation and have more modest time steps. Runge-Kutta strategy consistently relies upon the underlying conditions. Subsequently, it is a lot simpler and speedier as far as programming to receive DDE strategies.

2.5. Effect of vibration on machining

Kassab et al. [47] researched the impact of cutting device vibration on the workpiece's surface unpleasantness during dry turning. Utilizing vibration information, the surface unpleasantness of machined things was anticipated. At the finish of the investigation, the accompanying end was drawn.

- Cutting tool speed increase significantly affects the surface unpleasantness of the workpiece. The surface harshness of the workpiece is relative to cutting tool speed increase. This impact collaborates with other free factors, for example, feed rate cutting pace and profundity of cut.
- The speed increase of the cutting apparatus increments with the expansion of the cutting tool overhang for various cutting conditions. In this way, the vibration of the cutting apparatus relies unequivocally upon the cutting tool overhang.
- With the expanding feed rate, the surface harshness of the workpiece increments. The feed rate can be considered as the primary cutting variable in the machining activity.
- Increasing slicing speed prompts a diminishing in surface harshness of work-piece.
- Depth of cut small affects surface harshness of the workpiece in this examination.
- Parallel to the tool vibration the surface harshness of the workpiece increments with expanding the cutting apparatus overhang.
- The impact of cutting device vibration in feed heading could be disregard whenever contrasted and that the upward way.

It is observed that most of the researchers have worked to optimize the effect of single parameter for vibration study. The cumulative effect of feed, speed and depth of cut using experimentation investigation is found very less.

2.6. Experimental modal analysis

By and large, this trial perception in the field of underlying elements has three significant objectives, particularly for:

(1) Dynamic loading measurement of critical material properties

(2) Determining the type and scale of operational vibration response levels

(3) Validation of theoretical models and forecasts for a variety of complex phenomena.

Experimental modal analysis (EMA) might be used to achieve the third goal referenced previously. EMA is a strategy for deciding and examining the unique properties of designs when they are exposed to a known vibration excitation (frequently outside of typical help conditions). Modal Testing is another name for it. This part gives an outline of exploratory modular examination. Furthermore, a short outline of the essential vibration estimation strategy is incorporated. The reason for utilizing and clarifying a barrel-shaped metal workpiece is to acquire a comprehension of the elements of turned metal. The aftereffects of a modular report on the understudy's and her associates' workpieces are introduced and talked about.

The investigation of the unique attributes of a mechanical framework is known as modular examination. Also, measured testing appears as a method for deciding a plan's vibration qualities, like trademark frequencies, mode shapes, and mode collaboration factors. The measured examination has various benefits, including empowering the arrangement to stay away from resonation vibration or to vibrate at a particular recurrence, giving an expert comprehension of how the arrangement would respond to different kinds of dynamic loads, and aiding the assessment of game plan control (time-step, etc) for other special assessments. It is utilized to make a mathematical model of a real plan dependent on assessed vibration information. This vibration information incorporates response levels just as excitations on the construction, taking into consideration the foundation of a connection. To find Frequency response Functions (FRFs) or inspiration response works, these decided responses and excitations are frequently presented in time-space prior to being changed over to repeat region (IRFs). The direct examination can likewise be utilized to acquire a theoretical reaction model, as talked about underneath.

The spatial model is a mathematical portrayal that is utilized to convey the genuine qualities of the design, which are usually communicated as far as mass, strength, and damping properties. In the wake of exposing the spatial model to a speculative measured assessment, a model particular explanation of the plan's conduct as a grouping of vibration modes is gotten (normal frequencies, secluded damping components, and mode shapes). Ordinary plan techniques are usually characterized by the secluded model, wherein the construction vibrates typically without outside excitations. The third stage (response model) portrays how the plan will react to explicit excitation conditions by creating a variety of FRFs inside the basic repeat range.

In the meantime, the test way to deal with vibration assessment is turned around from the speculative methodology, with the FRFs approximated to build the reaction model and the measured model addressed. The secluded model includes trademark frequencies, particular damping, and mode shapes. At last, a spatial model can be made utilizing appropriate assessments to precisely address the genuine structure. Therefore, proper levels of opportunity (DOFs) ought to be recalled during the calculation, just as the incorporation of most vibration modes inside a specific repeat range.

All in all, a modular test has four fundamental advances or stages. A test arranging measure is the main stage. For different transductions, signal preparing, and examination capacities, it is critical to utilize the proper hardware. Another urgent state of a modular test is that the entirety of the essential boundaries be determined. This involves ensuring that the entirety of the amounts required for the possible application are remembered for the rundown of amounts to be determined, just as eliminating any superfluous information. Another piece of test arrangement is the choice of reaction estimation locales. This choice is guided by the expected application, and it's significant that the quantity of levels of opportunity (DOFs) required for a basic visual comprehension of enlivened mode structure shows isn't generally the best number for a more quantitative application like model approval, refreshing, or modification.

Following the arranging interaction, the subsequent stage is to set up the design for testing and gather the crude information that will be utilized to build the model of the construction's elements. The exactness of these deliberate information is the second most significant angle (in the wake of guaranteeing their culmination, that will be, that solitary the correct ones are estimated). The vital worry here is to keep away from fundamental blunders, for example, those brought about by improper hardware use or transducer establishment. These mistakes are considerably more hard to recognize and take out than blunders of a more irregular nature, for example, those brought about by commotion, and once implanted in the information, they can seriously corrupt the model's viability.

A directed excitation compelling should be applied and assessed alongside the subsequent reactions at however many focuses as are conceivable during the estimation interaction of a modular test. The determined information would then be introduced as reaction capacities, which are a bunch of proportions among reactions and excitations, either depicted by capacities that portray the reactions to a self-assertive symphonious excitation (FRFs) or an indiscreet excitation (IRFs). The Fourier change's properties permit reasonable signs preparing to change over crude information from both of these excitation designs into the fitting arrangement of FRF or IRF.

The translation or examination of reaction capacities task comes just after the information assortment and preparing step. The determined information are then exposed to a technique that plans to distinguish the fundamental boundaries of a nonexclusive numerical model that permits it to show a similar complex conduct as the test information. Since the model being referred to is regularly a modular model, the examination task is to figure out which of the framework's modular properties best depicts the mind boggling conduct found in the tests. The coefficients in a given polynomial capacity are dictated by requiring a base contrast between the deliberate curve(s) and the curve(s) recovered utilizing the polynomial articulation, which is usually done utilizing a bend fitting strategy. This isn't the best way to get the modular model, however it's the most famous.

The displaying period of the modular testing measure is the last advance. Assortments of steps are taken during the displaying cycle. In the first place, when clients play out an each capacity in turn modular investigation, they are given an assortment of modular boundaries that are probably going to contain a few irregularities. The way that there are many copy figures for the normal recurrence and damping factor for the majority of the modes will uncover these irregularities. Every individual FRF has an alternate worth, and these numerous qualities are inconsistent with the kind of different level of opportunities (MDOF) straight framework that the modular model depends on. Accordingly, a solitary incentive for the regular recurrence and damping factor for every mode should be separated from these numerous evaluations. During the worldwide type of modular investigation, such a technique is completed consequently (in which all FRFs are examined in a solitary advance, instead of separately, similar to the case with other examination systems). Despite the fact that figuring a normal worth from various assessments is simple, it should possibly be acknowledged as a reasonable worth if the change of the individual evaluations is little and the distinctions are irregular. The importance of the change ought not be disregarded regardless. It no doubt recommends a genuine defect or error in the first informational index or their modular investigations. Different tests on the subsequent model should be performed, for example, guaranteeing that the modes are reasonably genuine and not intricate, except if there are uncommon circumstances where modular intricacy can be defended. To confirm the factual and actual dependability of the end-product, an assortment of tests can be applied to the deliberate information and their separated models, and these checks ought to be performed consistently to guarantee that the necessary consistency is safeguarded in all phases of the test.

2.7. Optimization and Adaptive control for vibration applications

Numerous scholars have undertaken studies on the application of optimization techniques and adaptive control mechanisms, as well as a variety of other methodologies [30,34]. Adaptive control brings automation one step closer. When adaptive control techniques are used in conventional experimental processes, desired outcomes such as cost reduction, vibration reduction, and tool wear reduction can be achieved.

Al-Shayea et al. [21] used experimental exploration to optimize the effect of process parameters on machining vibration during the turning process of AISI 1040 steel. The response surface method (RSM) was used in that investigation to determine the optimal value of reaction components (vibration and chip recurrence). As pioneered by Montgomery, RSM is a useful collection of numerical and quantifiable processes for exhibiting and dissecting the effects of any component on a given issue in order to enhance the response. The RSM strategy in conjunction with the trial design is an effective way for determining the surface discomfort caused by the cycle's vibration and chip recurrence. The results obtained through the use of the RSM demonstrated a feasible, methodical, and logical strategy for improving the turning cycle. The cutting speed, depth of cut, and feed rate were all found to be significantly related to vibration and chip recurrence. RSM's 3-D surfaces can assist the client in seeing the effects of the limits on a superficial level of unpleasantness, by considering the preset range. The methodology and relationship between variables is shown in fig 2.1 and fig 2.2 respectively.

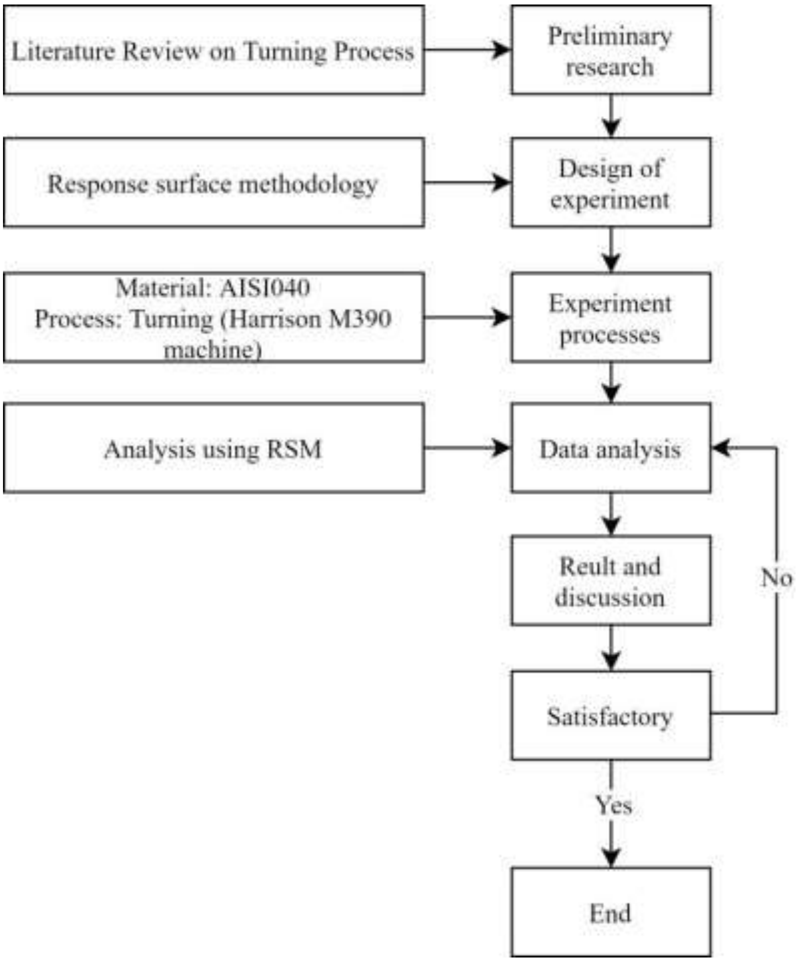

Fig.2.1. Flow chart of the proposed methodology [21]

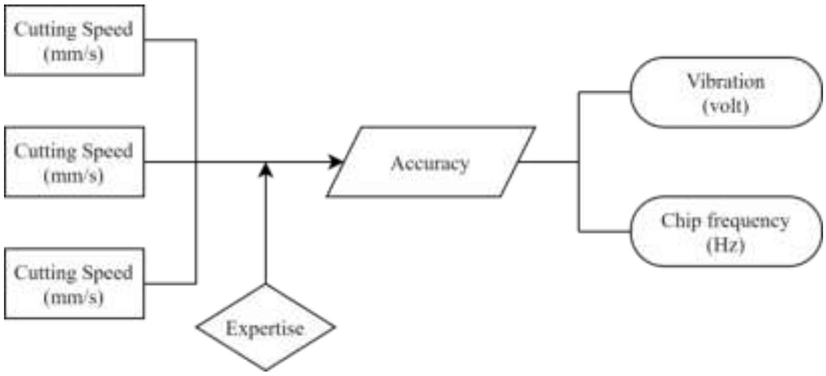

Fig.2.2. The relationship between the variables [21]

Bansal et al. [31] monitored the vibration signals by means of Aurdino UNO setup and ADXL345 Accelerometer devices[48]. The Aurdino UNO circuit with annotation is shown in fig 2.3 and ADXL345 accelerometer is shown in fig 2.4. The examination reasoned that the power of vibration force increments as the cutting velocity increments by keeping the feed rate and profundity of cut consistent for the metal and gentle steel and this work can be additionally reached out by changing the boundaries for some different materials.

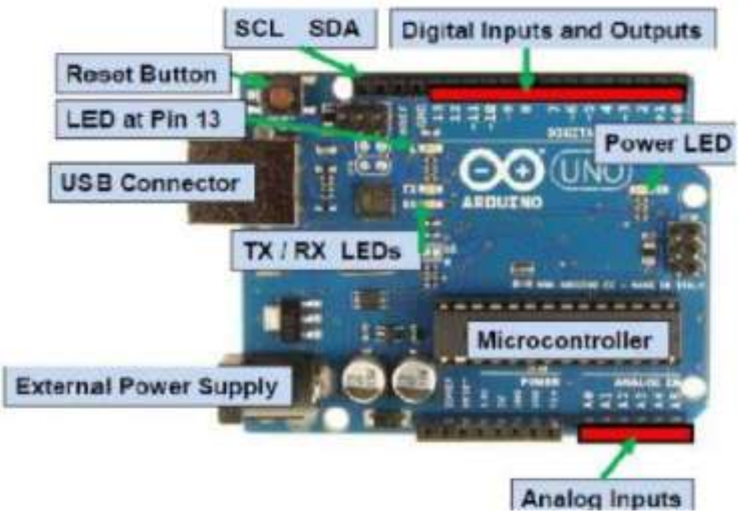

Fig.2.3. Aurdino UNO circuit with annotations[31]

Fig.2.4. ADXL345 Accelerometer[28]

Similarly, Shankar[28,29] utilized an accelerometer system on a lathe machine for low-cost vibration and process improvement. On the lathe apparatus, an ADXL335 accelerometer setup was attached for the purpose of measuring the experimental observations defined using the Taguchi technique of Design of Experiments (DOE) methodology.

Quintana et al. [33] provided an approach for investigating chatter vibrations in a vibration study. Fig 2.5 describe methodology of chatter vibration study. The report reviewed the state of research on the prattle issue and classified the present strategies for ensuring stable cutting into those that make use of the heave effect, out-of-processor in-measure, and those that affect the framework's behavior latently or effectively.

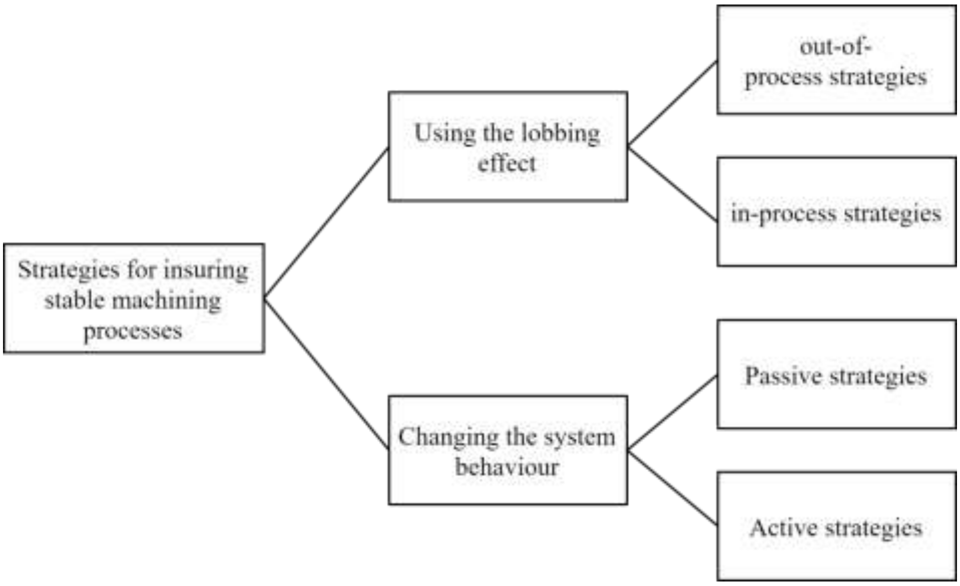

Fig.2.5. Methodology of chatter vibration study[33]

Bagci et al. [25] used acoustic sound pressure level to monitor and analyze the MRR-based feed rate optimization methodology and the impact of cutting conditions in free-form surface milling shown in fig 2.6. The experimental technique and findings demonstrate that sound pressure level monitoring is a very helpful and practical way for monitoring the effect of machining conditions and variable feed rate values obtained through optimization in the sculptured surface milling process. The next study will build an adaptive on-line control system based on the cutting sound pressure signal, enabling the CNC milling center to be integrated for more efficient surface milling (desired surface quality or machining cost) by modifying feed rate values.

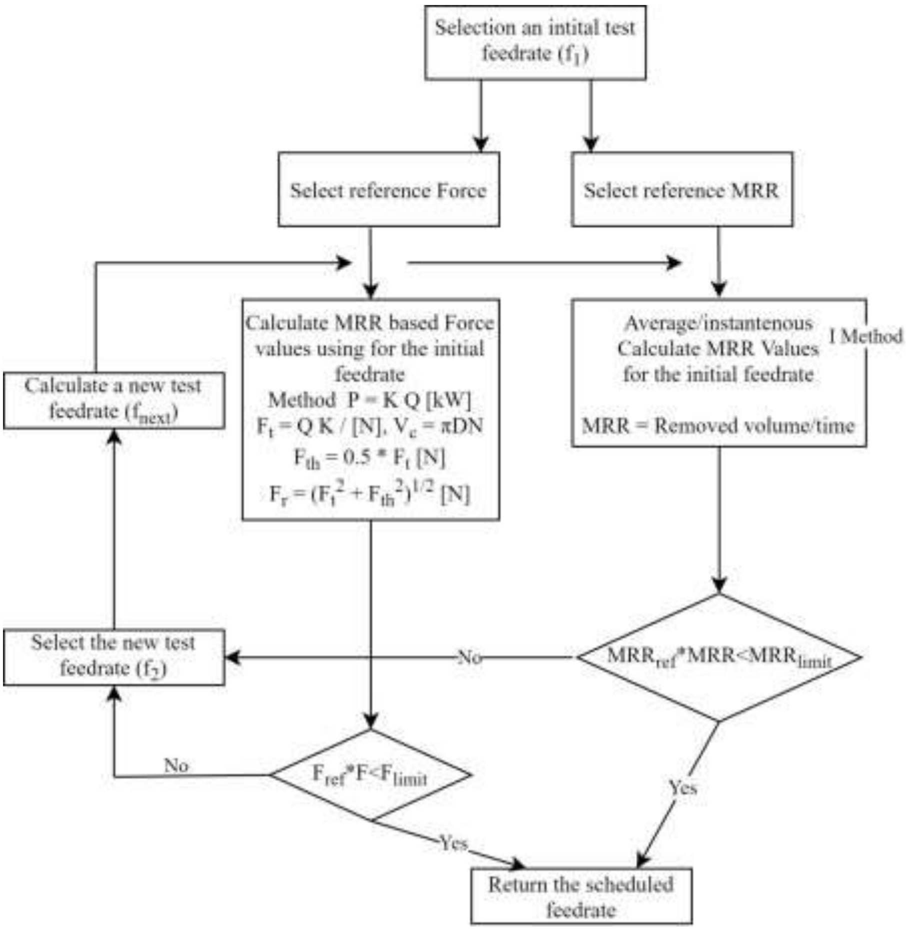

Fig.2.6. Traditional block diagram of feedrate optimization using MRR[25]

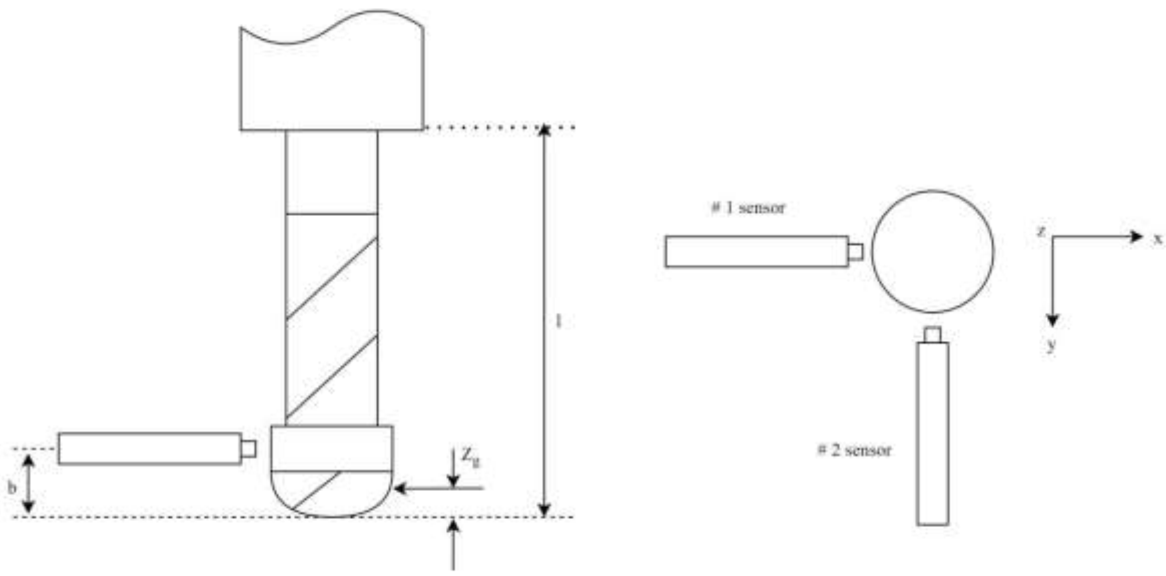

Fig.2.7. Schematic depiction of experimental set-up for deflection measurement[25]

Kalinski et al. [20] used optimal-linear spindle speed control to execute the chatter vibration surveillance. The trial findings obtained while milling at high speeds on the AlceraGambin 120CR machine demonstrated an extremely high level of vibration surveillance efficiency. The spindle speed optimal-linear control method for vibration surveillance has been successfully utilized. The chatter vibration's peak values are decreased substantially. Additionally, the root mean squared values are reduced. For a variety of materials, the results looked to be successful. As a result of the latter, we can conclude that the proposed strategy looks to be adaptable. Additionally, successful achievements in the area of chatter suppression have been produced with limited resources. Apart from the experimental tools, the milling machine's conventional CNC control system is used. This inexpensive strategy is easily applicable to industrial applications if the machine's control system enables us to modify the spindle speed during a milling process without interrupting work-piece flow as shown in fig 2.8.

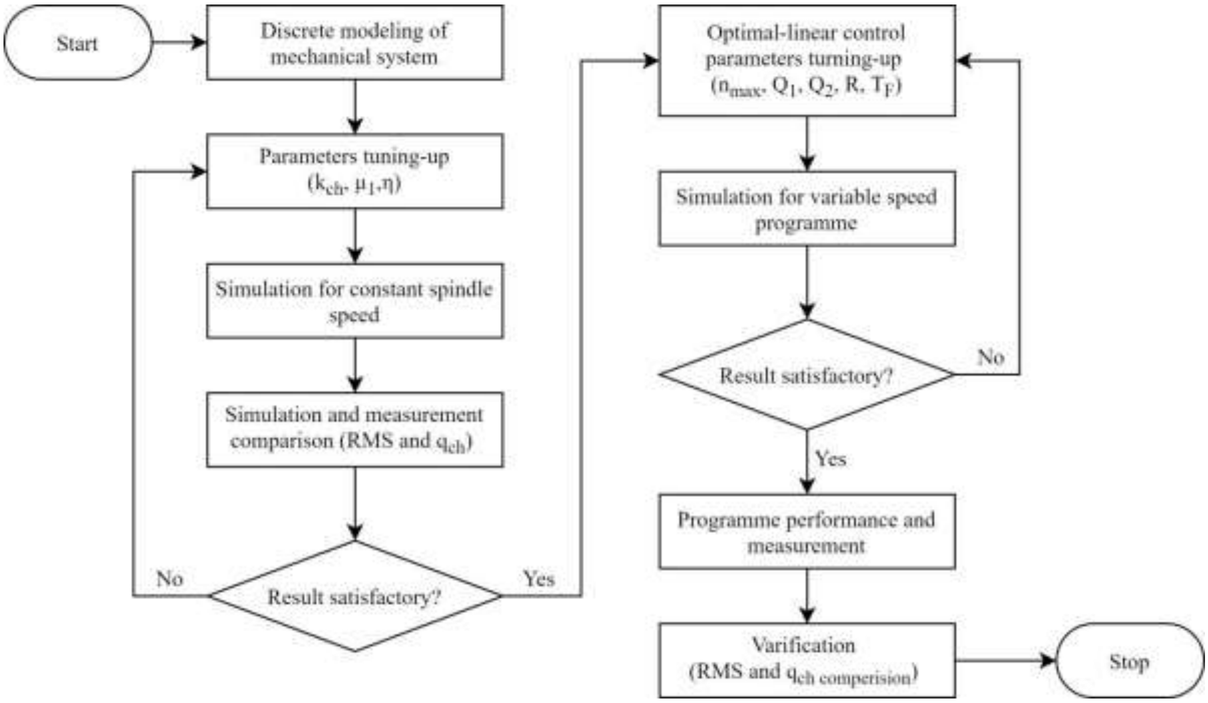

Fig.2.8. Overall procedure of vibration surveillance and generation of the spindle speed program[20]

2.8. Adaptive Control Constraints (ACC)

Watanabe et al. [11] led an investigation on the plan of a processing machine apparatus' ACC framework. To decide the ideal control calculation for a versatile control requirement framework for a processing machine device, four distinct kinds of control calculations are contemplated. The framework keeps a steady pinnacle worth of the slicing power through self-change of the feed rate. The framework is an examining information arrangement of a high request shown in fig 2.9. The framework's steadiness is then decided to utilize the Nyquist technique and the Linvill condition, and the framework's transient reactions to handling boundary variety are reproduced on a PC utilizing the state space approach. The four control calculations are as per the following: (1) an ordinal ceaseless essential calculation, (2) a discrete necessary calculation, (3) a nonlinear calculation wherein the ideal feed rate is determined by separating with the understanding that the power is corresponding to the feed rate, and (4) an improved division calculation wherein the genuine feed rate is estimated to ascertain the ideal feed rate all the more definitely. As indicated by the examination and testing results, the reexamined division calculation is the steadiest and has the best response when measure boundaries modify.

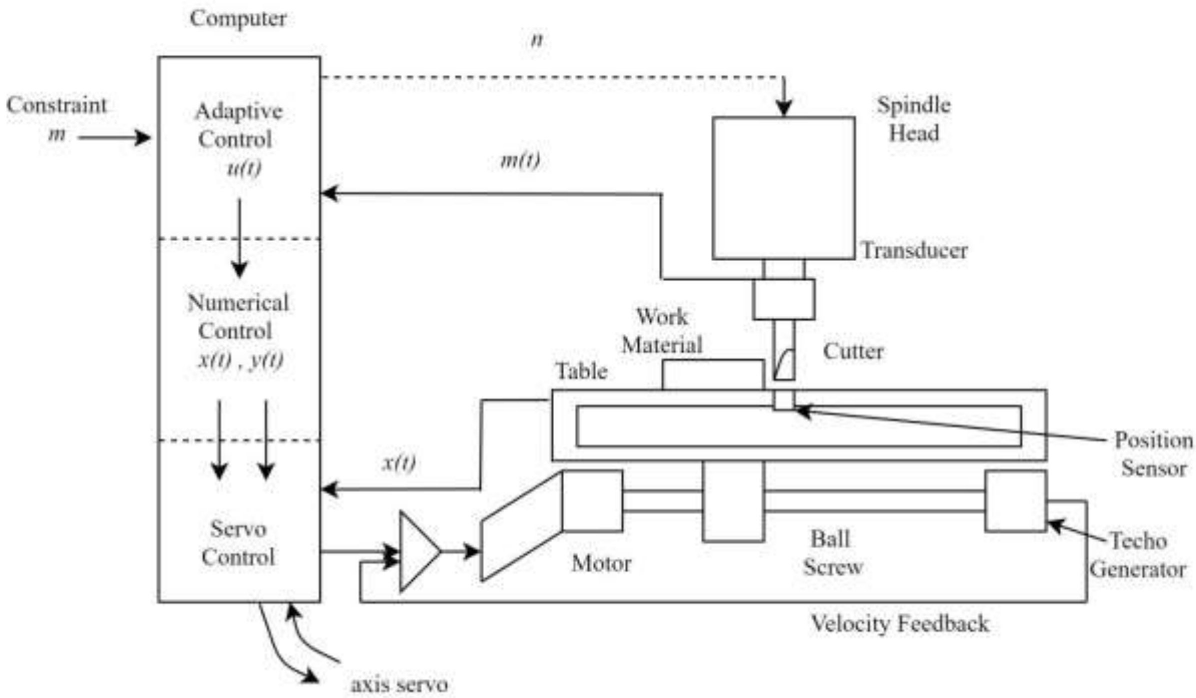

Fig.2.9. Composition of an adaptive control constraint (ACC) [11]

The ACC of machining tasks was analyzed by Liu et al. [10]. The examiner reasoned that while early ACC frameworks with consistent addition are incredibly straightforward for pragmatic applications, they become temperamental at high acquire and have a deferred reaction at low increase. A boundary versatile control/self-tuning control ACC framework can change the control acquire contingent upon assessed cutting cycle boundaries, in any case, it is just accessible for linear cutting cycles. While a versatile control framework dependent on a model reference can follow the direction of the reference model, choosing the ideal model isn't clear. While an ACC framework dependent on the inconsistent design can give fast response and power, it wavers about the sliding mode surface. While a neural organization based ACC framework doesn't depend on a cutting interaction model and is equipped for learning, its reaction speed is restricted. A fluffy control-based ACC framework, then again, doesn't depend on a cutting cycle model and has a serious level of heartiness, as it depends on a specialist's mastery shown in fig 2.10 and 2.11 respectively. Every ACC framework has various benefits and disservices, and consequently ought to be picked by the control objective.

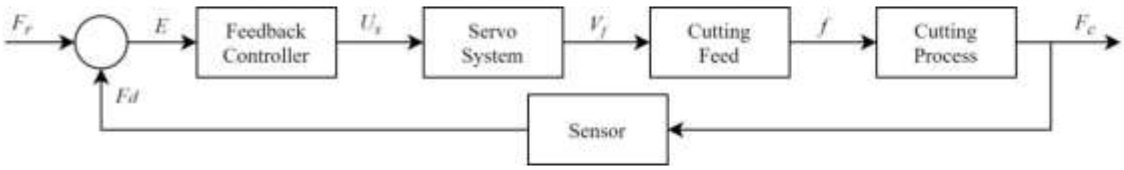

Fig.2.10. Parameter adaptive control based ACC system[10]

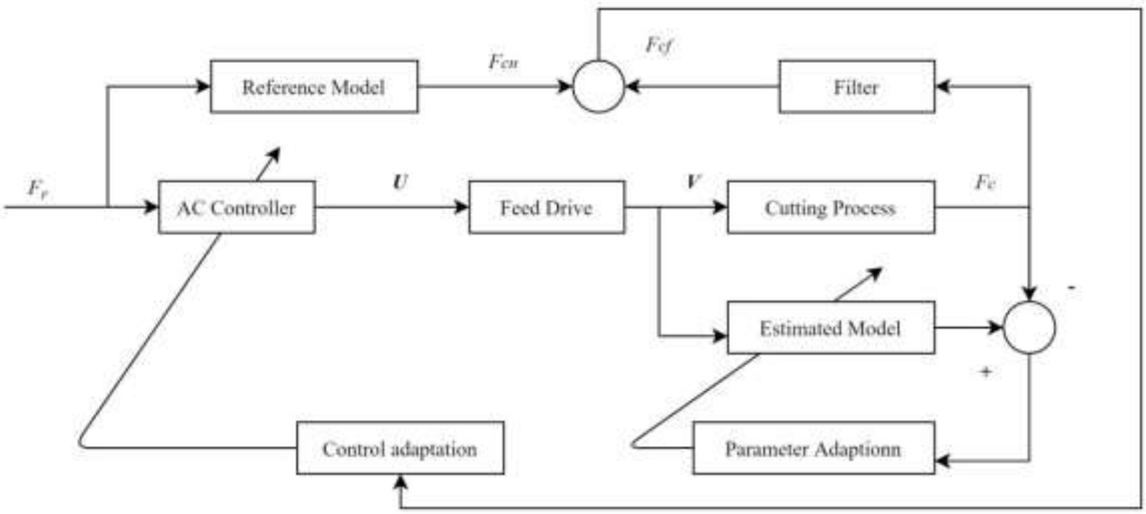

Fig.2.11. The model reference adaptive control based ACC system[10]

Srinivasa Prasad et al. [49] designed an adaptive control/self-tuning control system for computer numerical control (CNC) turning. The adaptive controlled system received the signals from the online measurement and transmitted them back to the machine tool controller, which adjusted the cutting settings to the point where the machining could be halted when a predetermined threshold was crossed. The primary objective of this work was to develop a reliable adaptive control system. The control system's objective was to regulate cutting parameters and maintain displacement and tool flank wear under constraint valves for a specific workpiece and tool combination in accordance with the ISO standard. The configuration of the proposed adaptive control constraint system displayed in fig 2.12.

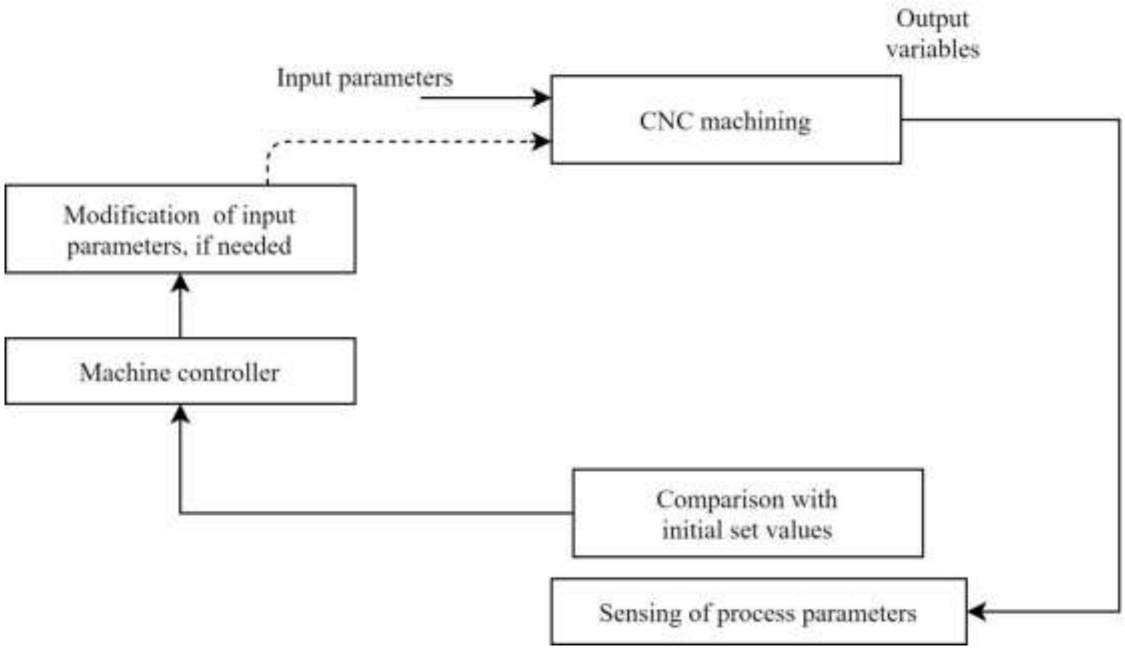

Fig.2.12. Configuration of the proposed adaptive control constraint system[49]

The digital adaptation of the cutting parameters for experimentation using MATLAB Simulink validated the efficacy of the adaptively controlled condition monitoring system, as demonstrated in several machining operations under diverse machining conditions [49]. The article discussed state-of-the-art ACC turning systems. The workpiece material was AISI4140 steel with a hardness of 150 BHN, and carbide inserts were used as the cutting tool material throughout the experiment. Methodology in condition monitoring system with ACC system is as per fig 2.13. When the surface roughness and feed are measured under identical conditions, it is possible to forecast the tool condition quite accurately using the presented technique.

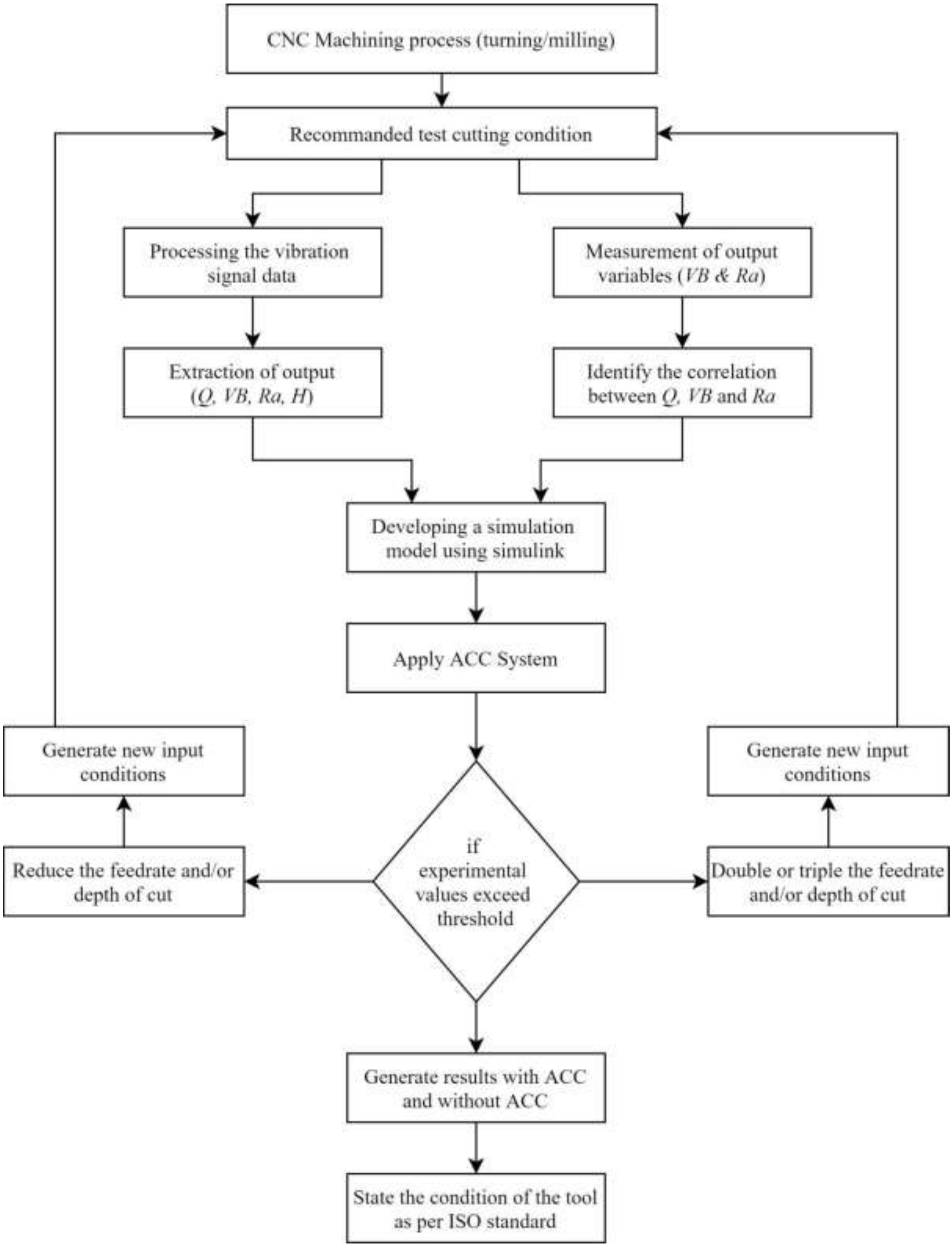

Fig.2.13. Methodology in condition monitoring system with ACC system[49]

2.9. Literature review Summary

Machining vibrations, also called chatter, compare to the overall development between the work-piece and the cutting instrument. The vibrations bring about waves on the machined surface. This influences average machining measures, like turning, processing and penetrating, and abnormal machining measures, like pounding. A chatter mark is a sporadic surface defect avoided by a wheel that is with regards to valid in grinding or standard imprint left when turning a long piece on a machine, due to machining vibrations.

As right on time as 1907, Frederick W. Taylor [50] portrayed machining vibrations as the most dark and fragile of the multitude of issues confronting the mechanic, a perception actually obvious today, as demonstrated in numerous distributions on machining. The clarification of the machine device regenerative chatter was made by S. A. Tobias [51] also, W. Fishwick in 1958 [51], by displaying the input circle between the metal cutting cycle and the machine device structure, and accompanied the strength projections chart. The design firmness, damping proportion and the machining cycle damping factor, are the principle boundaries that characterizes the breaking point where the machining interaction vibration is inclined to develop with time [17]. The numerical models make it conceivable to reproduce machining vibration precisely; yet practically speaking it is consistently hard to keep away from vibrations [29].

The utilization of high-speed machining (HSM) has empowered an increment in profitability and the acknowledgment of work-pieces that were inconceivable previously, like flimsy walled parts [43]. Tragically, machine focuses are less robust a result of the great powerful developments. In numerous applications, for example long instruments, meager work-pieces, the presence of vibrations is the most restricting element and urges the engineer to decrease cutting velocities and feeds well underneath the limits of machines or devices [32].

Vibration issues by and large outcome in commotion, awful surface quality and in some cases device breakage [28]. The fundamental sources are of two sorts: constrained vibrations and self-created vibrations. Constrained vibrations are mostly created by intruded on cutting (innate to processing), run-out, or vibrations from outside the machine. Self-created vibrations are identified with the way that the real chip thickness relies likewise upon the overall situation among instrument and work-piece during the past tooth section [27]. In this way expanding vibrations may show up to levels which can truly corrupt the machined surface quality.

The standard strategy for setting up a machining interaction is still basically dependent on chronicled specialized skill and on experimentation technique to decide the best boundaries [25]. As per the specific abilities of an organization, different boundaries are concentrated in need, like profundity of cut, device way, work-piece set-up, and mathematical meaning of the instrument [9]. At the point when a vibration issue happens, data is typically looked for from the instrument producer or the CAM (Computer-helped fabricating) programming retailer, and they may give a superior technique for machining the work-piece [21]. Now and again, when vibration issues are an over the top monetary bias, specialists can be called upon to recommend, after estimation and computation, axle velocities or instrument changes [45].

Contrasted with the mechanical stakes, business arrangements are uncommon. To examine the issues and to propose arrangements, just couple of specialists proposes their administrations [34]. Computational programming for solidness projections and estimation gadgets are proposed however, notwithstanding boundless exposure, they remain generally infrequently utilized [31]. Ultimately, vibration sensors are frequently incorporated into machining focuses however they are utilized mostly for wear finding of the apparatuses or the axle. New Generation Tool Holders and particularly the Hydraulic Expansion Tool Holders limit the unwanted impacts of vibration generally [30]. As a matter of first importance, the exact control of absolute pointer perusing to fewer than 3 micrometers decreases vibrations because of adjusted burden on front lines and the little vibration made subsequently is assimilated generally by the oil inside the offices of the Hydraulic Expansion Tool Holder.

From the above literature survey it is observed that vibration during turning operations is required to optimize, detailed gap is mentioned as below.

2.10. Research gaps

It is concluded that vibration during turning operation is a significant issue; it results in increased chatter noise, poor surface smoothness, increased tool wear, and occasionally damage to the tool or workpiece. The following research need was identified during the literature review:

1. Most of the researchers have focused the vibration problem solution by using mathematical techniques, very less touch found that focused directly on the issues of three axis vibration through experimentation.

2. Most of the researchers considered single parameter effect to optimize vibration, combine effect of multiple parameter for tool vibration optimization through experimental investigation is not considered.

3. No work found which suggest corrective actions to alter parameters to minimize cutting tool vibration by predictive experimental model.

4. Most of the research works focus on the analysis of the vibration by simplifying in beam, therefore, the real analysis has not been analyzed.

2.11. Objectives of the research

The purpose of this work is to evaluate the performance of cutting tools in terms of vibration and structural evaluations, as well as experimental validations. Depending on the problem definition and research gap, the following objectives can be directed at improving the performance of the considered system.

1. To identify the viability of measurement dynamic vibration of the cuttings tool in three axis during turning process.
2. To determine optimum parametric combination for experimental work which affect cutting tool vibration in turning operation.
3. To analyze the tool vibration during experimental investigation based on identified parameters.
4. To validate the results and suggest the corrective actions to implement adaptive control.

2.12. Research Methodology

The procedure of research comprises of several steps and collection of data through experimental investigation is required. The steps involved in the methodology are as follows

1. Study the mathematical formulation of Beam theory.
2. Develop the setup for measurement of three axis cutting tool vibration.
3. Check the feasibility for vibration measurement through conduction of pilot experiment.
4. Input parameter and range of parameter selection for tool vibration study.
5. Apply Taguchi (L-16) for experimentation parameter value selection.
6. Analysis of variance to find optimum machining parameters.

7. Root Mean Square of all three direction cutting tool vibration for resultant effect.
8. Regression analysis of available result for prediction of cutting tool vibration in selected range.
9. Prediction graphs for suggested adaptive control algorithm.
10. Adaptive control algorithm for obtaining optimum parameters which result minimization of cutting tool vibration.
11. Validation of results by comparing regression results with experimentation results.

2.13. Scope and original contribution of the present work

Vibrations transmitted through cutting tools during machining operations on lathes or CNC machines are a major source of worry for manufacturers. These vibrations can give adverse effect in machining output. The current research employs experiments to find out the cutting tool vibration in all directions. Root Mean Square of all three direction cutting tool vibration for resultant effect is considered. A regression methodology to develop the relationship between dependent variable and predicator. Adaptive control approaches to determine the optimal cutting parameters for decreasing cutting tool vibrations. This exhaustive examination of turning processes on lathe machines with the goal of minimizing tool vibrations is a distinctive and unique contribution of the current work.

2.14. Summary

This investigation explores the various approaches to resolving the complex model of turning activities. Recurrence Response Analysis, Transient Response Analysis, and the Runge-Kutta Approach are the methodologies utilized for jabber examination/mathematical mix strategies in vibration investigation. Approval of the exploratory model research, which is also conducted prior to reaching resolutions, may be used to select a satisfying cycle.

The problem definition was established and objectives were created based on the extensive literature review with the goal of resolving the present existing problem. This chapter presents the problem definition and expressed objectives along with research methodology. Further study has been undertaken in accordance with the aims.

3. CUTTING TOOL PERFORMANCE ASSESSMENT FOR CUTTING TOOL VIBRATION

3.1. Preamble

The purpose of this chapter is to examine the performance assessment of the cutting tool for tool vibration study. The mathematical modeling of the vibrations and stresses produced during cutting operations using the concept of lateral beam vibrations. The analysis's boundary conditions are analogous to the simply supported and fixed (clamped) end analogies for various tool operating modes. This chapter describes the experimental technique used to determine tool performance over a range of cutting parameter configurations and to validate theoretical findings. This chapter also describes the design, fabrication, and integration of the experimental equipment needed to validate the structural and analytical observations. Additionally, this chapter explains the procedures followed throughout the experiment and the tools used to capture the parameters. Finally, the experimental and analytical data are compared.

3.2. Mathematical Modeling for system parameters

The purpose of this chapter is to develop and examine the mathematical modeling of the vibrations and stresses produced during cutting operations using the concept of lateral beam vibrations. The analysis's boundary conditions are analogous to the simply supported and fixed (clamped) end analogies for various tool operating modes.

$$V_C = \frac{\pi D n}{1000} \tag{1}$$

Where V_C is cutting speed (m/min), D is the work-piece diameter (mm) and n is the main axis spindle speed RPM.

$$T_C = \frac{l}{l_C} \quad (2)$$

Where T_C is cutting time (min), l is the length of work-piece (mm) and l_C is cutting length per minute (mm/min).

$$h = \frac{f^2}{8 \cdot RE} \times 1000 \quad (3)$$

Where h is finished surface roughness (micron), f is the feed per revolution (mm/rev) and RE is insert corner radius (taken as 0.8 mm).

$$Q = V_C \times d_C \times f_n \quad (4)$$

Where, V_C is cutting speed (mm/min), d_C is depth of cut (mm) and f_n is feed rate per revolution (mm).

$$P_C = \frac{ap \cdot f \cdot V_C \cdot K_C}{60 \times 1000 \times \eta} \quad (5)$$

Where, P_C is the actual cutting power (kW), d_C is depth of cut (mm), f is feed per revolution (mm/rev), K_C is specific cutting force and η is machine coefficient.

Table 3.1 The values of specific cutting force for different work materials

(obtained from Keyence Corporation (https://www.keyence.com/ss/products/measure-sys/machining/formula/cutting.jsp)

Work Material	**Tensile Strength (*MPa*) or Stiffness**	**Specific Cutting Force (K_C) (*MPa*)**				
		0.1 (*mm/rev*)	**0.2 (*mm/rev*)**	**0.3 (*mm/rev*)**	**0.4 (*mm/rev*)**	**0.6 (*mm/rev*)**
Mild steel (SS400, S10C, etc.)	520	3610	3100	2720	2500	2280
Medium steel (S45C, S50C, etc.)	620	3080	2700	2570	2450	2300
Hard steel (S55C, S58C, etc.)	720	4050	3600	3250	2950	2640

Tool steel (Carbon tool steel (SK), etc.)	670	3040	2800	2630	2500	2400
Tool steel (Alloy tool steel (SKS), etc.)	770	3150	2850	2620	2450	2340
Chrome-manganese steel (Manganese carbide (MnC), etc.)	770	3830	3250	2900	2650	2400
Chrome-manganese steel (Manganese carbide (MnC), etc.)	630	4510	3900	3240	2900	2630
Chrome molybdenum steel (SCM grades, etc.)	730	4500	3900	3400	3150	2850
Chrome molybdenum steel (SCM grades, etc.)	600	3610	3200	2880	2700	2500
Nickel chrome molybdenum steel (SNCM415, etc.)	900	3070	2650	2350	2200	1980
Nickel chrome molybdenum steel (SNCM439, etc.)	352HB	3310	2900	2580	2400	2200
Hard cast iron	46HRC	3190	2800	2600	2450	2270
Meehanite cast iron (FC350, etc.)	360	2300	1930	1730	1600	1450
Gray cast iron (FC250, etc.)	200HB	2110	1800	1600	1400	1330

The above table 3.1 helps the find out the cutting power for the different materials from the value of the cutting force at the different feed.

3.3. Rotating Beam Moving Loads with Regenerative Chatter

The cutting tool's performance during turning operations is determined by the material's strength, structural design, and attachment configuration[33]. The structural strength of the tool varies along its length for various configurations such as simply supported and fixed (clamped) end [34]. The present study used numerical simulation techniques to conduct a structural analysis of a cutting tool in two distinct conditions: simply supported and fixed-end configurations. The analysis demonstrates that under simply supported conditions, stress distributions from minimum to maximum variations occur periodically along the length of the tool; whereas, under fixed/clamped conditions, the maximum value occurs at the end of the tool other than the clamped end, along with distributions of minimum to mid-range values along the length of the cutting tool [19].

Tool vibration is a broad phrase that refers to the intermittent nature of the general uprooting between apparatus and workpiece when the source of the vibration is not readily apparent or perceptible [17]. A certain level of relative vibration between the apparatus and the workpiece is unavoidably experienced, eroding the surface quality and profile of the workpiece on a microscopic level [18]. Due to the detrimental effect of vibration on surface age, scientists have considered the point speculatively and hypothetically [20].

Vibration plays a key role in determining the surface age of machining [8]. A thorough analysis of vibration characteristics and their effect on surface aging has been conducted. Certain types of vibration have been perceived, including apparatus tip vibration and material-induced vibration, referred to as latent vibration [21]. Additionally, vibration applications have made significant advancements, such as rapid apparatus servos/moderate device servos and supersonic vibration, dubbed dynamic vibration [22]. Regardless, online estimation for vibration ID, vibration tool, prattle vibration, and vibration birthplaces has not been thoroughly investigated [23]. Essentially, dynamic vibration can be used to enhance the nano-metric surface quality degraded by inactive vibration [24].

A solid model isn't characterized as a period changing measure, yet rather as one in which the state of the cycle at last to is subject to the advancement of the state of the connection over the interval of time [0, t_0]. Furthermore, it is used to convey and show the structure's conduct over the long haul [25]. Another mathematical model for turning metal workpiece is created in this examination by joining thoughts from two huge social affairs of trained professionals: basic dynamists and gathering engineers [26]. This model considers the workpiece as a versatile workpiece and the cutting device as a versatile cutting gadget with regenerative chatter impacts. Already, most of examinations concerning dynamic models of turning action accepted the workpiece was unbendable and subsequently disregarded work-piece twisting [27]. The workpiece, at last, goes through mutilation because of an outer power applied by the cutting mechanical assembly [28]. This affects and changes the chip thickness [29]. There are no incredible models that have been found already that treat the workpiece and cutting mechanical assemblies as versatile, thus this examination is important [30]. The subtleties of fostering the mathematical itemizing of this stand-out model are altogether considered and examined beneath [31].

The turned workpiece is portrayed as a roundabout pillar that is exposed to three bearings of power along the x-hub and pivots along its longitudinal hub x. The disfigurements made in the y and z tomahawks by the moving cutting powers during turning are signified by v and w. The three directional moving cutting powers follow up on the shaft's surface and have been meant the bar's unbiased hub.

3.3.1. Lateral Vibration of Beams

Consider the free-body graph of a component of a pillar, where *M(x, t)* is the bowing second, *V(x, t)* is the cutting power, and *f(x, t)* is the outside power per unit length of the bar. Since the idleness power following up on the component of the shaft is the power condition of movement in the z heading gives [32],

$$\rho A(x)dx\frac{\partial^2 w}{\partial t^2}(x,t) \tag{6}$$

$$-(V+dV)+f(x,t)dx + V = \rho A(x)dx\,\frac{\partial^2 w}{\partial t^2}(x,t) \tag{7}$$

Where ρ is the mass density and *A(x)* is the cross-sectional area of the beam. The moment equation of motion about the *y*-axis passing through point *O* leads to *A* beam in bending.

$$(M+dM) - (V + dV)dx + f\,(x,t)\ dx\frac{dx}{2} - M = 0$$

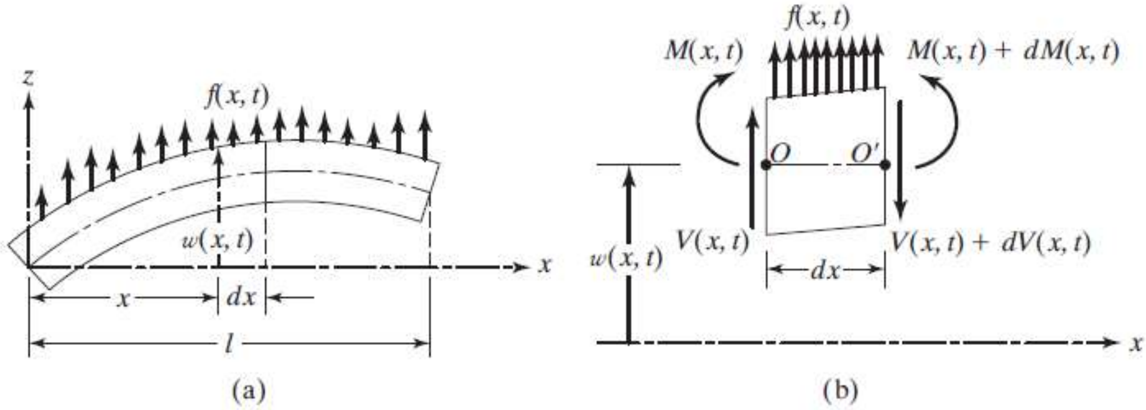

Fig.3.1. Lateral vibrations of beam

By writing,

$$dV = \frac{\partial V}{\partial x}\,dx \quad and \quad dM = \frac{\partial M}{\partial x}\,dx$$

and disregarding terms involving second powers in *dx*,

$$-\frac{\partial V}{\partial x}(x,t) + f(x,t) == \rho A(x)dx\,\frac{\partial^2 w}{\partial t^2}(x,t)$$

(8)

$$\frac{\partial M}{\partial x}(x,t) - V(x,t) = 0$$

(9)

By using the relation, V= *∂M/∂x*

$$\frac{\partial^2 M}{\partial^2 x}(x,t) + f(x,t) = \rho A(x)\frac{\partial^2 w}{\partial t^2}(x,t)$$

(10)

From the elementary theory of bending of beams (also known as the Euler-Bernoulli or thin beam theory), the relationship between bending moment and deflection can be expressed as,

$$M(x,t) = EI(x)\frac{\partial^2 w}{\partial t^2}(x,t)$$

(11)

Where, *E*is Young's modulus and *I*(*x*) is the moment of inertia of the beam cross-section about the *y*-axis. The equation of motion for the forced lateral vibration of a non-uniform beam can be obtained as:

$$\frac{\partial^2}{\partial^2 x}\left[EI\,(x)\frac{\partial^2 w}{\partial t^2}(x,t)\right] + \rho A(x)\frac{\partial^2 w}{\partial t^2}(x,t) = f\,(x,t)$$

(12)

For a uniform beam,

$$EI\frac{\partial^4 w}{\partial x^4}(x,t) + \rho A(x)\frac{\partial^2 w}{\partial t^2}(x,t) = f\,(x,t)$$

(13)

For free vibration, $(x, t$, and so the equation of motion becomes

$$c^2 \frac{\partial^4 w}{\partial x^4}(x,t) + \frac{\partial^2 w}{\partial t^2}(x,t) = 0$$

(14)

where,

$$c = \sqrt{\frac{EI}{\rho A}}$$

3.3.2. Initial Conditions

Since the condition of movement includes a second-request subordinate as for time and a fourth-request subsidiary as for *x*, two beginning conditions and four limit conditions are required for tracking down a remarkable answer for *w(x,t)* [52]. Normally, the upsides of parallel dislodging and speed are indicated as $w_0(x)$ and $w_0(x)$ at $t = 0$, with the goal that the underlying conditions become,

$$w(x, t = 0) = w_0(x)$$

$$\frac{\partial w}{\partial t}(x, t = 0) = w_0(x)$$

(15)

3.3.3. Free Vibration

The free-vibration solution can be found using the method of separation of variables as,

$$w(x,t) = W(x)T(t)$$

$$\frac{c^2}{W(x)} \frac{d^4 W(x)}{dx^4} = -\frac{1}{T(t)} \frac{d^2 T(t)}{dt^2} = a = \omega^2$$

(16)

where, $a = \omega^2$ a positive constant. The above expression can be written as following two equations:

$$\frac{d^4W(x)}{dx^4} - \beta^4 W(x) = 0 \qquad \textbf{(17)}$$

$$\frac{d^2W(x)}{d2} + \omega^2 T(t) = 0 \qquad \textbf{(18)}$$

where,

$$\beta^4 = \frac{\omega^2}{c^2} = \frac{\rho A \omega^2}{EI}$$

The solution can be expressed as

$$T(t) = A\ cos\ cos\omega t + B\ sin\ sin\omega t$$

where *A* and *B* are constants that can be found from the initial conditions. For the solution, we assume,

$$W(x) = Ce^{sx}$$

where, *C* and *S* are constants, and derive the auxiliary equation as,

$$s^4 - \beta^4 = 0$$

The roots of this equation are:

$$S_{1,2} = \pm\beta, \qquad S_{3,4} = \pm i\beta$$

Hence, the solution becomes,

$$W(x) = C_1 e^{\beta x} + C_2 e^{-\beta x} + C_3 e^{i\beta x} + C_4 e^{-i\beta x} \qquad \textbf{(19)}$$

where, C_1 , C_2 , C_3 and C_4 are constants. The equation can also be expressed as,

$$W(x) = C_1\ cos\ cos\beta x + C_2\ cos\ cos\beta x + C_3\ cos\ cos\beta x + C_4\ cos\ cos\beta x$$

$$W(x) = C_1\beta x + \cos\cos\beta x) + C_2(\cos\cos\beta x - C_4\cos\cos\beta x) + C_3(\cos\cos\beta x + C_2 \cos\cos\beta x) + C_3(\cos\cos\beta x - C_4\cos\cos\beta x)$$

(20)

where, C_1 , C_2 , C_3 and C_4 in each case, are different constants. The constants C_1, C_2 ,C_3 and C_4 can be found from the boundary conditions. The natural frequencies of the beam are computed as

$$\omega = \beta^2\sqrt{\frac{EI}{\rho A}} = (\beta l^2)\sqrt{\frac{EI}{\rho A l^4}}$$

(21)

The function $W(x)$ is known as the normal mode or characteristic function of the beam and is called the natural frequency of vibration. For any beam, there will be an infinite number of normal modes with one natural frequency associated with each normal mode. The unknown constants C_1 to C_4 and the value of β can be determined from the boundary conditions of the beam as indicated below.

For any beams, there will be an infinite number of normal modes with one natural frequency associated with each normal mode. The other collaborator group from Dalian University of Technology in China has done the modal testing for boundary work-piece in the lathe in order to determine its natural frequencies and mode shapes.

3.3.4. Boundary Conditions

3.3.4.1. Case 1: simply supported

Deflection, $w = 0$ Bending moment = E

Free – Free

$$W_n(x) = C_n[\sin\sin\beta_n x]$$

(22)

$$\beta_1 l = \pi$$

$$\beta_2 l = 2\pi$$

$$\beta_3 l = 3\pi$$

$$\beta_4 l = 4\pi$$

3.3.4.2. Case 2: fixed (clamped) end or Cantilever

Deflection= 0 slope = $\partial w/\partial x = 0$

The frequency equations, the mode shapes (normal functions), and the natural frequencies for beams with common boundary conditions are. We shall now consider some other possible boundary conditions for a beam

$$cos\ cos\beta_n l \ \cdot cos\ cos\beta_n l = 1$$

$$W_n(x) = C_n[sin\ sin\beta_n x - sinh\ sinh\beta_n x - \alpha_n(cos\ cos\beta_n x - cosh\ cosh\beta_n x)]$$

(23)

Where

$$\alpha_n = \left(\frac{\sin\beta_n l + \sinh\beta_n l}{\cos h\beta_n l + \cos\beta_n l}\right)$$

$$\beta_1 l = 3.926602$$

$$\beta_2 l = 7.068583$$

$$\beta_3 l = 10.21017$$

$$\beta_4 l = 13.35176$$

$$\beta l = 0\ for\ rigid\ body\ mode$$

The present study used Numerical techniques for the two distinct conditions: simply supported and fixed-end (cantilever) configurations. it is challenging to build a mathematical model that encompasses all the factors in a system subjected to vibration and is capable of accurately predicting the system's behavior. From the mathematical model, equation of Vc, T_c, Pc, & h help to analysis the experimental output. As a result, we have performed the experiments using this study as a base reference.

3.4. Background for Experimental Investigation.

Machining vibrations casually alluded to as gab, are estimated comparable to the general improvement between the workpiece and the cutting tool. On the machined surface, the vibrations produce waves. This affects both standard machining tasks like turning, handling, and penetrating, just as unpredictable machining activities like beating. A babble mark is an irregular surface blemish brought about by machining vibrations that are kept away from by a wheel when crushing or a standard engraving left when turning a long thing on a machine.

As ahead of schedule as 1907, Frederick W. Taylor [50] described machining vibrations as the riskiest and delicate of the numerous difficulties defying the technician, a view that is as yet clear today, as seen by different machining circulations. S. A. Tobias [51] and W. Fishwick in 1958 [51] explained the machine gadget recovery jabber by displaying the info circle between the metal cutting cycle and the machine gadget structure, which was joined by a strength projections diagram. The plan immovability, damping extent, and machining cycle damping factor are the essential limits that characterize where the machining collaboration vibration starts to happen [17]. Albeit mathematical models give ideal proliferation of machining vibration, it is continually hard to stay away from vibrations by and by [29].

High speed machining has empowered an expansion in productivity and the acknowledgment of already unimaginable workpieces, for example, delicate walled segments [43]. Unfortunately, machine centers are getting less strong because of fast innovative headways. In an assortment of uses, like long tools and little workpieces, the presence of vibrations is the most restricting component, convincing the specialist to decrease cutting speeds and feeds extensively underneath the capacities of machines or gadgets [32].

Vibration issues by and large outcome in commotion, awful surface quality and in some cases device breakage [28]. There are two essential sources: confined vibrations and self-made vibrations. Obliged vibrations are produced for the most part by barged in on cutting (an inborn property of handling), run-out, or vibrations from outside the machine. Self-created vibrations are identified with the way that the genuine chip thickness is likewise subject to the general state of the tool and workpiece during the previous tooth portion [27]. Consequently, developing vibrations may show to levels that fundamentally corrupt the machined surface quality.

The ordinary route for setting up machining cooperation is still intensely dependent on reported particular ability and experimentation to decide the ideal limits [25]. Various limits are fixated in prerequisite dependent on an association's one of a kind abilities, like cut profundity, device way, workpiece arrangement, and numerical significance of the tool [9]. At the point when a vibration issue happens, information is regularly looked for from the tool producer or a CAM (Computer-Assisted Manufacturing) programming merchant, who may recommend the best technique for cutting the workpiece [21]. Periodically, when extreme financial predisposition exists because of vibration concerns, experts might be counseled to advocate hub speeds or tool changes following assessment and calculation [45].

In contrast with mechanical stakes, business plans are generally rare. A couple of experts present their organizations to examine the difficulties and give arrangements [34]. Albeit computational programming for strong projections and assessing devices has been proposed, regardless of their limitless openness, they are frequently underutilized [31]. At last, vibration sensors are commonly incorporated into machining focuses, yet they are for the most part used to distinguish wear on the gear or the hub. The New Generation Tool Holders, especially the Hydraulic Expansion Tool Holders, essentially decrease the antagonistic impacts of vibration [30]. To start, exact administration of the outright pointer looking to under 3 micrometers diminishes vibrations brought about by changed burden on cutting edges, and any resulting vibration is by and largely consumed by the oil inside the workplaces of the Hydraulic Expansion Tool Holder.

According to previous research, vibration during turning operations is a significant issue; it results in increased chatter noise, poor surface smoothness, increased tool wear, and even damage to the tool or workpiece. The following research gap was identified throughout the literature review. Only a few studies have been conducted on vibration in three axes. Very little work has been done to optimize the vibration parameter through experimental methods. Additionally, relatively few literatures provide corrections to parameters based on optimization. Additionally, the majority of the literature concentrates on the study of vibration by simplifying in beam, obviating the need for genuine analysis. Additionally, relatively little study has been conducted from experimental work. Based on the mentioned research gap, the prime objective of the present work is to study the vibration behavior of cutting tool during turning operation under different experimental parameter conditions.

3.5. Methodology for Experimentation

The experimentation process under various parametric conditions is the central component of this study. As a result, the material selection task comes first, followed by the component selection task. Apart from the typical lathe machine setup, the system is comprised of the ADXL335 vibration sensor (accelerometer) and the Arduino UNO software tool [48]. Following the preparation of the experimental setup and execution of the experimentation process, the system elements are identified. The Design of Experiment (DOE) procedure was used to identify dependable system configurations prior to executing the experimentation process under various configurations. DOE is carried out using Taguchi L16 orthogonal array. The experimentation and recording of observations were carried out using the configurations derived by DOE. Based on the observation, different order regression expressions are generated to identify the system performance for diverse combinations of input parameters without conducting experiments. ANOVA (Analysis of variance) is used to find the parametric effect on the Vibration.

3.6. Experimental Setup

The experimental equipment consists of a standard lathe machine supplemented with an ADXL335 vibration sensor and the Arduino UNO software tool for vibration analysis of various equipment combinations [48,53]. Experimental Setups consist of the following components:

- Lathe Machine (Back Geared – 4+4 Speed)
- Single Point Cutting tool (With Carbide Insert)
- Work Samples (EN8 – Max Dia 45mm)
- Vibration Sensor (Accelerometer ADXL335)
- Arduino UNO (ATmega328P)

3.6.1. Components/Equipment used in the experimental setup

3.6.1.1. Lathe Machine

The lathe is a very versatile and important machine to know how to operate. This machine rotates a cylindrical workpiece against a tool that the individual controls. The lathe is considered to be the forefather of all machine tools. While holding and rotating the work on its axis, the cutting tool is advanced along the desired cut line. The lathe is a highly versatile machine tool that is widely utilized in industry. The lather can be used for turning, tapering, form turning, screw cutting, facing, dulling, drilling, spinning, grinding, and polishing operations with the appropriate attachments. Cutting operations are carried out with a cutting tool fed parallel or perpendicular to the work axis. Additionally, the cutting tool may be supplied at an angle relative to the work axis for machining taper and angles. The tailstock does not revolve on a lathe. Rather than that, the spindle that supports the stock revolves. Collets, centers, three-jaw chucks, and other work holding accessories can all be mounted on the spindle. The tailstock can be used to store tools for drilling, threading, reaming, and taper cutting. Additionally, it may support the workpiece end with the aid of a center and can be changed to accommodate a variety of workpiece lengths.

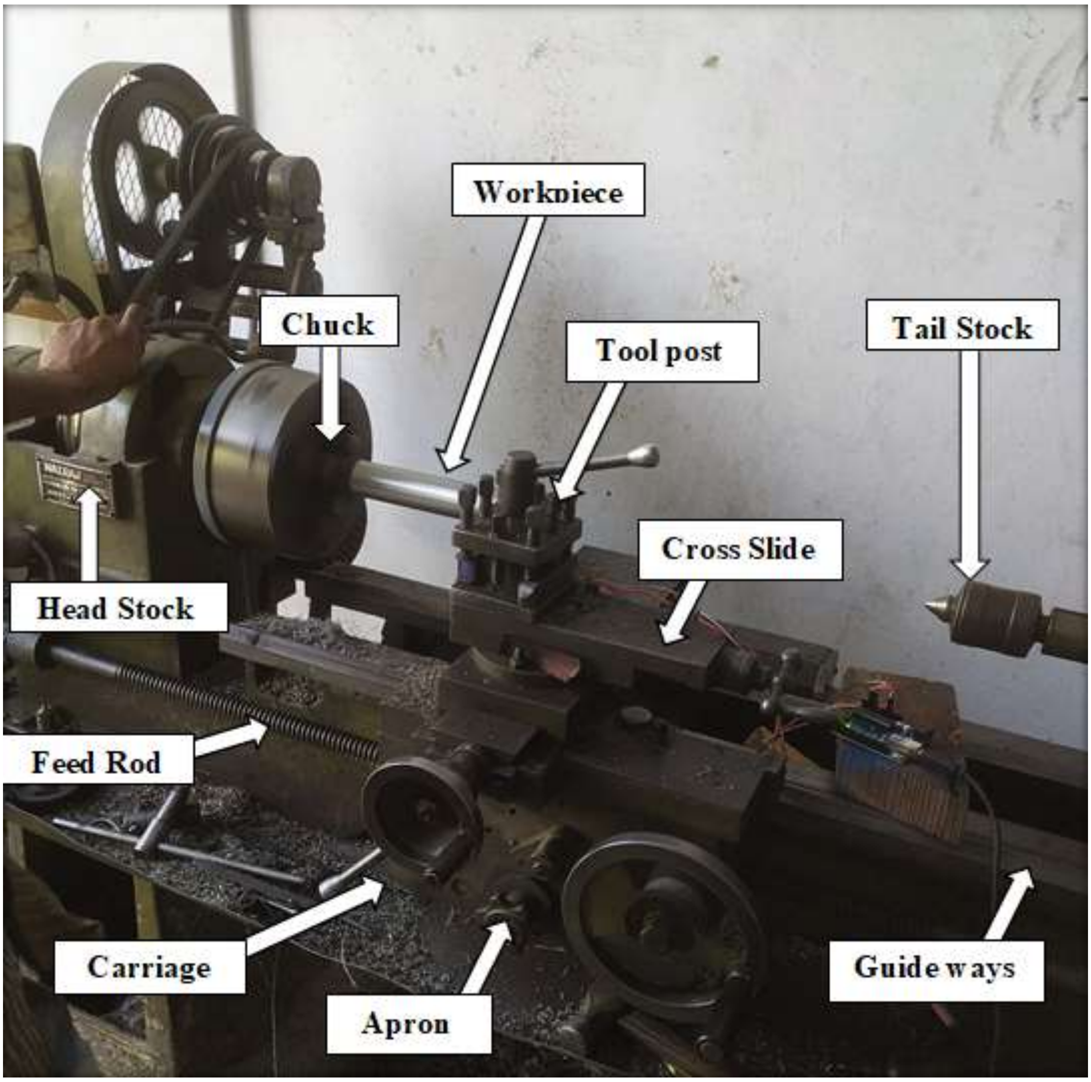

Fig.3.2. Lathe machine used for the experimental study

Table 3.2Technical specifications of lathe machine

Specification of Lathe Machine	
Make	Nataraj
Model	RXZ
Hight of Center	165 *mm*
Length of Bed	1220 *mm*
Width of Bed	238 *mm*
Max. Swing over Bed	350 *mm*
Max. Swing over Carriage	190 *mm*
Spindle Bore	40 *mm*

Spindle Nose	6 *TPI*
Speed 8 (RPM)	45-900 *RPM*
Lead Screw TPI	4 *TPI*
Tail Stock Sleeve	MT-3
Power Required	1.5 *HP*

3.6.1.2. Single Point Cutting tool (With Carbide brazed Insert)

Experiments were conducted using the Carbide tool. Carbide-tipped tools maintain their cutting edge hardness at elevated machining temperatures caused by increased cutting rates and feeds that shorten the machining cycle. Carbide-tipped tools increase surface polish and maintain size far longer, resulting in higher quality. Carbide tools do not require sharpening and have a low learning curve. Carbide tips retain their sharpness longer than HSS tips. To conduct the trials, position the tool holder 30 mm away from the tool holder. The vibration sensor is attached to the tool near the tip, where vibration is greatest. Fig 3.3 shows tungsten-cobalt cemented carbide (*YG6*) cutting tool used in experimentation. Cutting tool and the work-piece mounted on the lathe machine used for the experimental study is illustrated in fig 3.4.

Carbide tools have strong wear resistance, allowing the user to work at higher speeds and for longer periods than tools made of other materials, such as HSS. Carbide tools are more cost-effective than steel tools. Carbide tools are capable of milling Hardened Steel. Cemented Carbide is a recommended tool material for EN8 operations.

Tungsten carbide (WC) and cobalt are the primary components. The grade is denoted by the code YG, followed by the cobalt concentration expressed as a percentage. *YG6* is cemented carbide of tungsten and cobalt having a cobalt content of 6% and a tungsten carbide concentration of 94%.

Fig.3.3. Cutting tool of material: tungsten-cobalt cemented carbide (*YG6*)

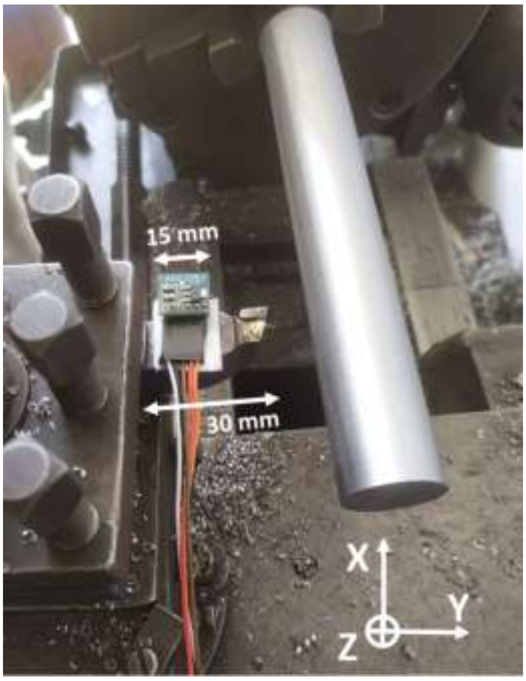

Fig. 3.4. Cutting tool and the work-piece mounted on the lathe machine used for the experimental study

3.6.1.3. Work Samples

EN8 is an unalloyed medium carbon steel that is used in applications where unique features are sought but the costs do not justify the purchase of composites [54]. By applying the appropriate heat treatment, EN8 can be surface toughened while maintaining its reasonable wear obstruction qualities. EN8 is used in automobile components such as roadways, studs, bolts, axles, and general design elements.

For the experiment, EN8 material is selected because EN8 is widely used in industries. EN8 is an unalloyed medium carbon steel which is used in applications where better properties than mild steel. EN8 can be heat treated to provide a good surface hardness and moderate wear resistance by flame or induction hardening processes. From the automotive trade to wider general engineering applications. EN8 used in automotive parts, connecting roads, studs, bolts, axles, spindles, general engineering components etc as shown in table 3.3. Fig 3.5 shows the specimen of work-piece. Table 3.8 and 3.9 describe the chemical composition and mechanical properties of EN8.

Table 3.3 Different applications of EN8 Material

	
general-purpose axles	**Shafts**
	
bolts and studs	**Connecting Rods**
	
Hydraulic Rams	**Automobile Components**

Fig. 3.5. Experimental specimen of work-piece

Table 3.4 EN8 chemical composition

Parameter	Value
Carbon	0.36-0.44%
Silicon	0.10-0.40%
Manganese	0.60-1.00%
Sulphur	0.050 Max
Phosphorus	0.050 Max
Chromium	-
Molybdenum	-
Nickel	-

Table 3.5 EN8 mechanical properties

Parameter	Value
Max Stress	700-850 N/mm^2
Yield Stress	465 N/mm^2 Min
0.2% Proof Stress	450 N/mm^2 Min
Elongation	16% Min
Impact KCV	28 Joules Min
Hardness	201-255 Brinell

3.6.1.4. Vibration Sensor

Vibration sensors are used to measure linear velocity, displacement, and acceleration. Vibration can be expressed in metric units (m/s^2) or units of gravitational constant "g," where **1 g = 9.81 m/s²**. To measure vibration in 3-axis, ADXL335 sensor used shown in fig 3.6. The ADXL335 is a petite, low-power total-three-pivot accelerometer with signal-adapted voltage yields. It evaluates the speed increase using a 3 g full-scale scope as a baseline. This sensor has an accuracy of 0.05 g. It is capable of quantifying the static speed increase caused by gravity in slant detecting applications, as well as the dynamic speed increase caused by movement, stun, or vibration [35].

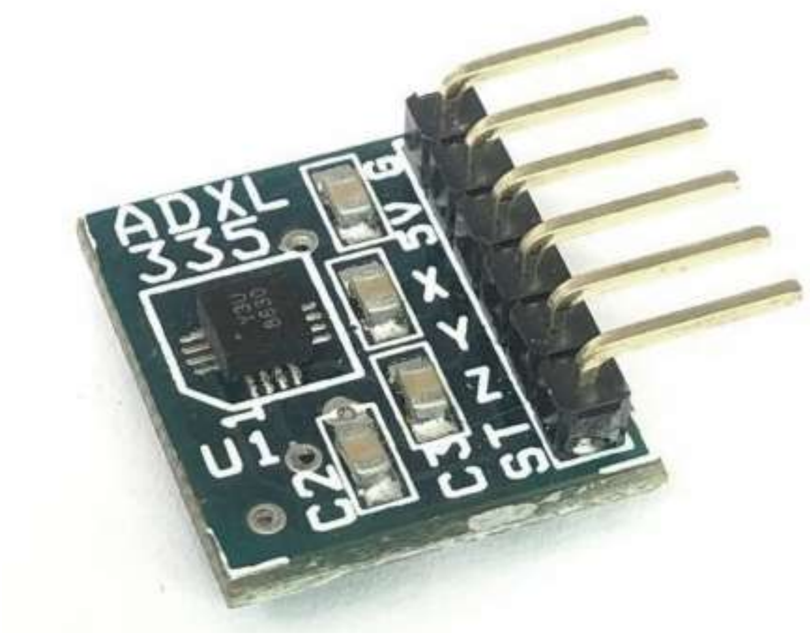

Fig. 3.6 ADXL335 vibration sensor

3.6.1.5. Arduino UNO (ATmega328P)

Arduino is an open-source platform for building devices that is based on simple-to-use hardware and programming. Arduino sheets are capable of deciphering inputs - light from a sensor, a finger on a catch, or a Twitter tweet - and converting them to outputs - actuating an engine, turning on an LED, or distributing something on the web [29]. You may guide your board by sending a series of commands to the board's microcontroller.

Arduino Uno is a board based on the ATmega328P microcontroller (datasheet) [28]. It features 14 advanced data/yield pins (six of which are PWM yields), six simple data sources, a 16 MHz ceramic resonator (CSTCE16M0V53-R0), a USB connection, a force jack, an ICSP header, and a reset button. It includes everything necessary to assist the microcontroller; simply connect it to a PC through USB or force it to start through an AC-to-DC adapter or battery shown in fig 3.7. Perusing is accomplished through Arduino programming. Appendix A1 contains the Arduino UNO code.

Fig. 3.7 Arduino UNO

3.6.2. Experimental Setup

The schematic depiction and the actual photograph of the experimental setup are as shown in the following Figures (Fig 3.8 and fig 3.9).

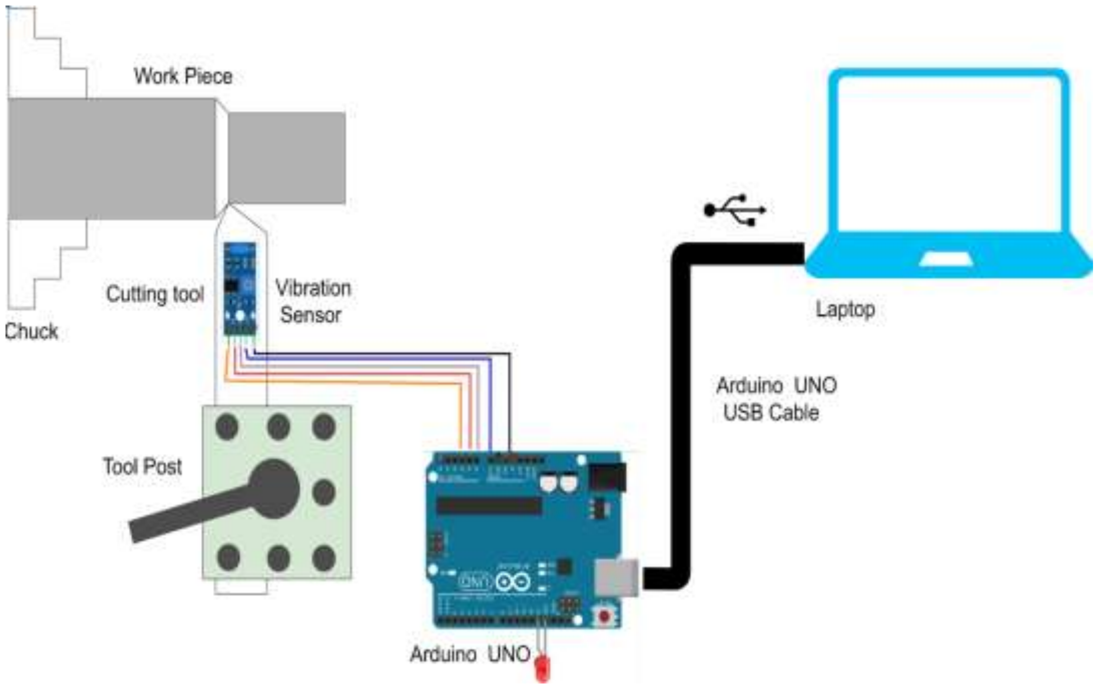

Fig. 3.8. Schematic representation of the experimental setup with Arduino UNO

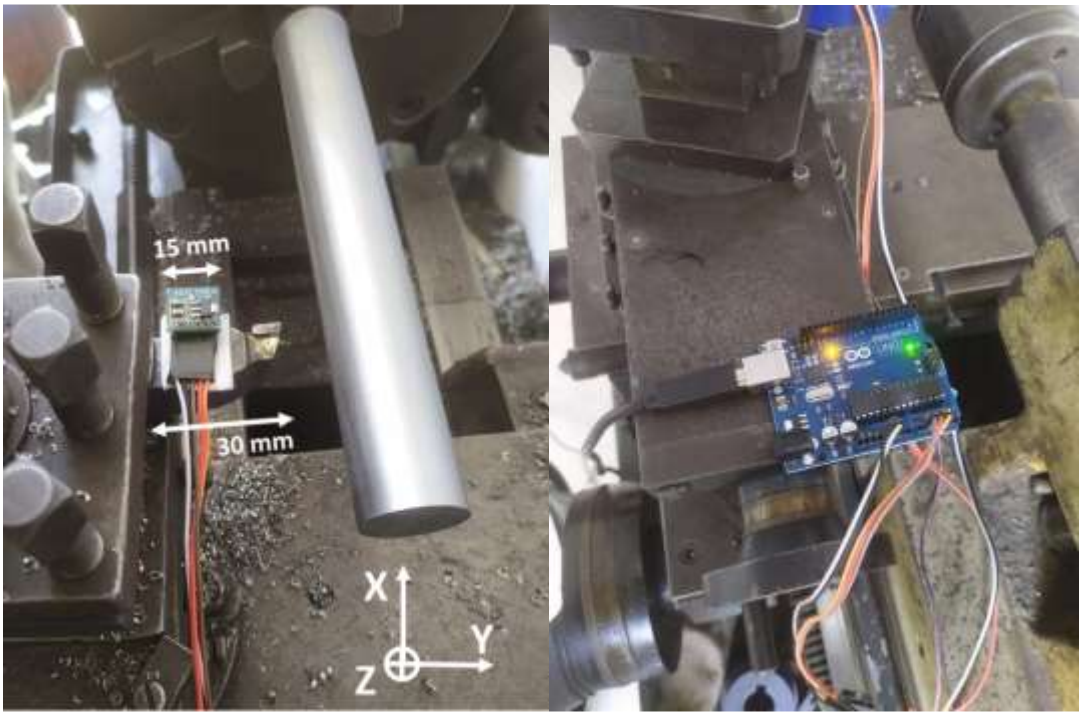

Fig. 3.9. Experimental setup with dimensional depiction

3.7. Selection of Parameters

The factors and levels are chosen in accordance with the findings of the literature review. Four levels were chosen for the studies based on the idea that the greater the number of levels, the more accurate the analysis. The parameter ranges are defined in accordance with previous research, published literature, and available machine capacity, as detailed below.

- **Speed (*N*)** - Selection of Spindle Speed is according to available machine tool speeds (4 Direct Speed is utilized)
- **Feed Rate (*f*)** - According to available automatic feed rate in Machine Tool
- **Depth of Cut (d_c)** - Range of depth of cut is selected from the literature review
- **Workpiece Diameter (*D*)** - Work diameter is considered for general industrial work and literature review.

3.8. Experimentation

Experimentation is the primary method for obtaining trustworthy results and validating data acquired through mathematical modeling and computer simulations [55–58]. A 270 mm long workpiece with varying diameters (as determined by the parameter levels) is used in the tests. Where 70 mm is retained in the chuck and 200 mm is used for experimenting. The turning procedure is performed with a carbide tool. To monitor vibrations at a minimal cost, the ADXL335 vibration sensor and the Arduino UNO are used shown in fig 3.10. Conduct all trials in accordance with the DOE table, with the vibration output directly stored in an excel file.

Carbide-tipped devices maintain their front line hardness at elevated machining temperatures caused by increased cutting speeds and feed that shorten the machining process length [54]. Additionally, carbide-tipped tools improve surface completeness and maintain size for a significantly longer period of time, resulting in higher quality. Carbide tools do not require honing or have a steep learning curve, and carbide tips retain their sharpness longer than high-speed steel tips. As a result, the experiments were conducted using the carbide tool. The tool was held 30 mm away from the tool holder for the testing. The vibration sensor was mounted towards the tip of the tool, where vibrations are greatest. Throughout the experiments, a speed range of 225-800 RPM was maintained.

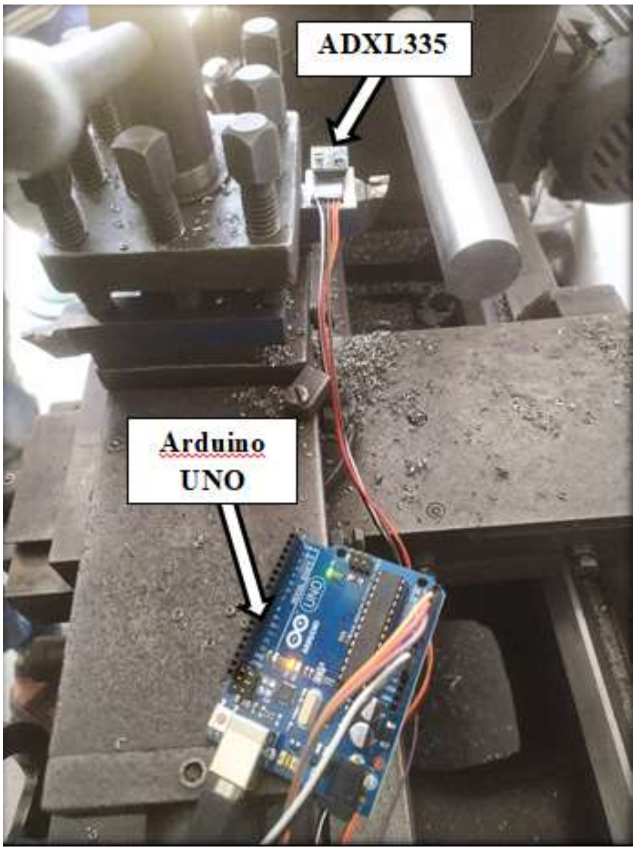

Fig. 3.10 Experimental setup with Arduino UNO and ADXL335

3.8.1. Design of Experiments Introduction

3.8.1.1. DOE

As detailed in the methodology, DOE was used to derive the parameter combinations for the experiment. The study considers the spindle's rotational speed, i.e. the work-piece, the feed rate, the depth of cut (DOC), and the work-piece diameter. With variable ranges of 225-800 RPM, 0.3-0.6 mm/rev, 0.5-1.25 mm, and 20-50 mm. Table 3.6 summarizes the factor levels for the parameter settings.

3.8.1.2. Taguchi

In light of our boundaries and levels, the feasible cluster is the Taguchi technique's L16 symmetrical display (allude to Table 3.9 with regards to the current examination). Dr. Taguchi designed his assessments using an unusual arrangement of symmetrical clusters. Each line addresses a pre-condition with a factor level indicated by the line's number. The ascending part is concerned with the variables identified throughout the inquiry [18].

3.8.1.3. ANOVA (Analysis of Variance)

ANOVA is a collection of quantifiable models and their associated evaluation techniques (for example, the "diversity" within and between groups) that is used to study the distinctions between means. ANOVA can assist in determining whether there are important differences in the methodologies used to calculate your autonomous factors. The combinations of input parameters and their related outputs are listed in Table 3.15. The ideal parameter values discovered from the observations are: N = 350 RPM, f = 0.15mm/rev, d_c = 0.3 mm, and D = 40 mm. Section 3.8 illustrate the complying main effect plot and the SN ratio, respectively. Additionally, Table 3.17 summarizes the percentage impact of each input parameter and illustrates it in Fig. 3.39.

3.8.2. Pilot Experiment

Prior to proceeding with the experiments, a pilot study based on the formulated DOE is for to find out the actual process way of the experimentation. This pilot study data and results are not for any further study. This is just for verification of the path for actual experiments.

The Factor and Levels tables, as well as the experimentation sets for four independent parameters (Table 3.7 – L16 table), are generated (Table 3.6), and the reactions of vibration components recorded during the pilot study are tabulated using the graphical representation. Table 3.8 is Response table pilot study and fig 3.11 is graphical representation of pilot study.

Table 3.6 Factors and levels for DOE

Factors	Levels			
	Level 1	Level 2	Level 3	Level 4
Rotational Speed(*N*)(*RPM*)	225	350	500	800
Feed rate (*f*)(*mm/rev*)	0.3	0.4	0.5	0.6
Depth of cut (d_c)(*mm*)	0.5	0.75	1.0	1.25
Diameter (*D*)(*mm*)	20	30	40	50

Table 3.7 L16 table of the pilot study

Sr. No.	Speed(*N*) (*RPM*)	Feed rate (*f*) (*mm/rev*)	Depth of cut (d_c) (*mm*)	Diameter (*D*) (*mm*)
1	225	0.3	0.50	20
2	225	0.4	0.75	30
3	225	0.5	1.00	40
4	225	0.6	1.25	50
5	350	0.3	0.75	40
6	350	0.4	0.50	50
7	350	0.5	1.25	20
8	350	0.6	1.00	30
9	500	0.3	1.00	50
10	500	0.4	1.25	40
11	500	0.5	0.50	30
12	500	0.6	0.75	20
13	800	0.3	1.25	30
14	800	0.4	1.00	20
15	800	0.5	0.75	50
16	800	0.6	0.50	40

Table 3.8 L16 table of pilot study – Response table

Sr. No.	Vibration (g) in three axis		
	$\Delta X_{max\ g}$	$\Delta Y_{max\ g}$	$\Delta Z_{max\ g}$
1	0.67	2.05	2.8
2	0.55	0.2	0.61
3	1.7	1.21	0.63
4	1.1	0.64	0.39
5	0.50	0.18	0.87
6	0.69	0.80	0.99
7	0.18	0.93	0.64
8	0.65	0.11	1.55
9	1.01	0.34	2.11
10	0.33	0.99	1.06
11	1.77	0.76	0.6
12	0.39	1.17	0.54
13	0.54	1.56	1.05
14	1.30	0.86	1.51
15	0.90	1.36	1.08
16	1.18	2.15	0.34

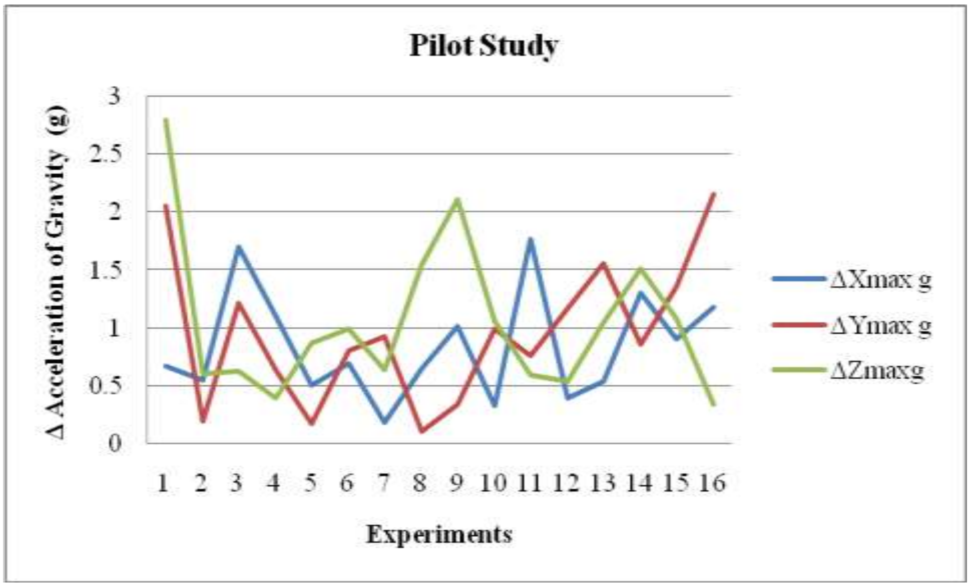

Fig.3.11 Response values of the pilot study

The result consistency of the vibration measurement is found satisfactory by developed setup in all three directions. With the discussed setup we retrieve the vibration results of all three direction at interval of every second which satisfy our first objective.

3.8.3. Final Experimentation (Actual Work)

Based on the study of the pilot process, found out the actual process of the experimentation. This process is further carried out in actual experimentation. The L16 parameter combination table for the final experimentation is prepared consisting of the four earlier explained input parameters (levels are different) and listed as shown in Table 3.9.

Table 3.9 L16 Parameter Combination

Sr. no.	**Speed (*N*) (*RPM*)**	**Feed rate (*f*) (*mm/rev*)**	**Depth of cut (d_c) (*mm*)**	**Diameter (*D*) (*mm*)**
1	225	0.12	0.1	30
2	225	0.13	0.3	35
3	225	0.14	0.5	40
4	225	0.15	0.7	45
5	350	0.12	0.3	40
6	350	0.13	0.1	45
7	350	0.14	0.7	30
8	350	0.15	0.5	35
9	500	0.12	0.5	45
10	500	0.13	0.7	40
11	500	0.14	0.1	35
12	500	0.15	0.3	30
13	800	0.12	0.7	35
14	800	0.13	0.5	30
15	800	0.14	0.3	45
16	800	0.15	0.1	40

The experimental sets of L16 combinations have been performed in segments based on the distance from the free end, e.g. 0-50 mm, 50-100 mm, 100-150 mm, and 150-200 mm; and at last as whole portion i.e. 0-200 mm as shown in fig 3.12. The element discretization is depicted in the following illustration. Which satisfy the second objective.

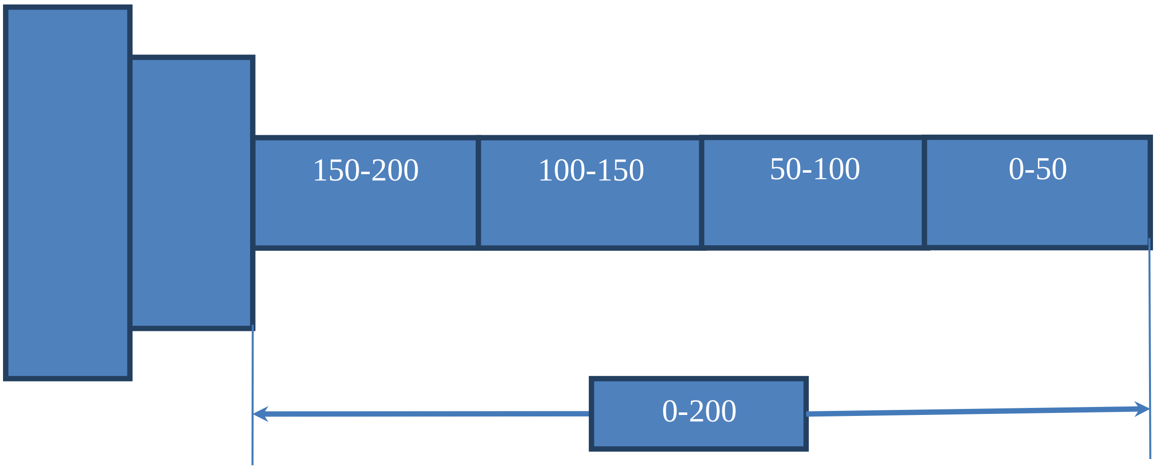

Fig.3.12 Division of workpiece in 4 segments

Prior to proceeding further with the experimentation, the system parameters are computed based on the mathematical model for the experimentation combination prescribed in L16 sets, as given in Table 3.10. Fig 3.13 to fig 3.28 shows the experimental observations for L16 parameter combination.

Table 3.10 Calculated values of the system parameters for the L16 sets of experimentation based on the mathematical model

sr. no	*N (rpm)*	*f (mm/rev)*	*dc (mm)*	*D (mm)*	$\Delta X_{max\ g}$	$\Delta Y_{max\ g}$	$\Delta Z_{max\ g}$	*RMS*	*Vc (m/min)*	P_c *(KW)*	T_c *(min)*	*MRR* (mm^3/min)	*h (μm)*
1	225	0.12	0.1	30	0.58	5.03	3.47	1.863	21.21	0.001749	7.407	0.2545	2.25
2	225	0.13	0.3	35	0.22	0.12	0.41	0.6403	24.74	0.006633	6.838	0.9649	2.641
3	225	0.14	0.5	40	1.18	0.21	0.46	0.6782	28.27	0.01361	6.349	1.979	3.063
4	225	0.15	0.7	45	0.97	0.24	0.31	0.5568	31.81	0.02296	5.926	3.34	3.516
5	350	0.12	0.3	40	0.8	0.18	0.33	0.5745	43.98	0.01089	4.762	1.583	2.25
6	350	0.13	0.1	45	0.65	0.1	0.16	0.4	49.48	0.004422	4.396	0.6432	2.641
7	350	0.14	0.7	30	0.81	0.23	0.31	0.5568	32.99	0.02222	4.082	3.233	3.063
8	350	0.15	0.5	35	0.25	0.16	0.37	0.6083	38.48	0.01984	3.81	2.886	3.516
9	500	0.12	0.5	45	1.31	0.69	1.58	1.257	70.69	0.02916	3.333	4.241	2.25
10	500	0.13	0.7	40	0.63	0.69	0.56	0.7483	62.83	0.03931	3.077	5.718	2.641
11	500	0.14	0.1	35	1.12	0.21	0.36	0.6	54.98	0.005292	2.857	0.7697	3.063
12	500	0.15	0.3	30	0.19	0.17	0.25	0.5	47.12	0.01458	2.667	2.121	3.516
13	800	0.12	0.7	35	1.51	1.21	1.65	1.285	87.96	0.0508	2.083	7.389	2.25
14	800	0.13	0.5	30	0.55	0.66	0.51	0.7141	75.4	0.03369	1.923	4.901	2.641
15	800	0.14	0.3	45	0.6	0.36	0.88	0.9381	113.1	0.03266	1.786	4.75	3.063
16	800	0.15	0.1	40	0.18	0.15	0.23	0.4796	100.5	0.01037	1.667	1.508	3.516

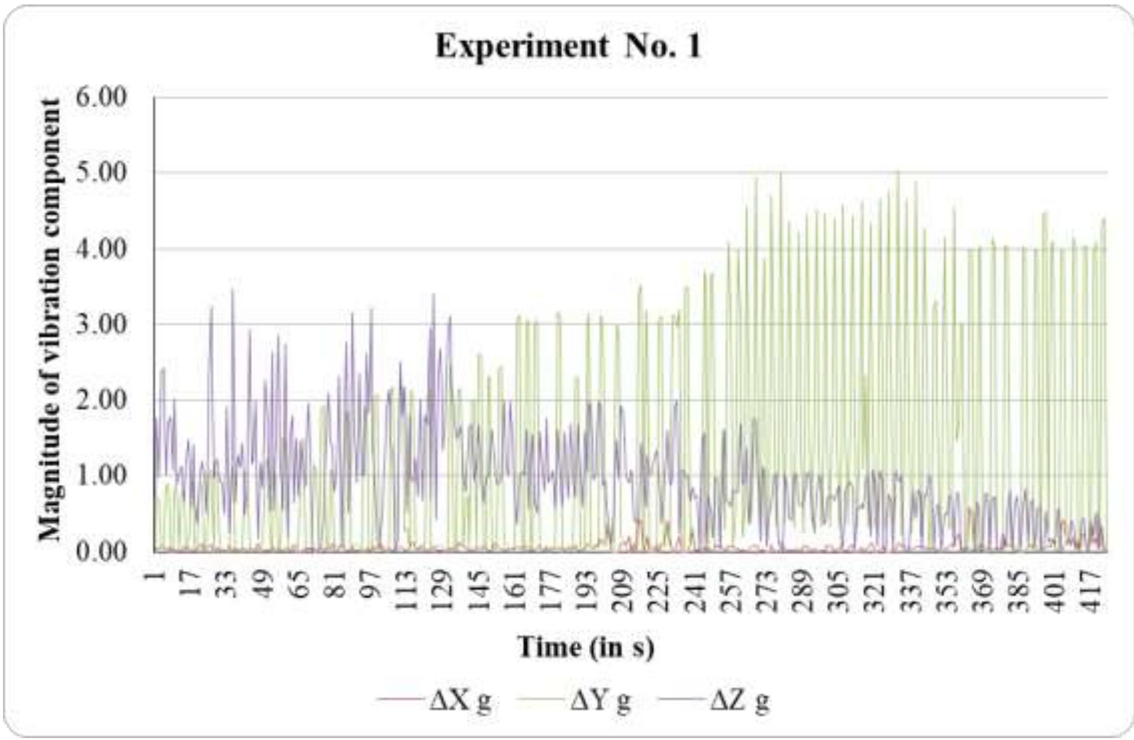

Fig.3.13 Outcome of Experimental set 1

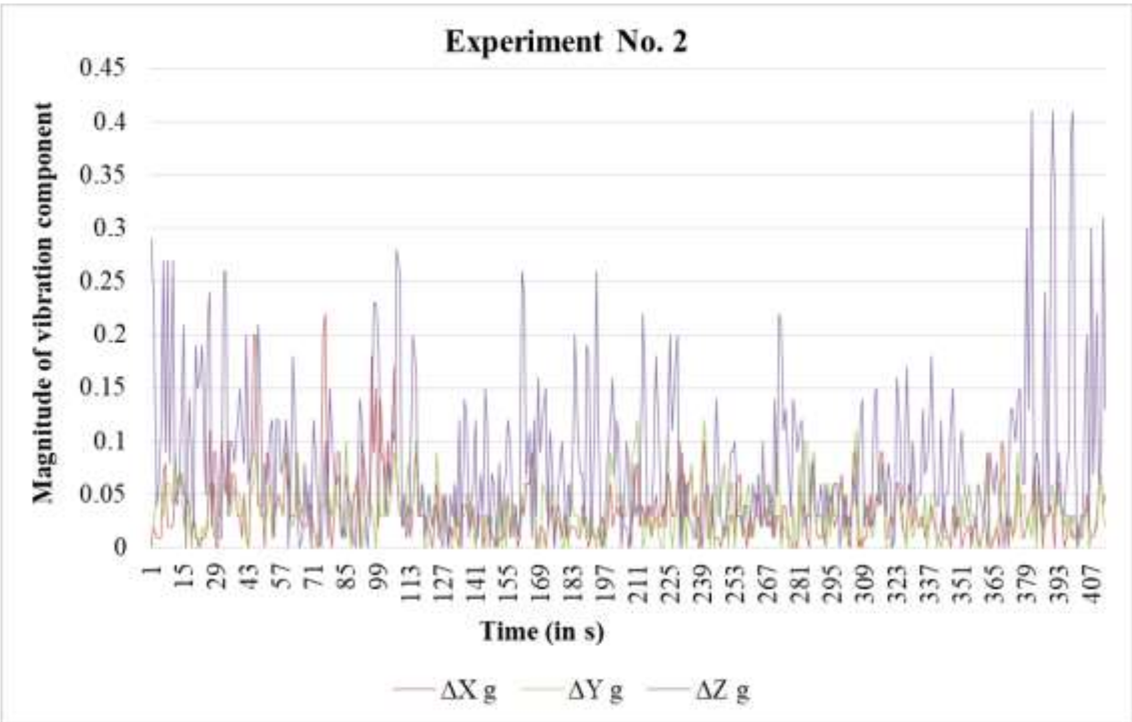

Fig.3.14 Outcome of Experimental set 2

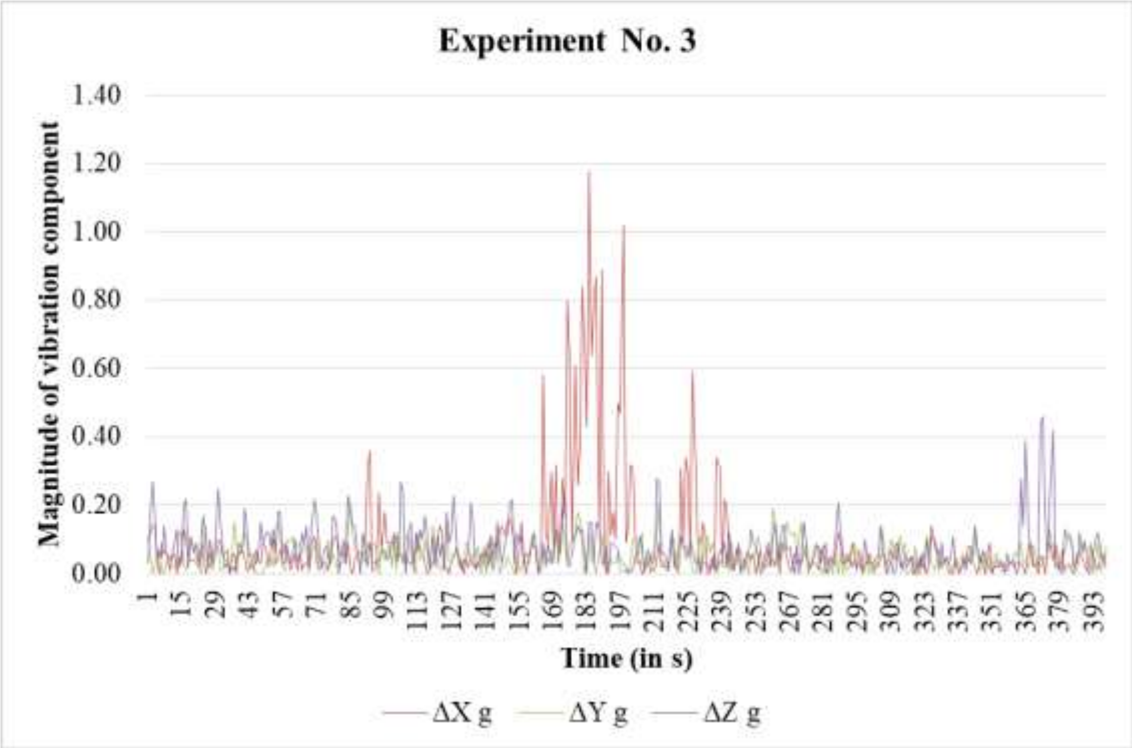

Fig.3.15 Outcome of Experimental set 3

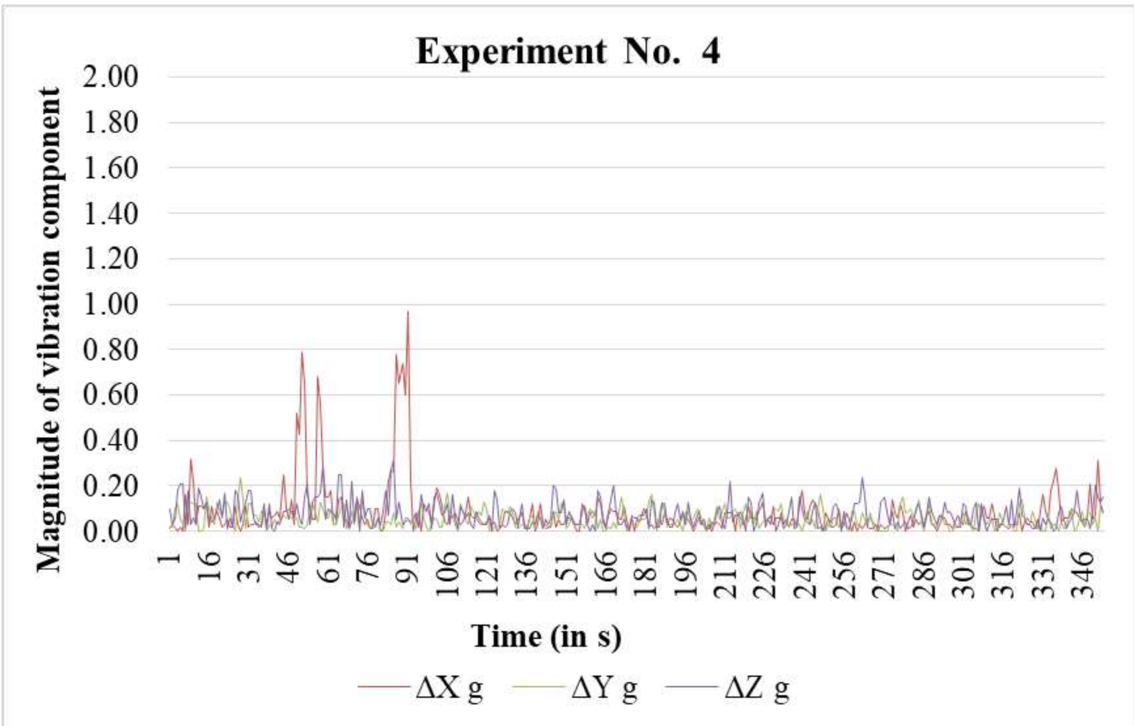

Fig.3.16 Outcome of Experimental set 4

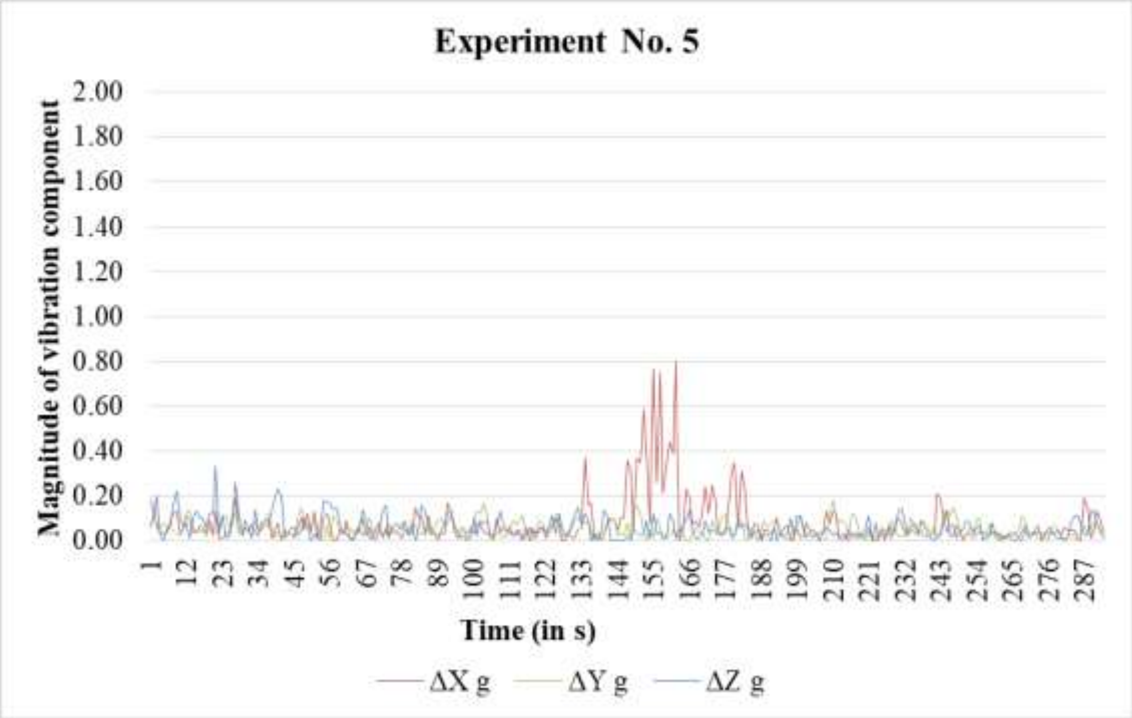

Fig.3.17 Outcome of Experimental set 5

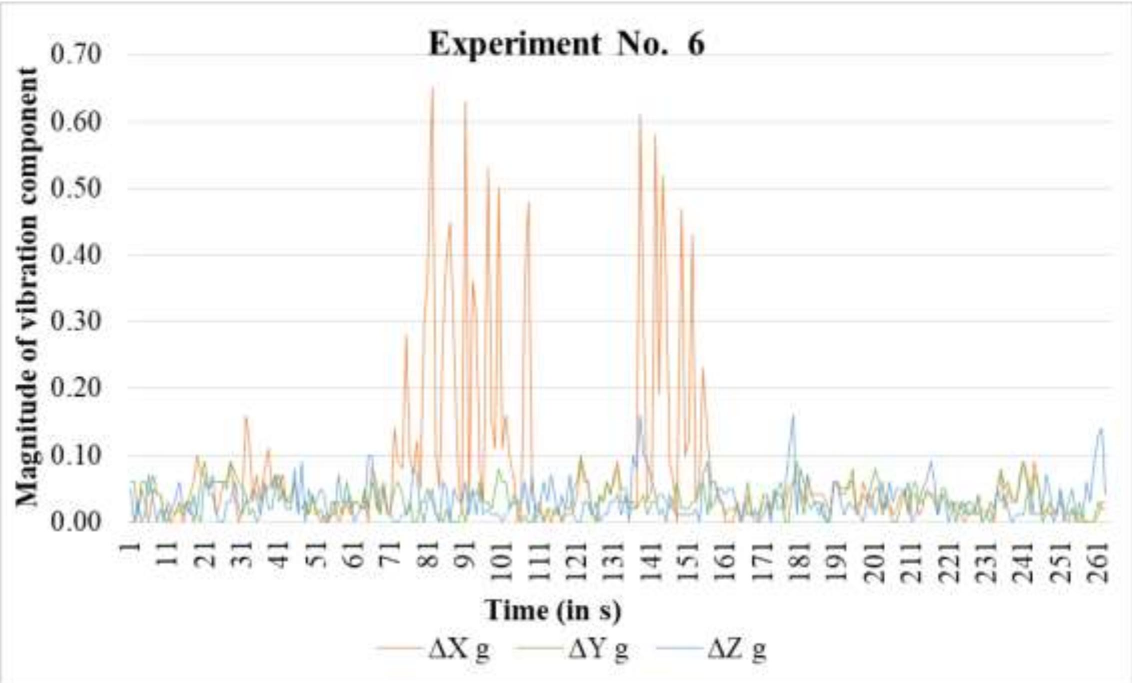

Fig.3.18 Outcome of Experimental set 6

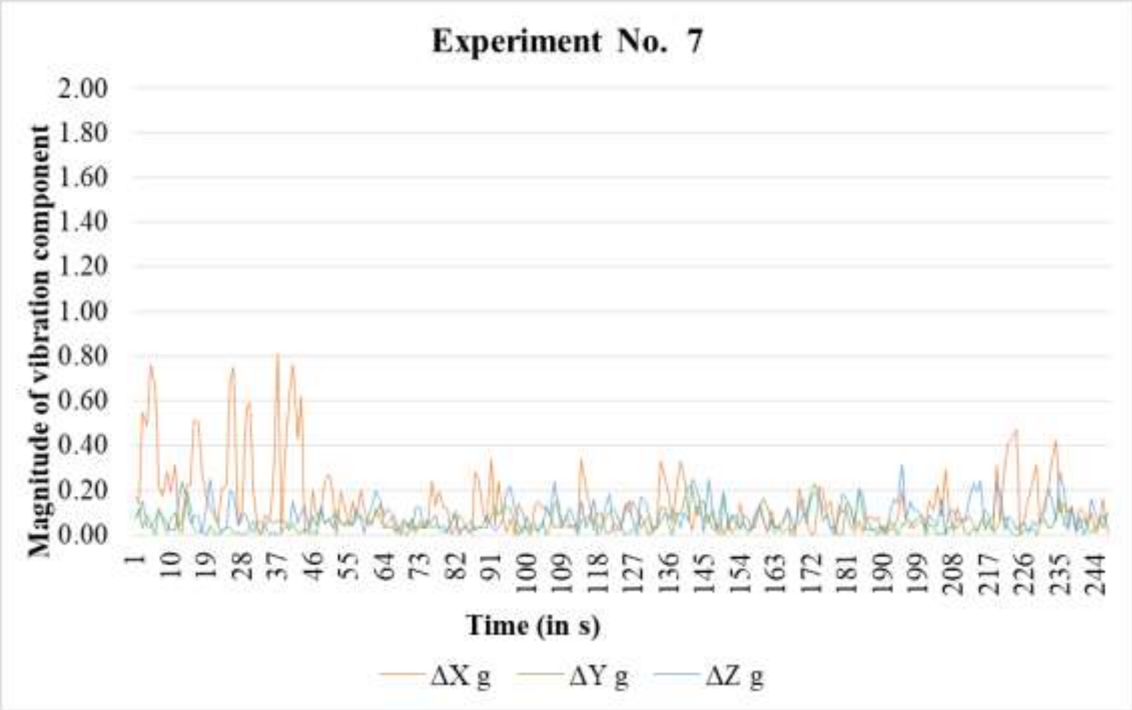

Fig.3.19 Outcome of Experimental set 7

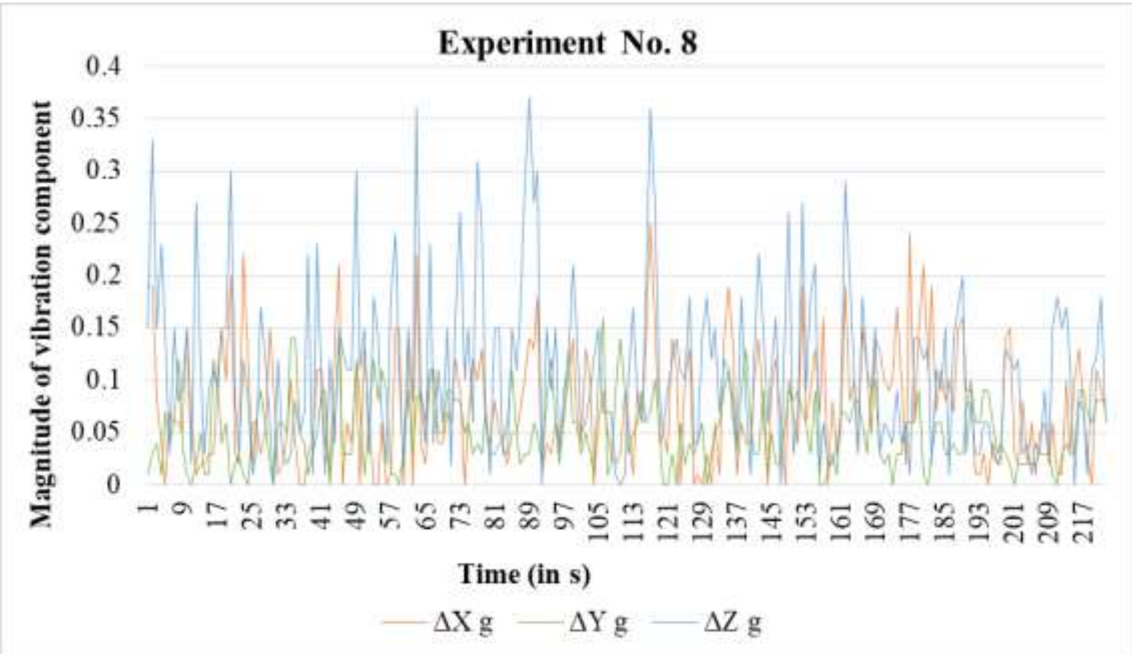

Fig.3.20 Outcome of Experimental set 8

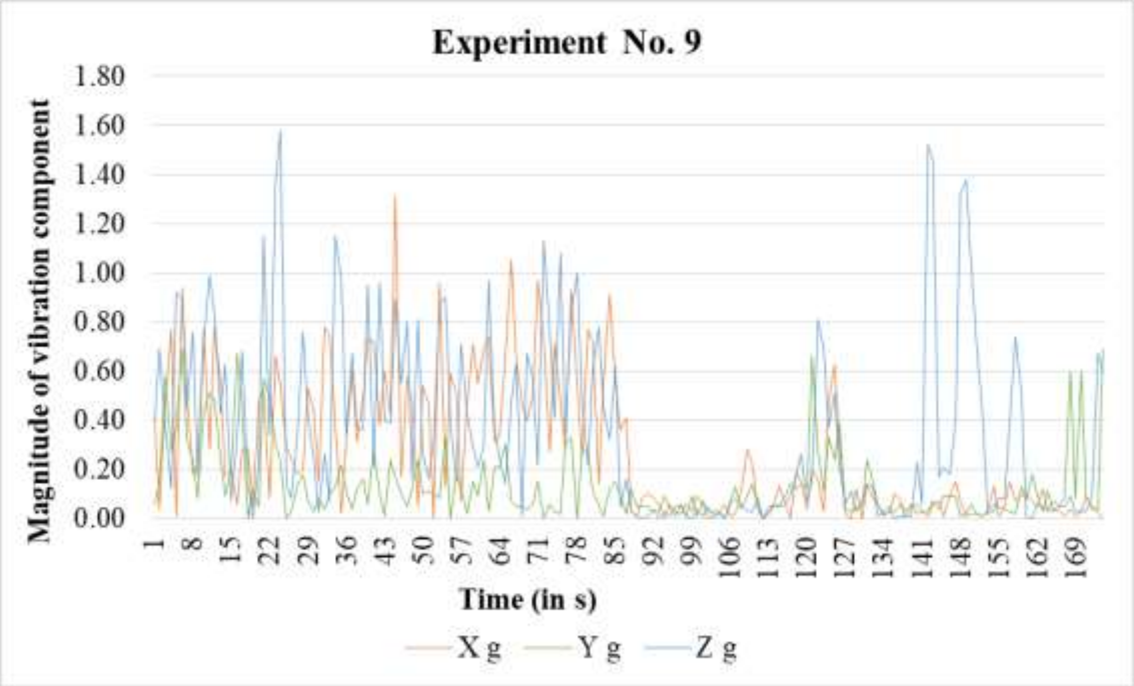

Fig.3.21 Outcome of Experimental set 9

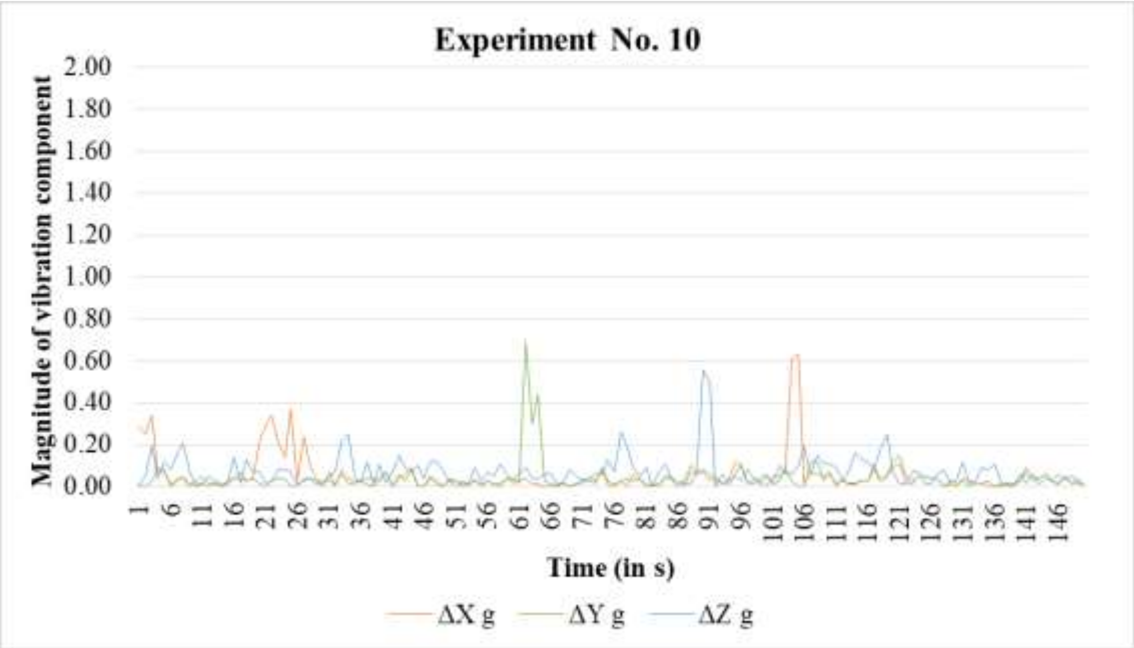

Fig.3.22 Outcome of Experimental set 10

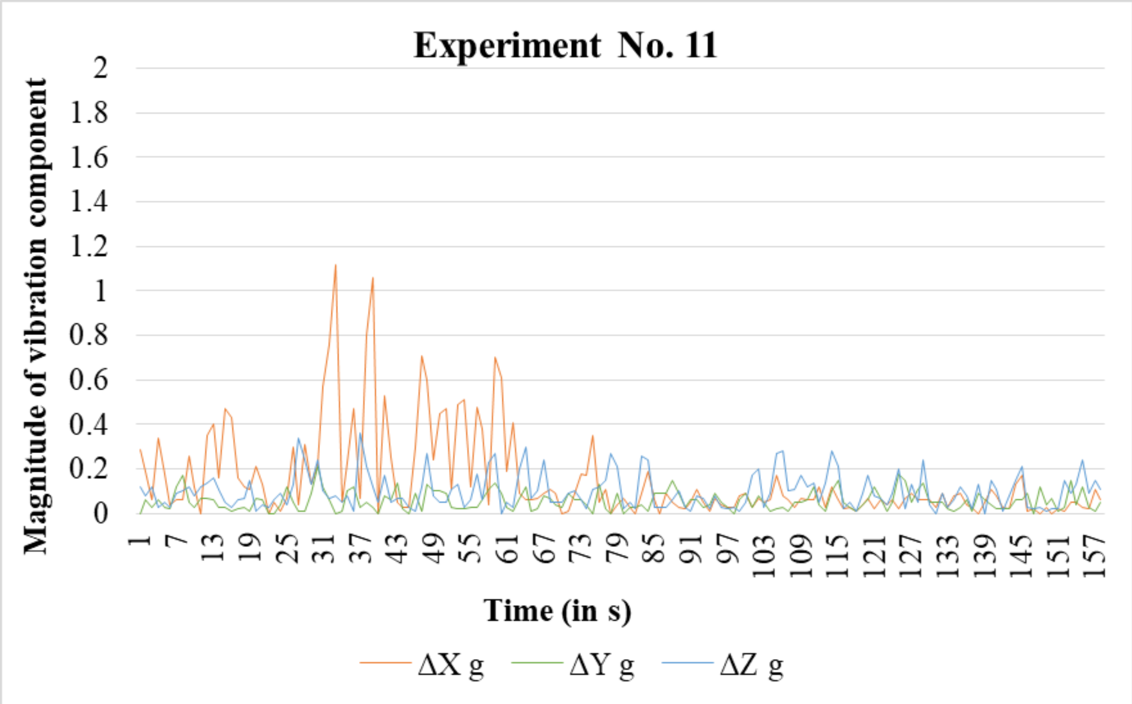

Fig.3.23 Outcome of Experimental set 11

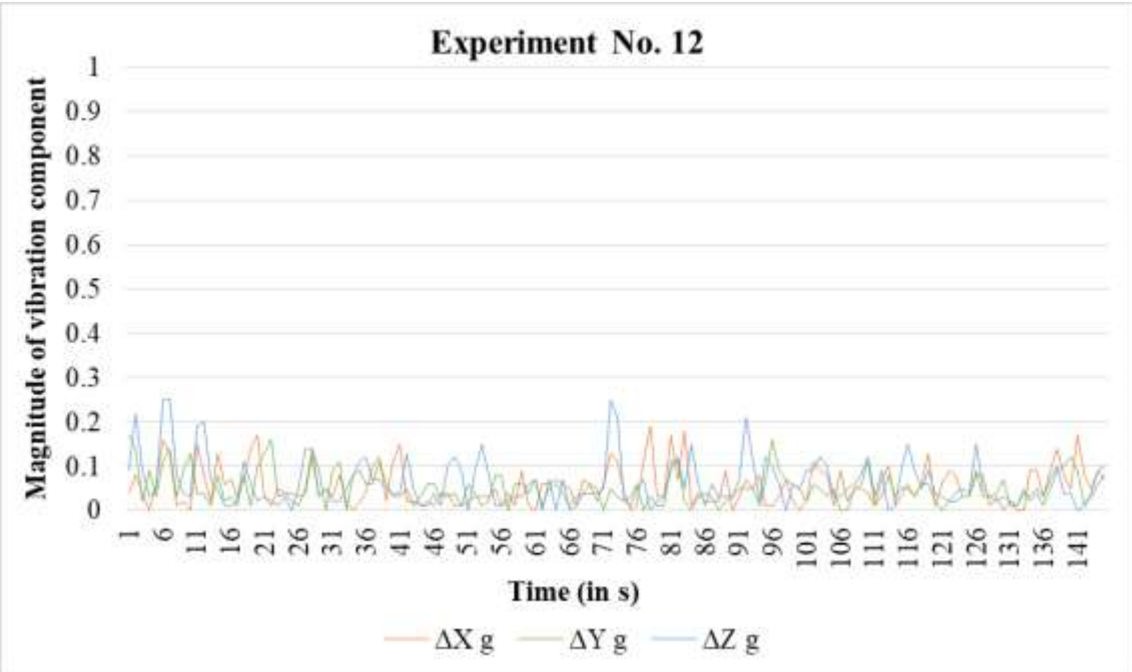

Fig.3.24 Outcome of Experimental set 12

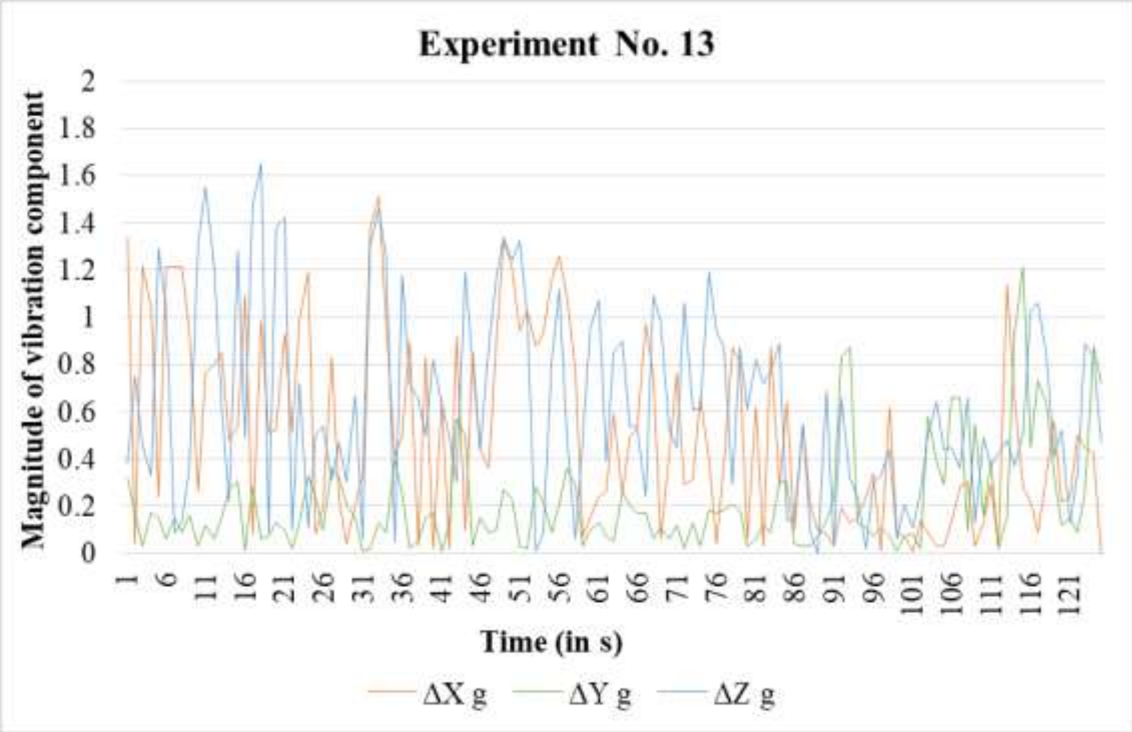

Fig.3.25 Outcome of Experimental set 13

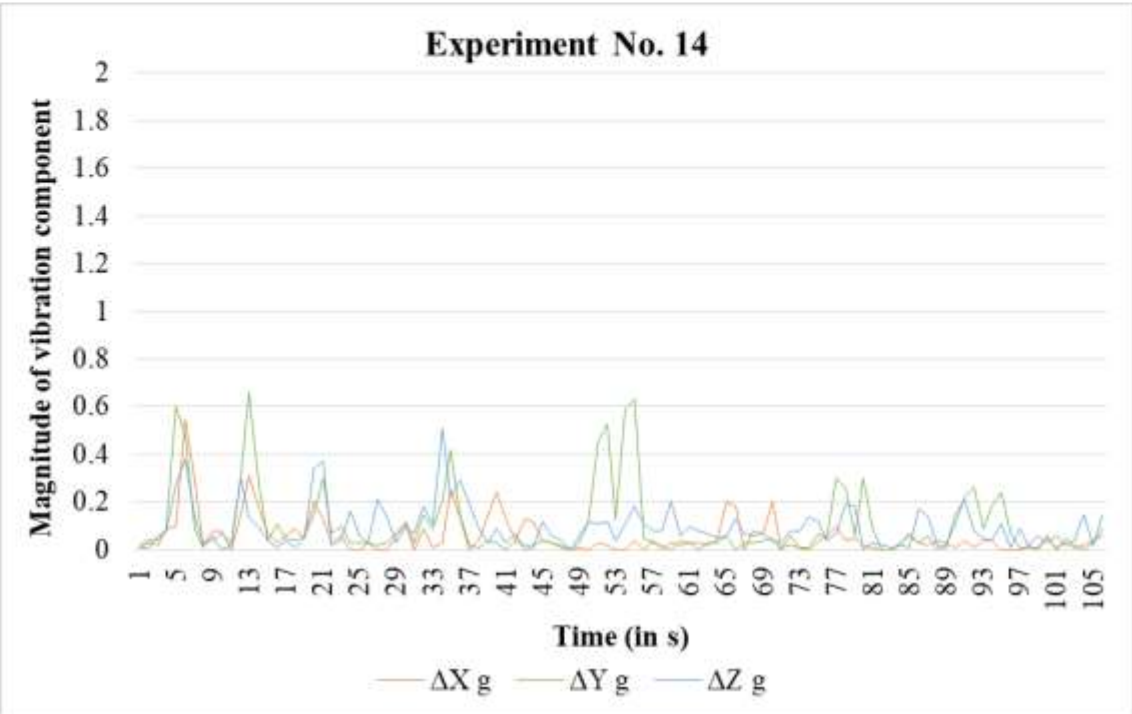

Fig.3.26 Outcome of Experimental set 14

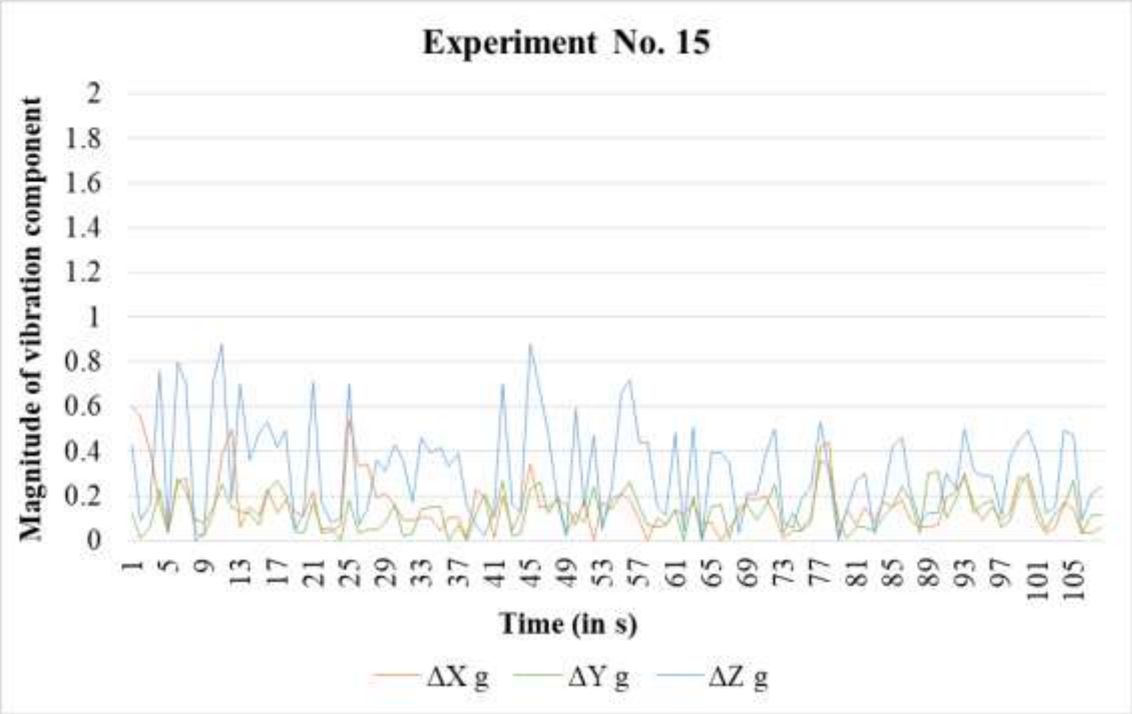

Fig.3.27 Outcome of Experimental set 15

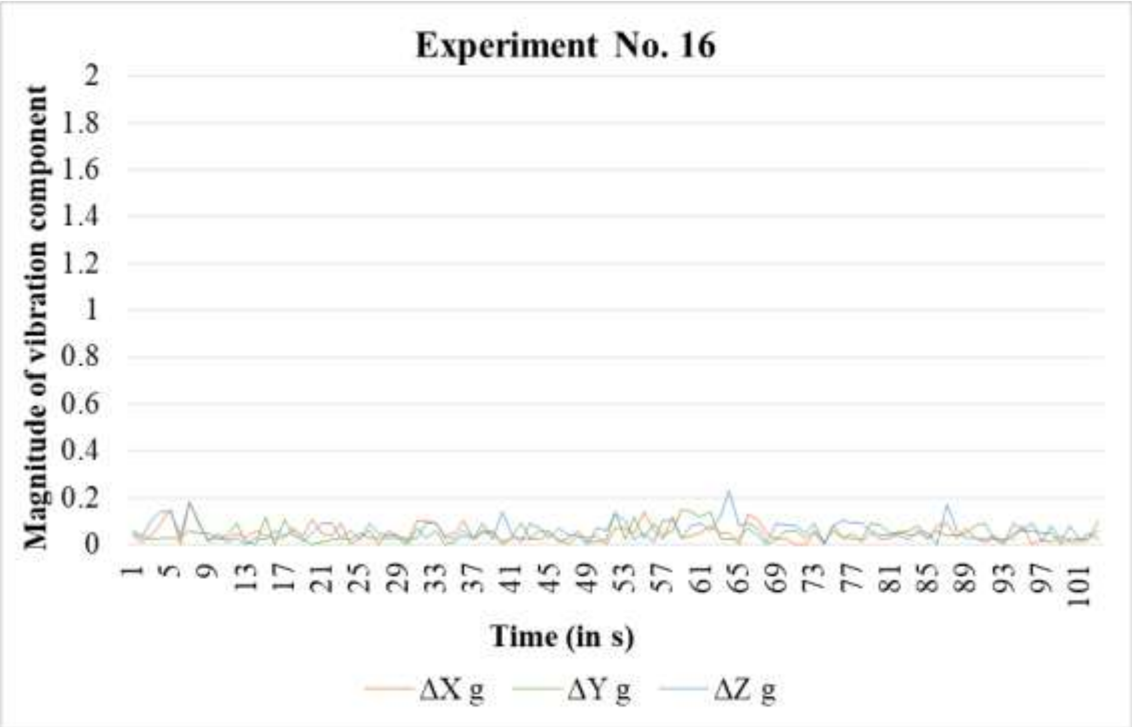

Fig.3.28 Outcome of Experimental set 16

3.8.3.1. Response table for 0-50 mm

The response vibration components derived for the element of 0-50 mm from the free end with respect to L16 set of the independent parameters are as given in Table 3.11.

Table 3.11 DOE parameters for 0-50 mm size from the free end

Sr. no.	Speed (*N*) (*RPM*)	Feed rate (*f*) (*mm/rev*)	Depth of cut (d_c) (*mm*)	Diameter (*D*) (*mm*)	$\Delta X_{max\ g}$	$\Delta Y_{max\ g}$	$\Delta Z_{max\ g}$
1	225	0.12	0.1	30	0.11	0.14	3.47
2	225	0.13	0.3	35	0.22	0.11	0.29
3	225	0.14	0.5	40	0.36	0.21	0.27
4	225	0.15	0.7	45	0.79	0.24	0.31
5	350	0.12	0.3	40	0.19	0.15	0.33
6	350	0.13	0.1	45	0.16	0.09	0.10
7	350	0.14	0.7	30	0.81	0.19	0.25
8	350	0.15	0.5	35	0.22	0.14	0.33
9	500	0.12	0.5	45	0.94	0.69	1.58
10	500	0.13	0.7	40	0.37	0.09	0.25
11	500	0.14	0.1	35	1.12	0.21	0.36
12	500	0.15	0.3	30	0.17	0.17	0.25
13	800	0.12	0.7	35	1.34	0.36	1.65
14	800	0.13	0.5	30	0.55	0.66	0.38
15	800	0.14	0.3	45	0.60	0.28	0.88
16	800	0.15	0.1	40	0.18	0.12	0.18

3.8.3.2. ANOVA for 0-50 mm

Performing the ANOVA methodology for the earlier presented tool element (0-50 mm), the main effect plot for the three components of tool vibrations and the S-N diagram are developed as given below in fig 3.29 and fig 3.30 respectively.

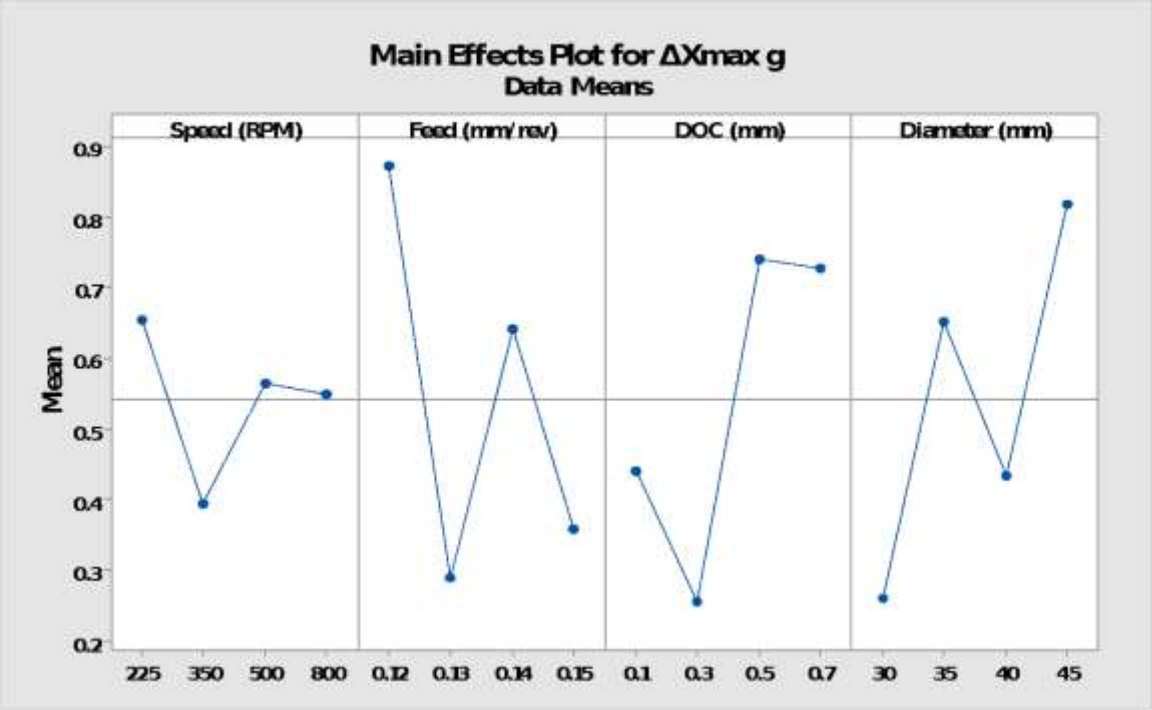

(a)

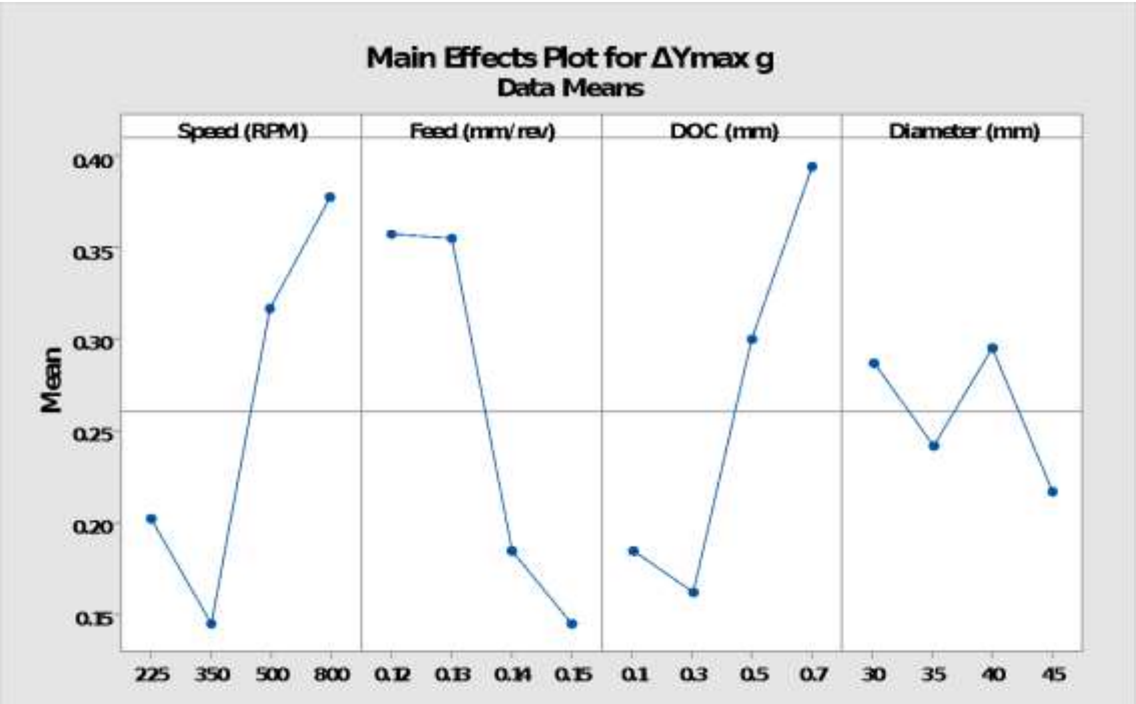

(b)

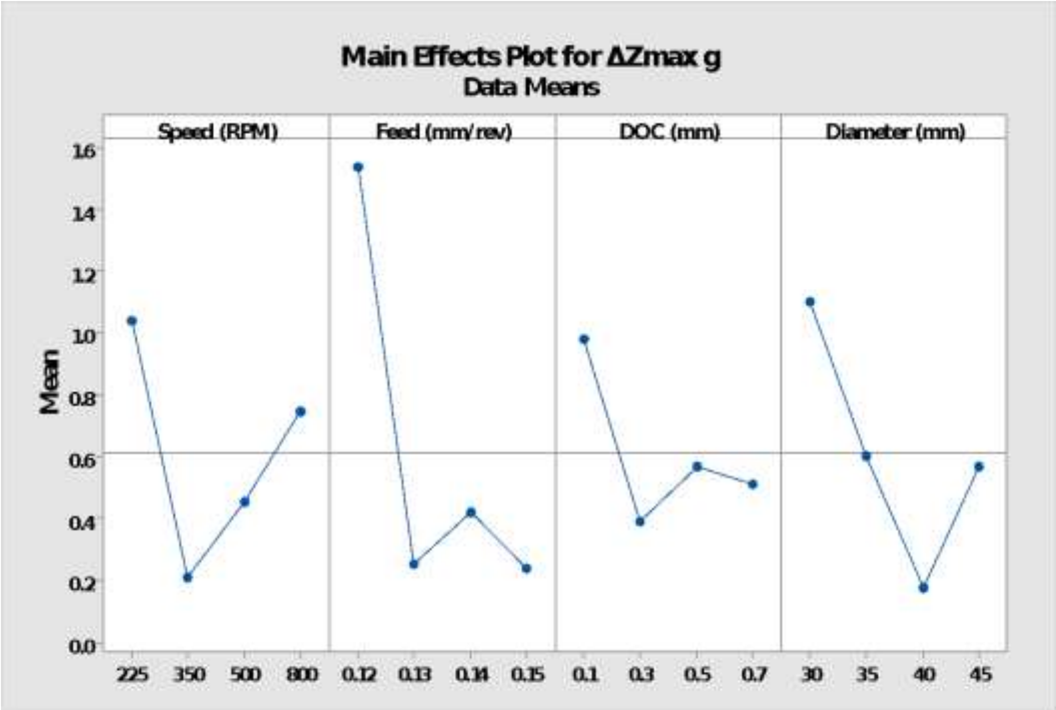

(c)

Fig.3.29 Main effect plot (0-50 mm size from the free end) for (a) ΔX_{maxg}, (b) ΔY_{maxg}, and (c) ΔZ_{maxg}

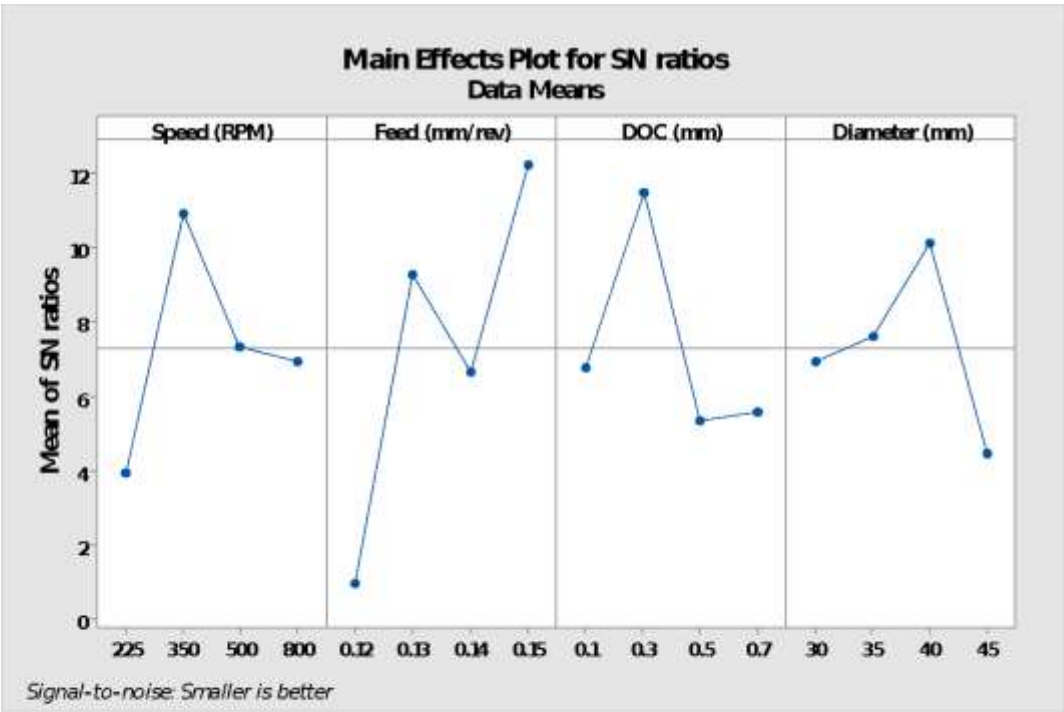

Fig.3.30 S-N ratio (0-50 mm from the free end)

3.8.3.3. Response table for 50-100 mm

The response vibration components derived for the element of 50-100 mm from the free end with respect to L16 set of the independent parameters are as given in Table 3.12.

Table 3.12 DOE parameters for 50-100 mm size from the free end

Sr. no.	Speed (*N*) (*RPM*)	Feed rate (*f*) (*mm/rev*)	Depth of cut (d_c) (*mm*)	Diameter (*D*) (*mm*)	$\Delta X_{max\ g}$	$\Delta Y_{max\ g}$	$\Delta Z_{max\ g}$
1	225	0.12	0.1	30	0.30	0.36	3.40
2	225	0.13	0.3	35	0.17	0.10	0.28
3	225	0.14	0.5	40	1.18	0.18	0.27
4	225	0.15	0.7	45	0.97	0.17	0.20
5	350	0.12	0.3	40	0.37	0.17	0.16
6	350	0.13	0.1	45	0.65	0.10	0.08
7	350	0.14	0.7	30	0.34	0.15	0.24
8	350	0.15	0.5	35	0.22	0.16	0.37
9	500	0.12	0.5	45	1.31	0.33	1.13
10	500	0.13	0.7	40	0.09	0.69	0.15
11	500	0.14	0.1	35	0.71	0.14	0.30
12	500	0.15	0.3	30	0.15	0.11	0.25
13	800	0.12	0.7	35	1.51	0.57	1.46
14	800	0.13	0.5	30	0.25	0.53	0.51
15	800	0.14	0.3	45	0.34	0.27	0.88
16	800	0.15	0.1	40	0.10	0.14	0.14

3.8.3.4. ANOVA for 50-100 mm

Performing the ANOVA methodology for the earlier presented tool element (50-100 mm), the main effect plot for the three components of tool vibrations and the S-N diagram are developed as given below in fig 3.31 and fig 3.32 respectively.

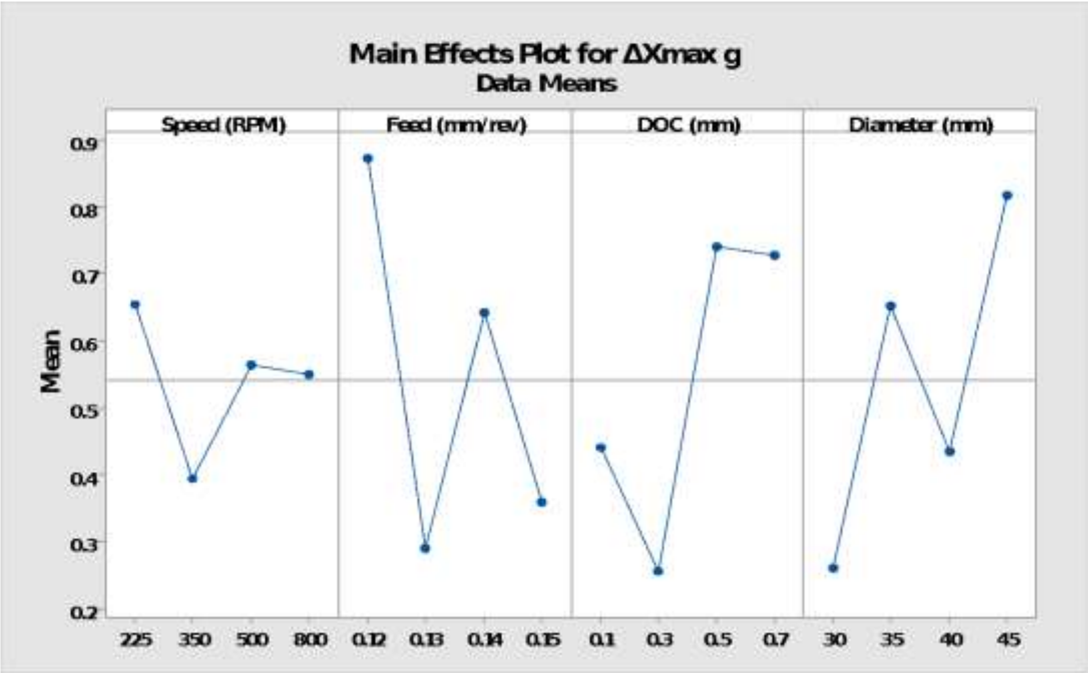

(a)

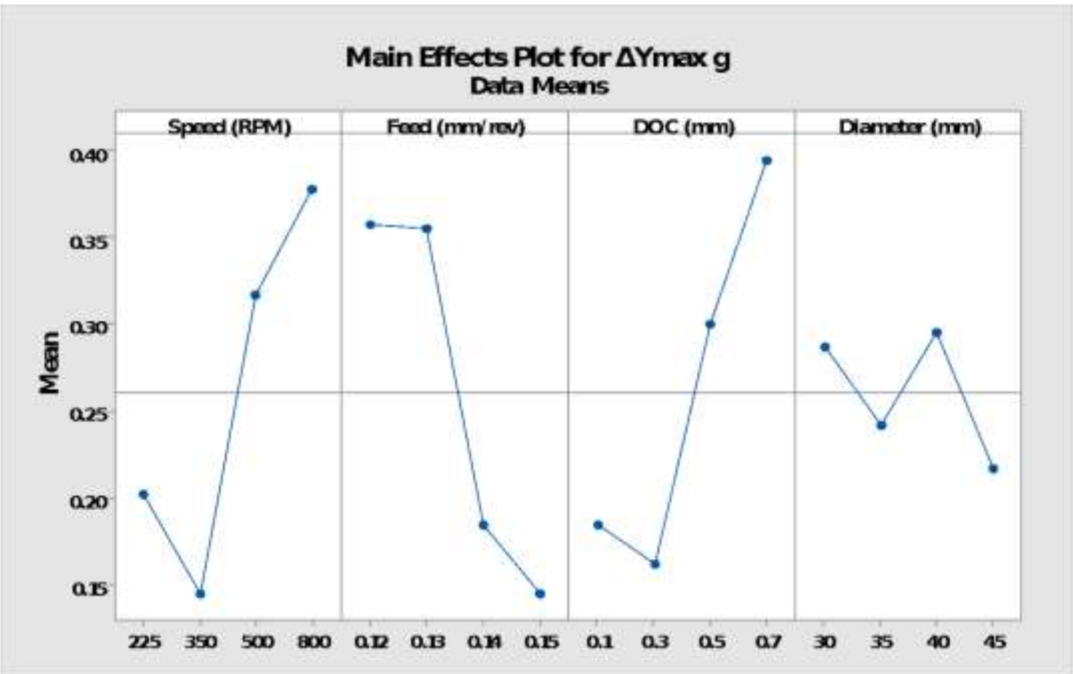

(b)

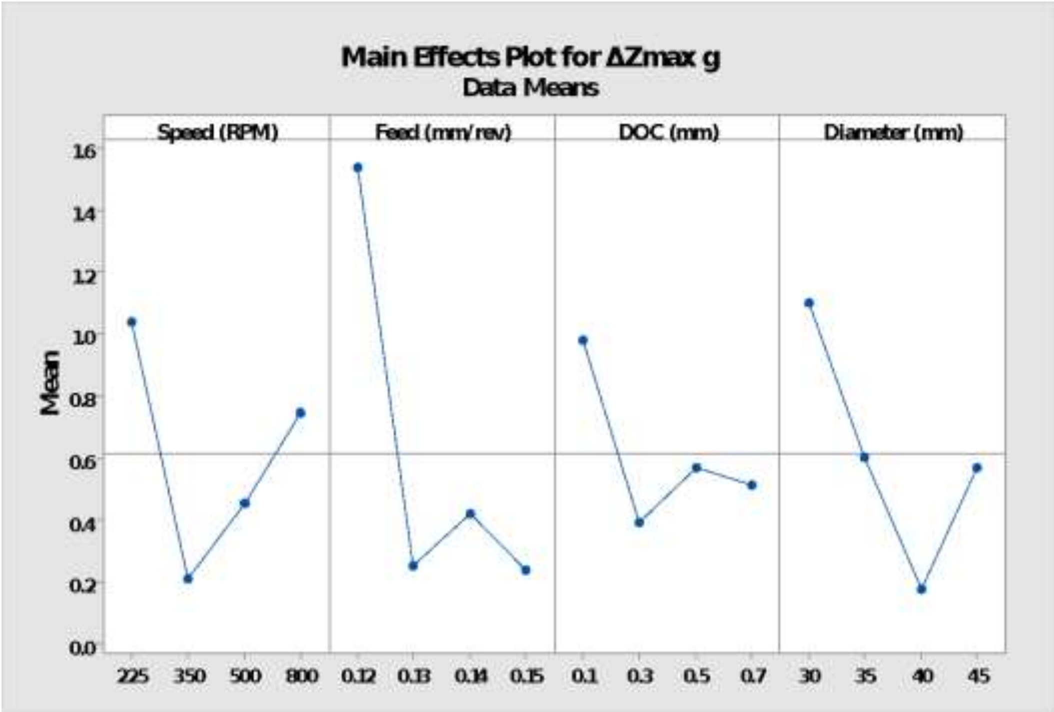

(c)

Fig.3.31 Main effect plot (50-100 mm size from the free end) for (a) ΔX_{maxg}, (b) ΔY_{maxg} and (c) ΔZ_{maxg}

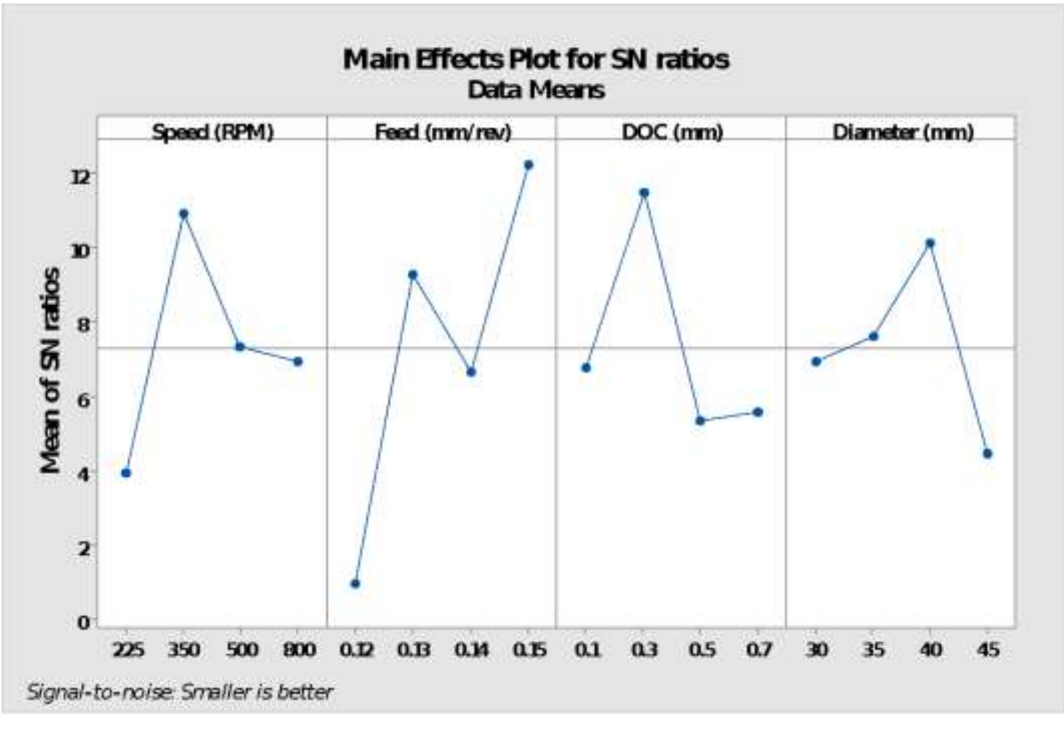

Fig.3.32 S-N ratio (0-50 mm from the free end)

3.8.3.5. Response table for 100-150 mm

The response vibration components derived for the element of 100-150 mm from the free end with respect to L16 set of the independent parameters are as given in Table 3.13.

Table 3.13 DOE parameters for 100-150 mm size from the free end

Sr. no.	Speed (*N*) (*RPM*)	Feed rate (*f*) (*mm/rev*)	Depth of cut (d_c) (*mm*)	Diameter (*D*) (*mm*)	$\Delta X_{max\ g}$	$\Delta Y_{max\ g}$	$\Delta Z_{max\ g}$
1	225	0.12	0.1	30	0.40	5.01	0.43
2	225	0.13	0.3	35	0.10	0.12	0.22
3	225	0.14	0.5	40	0.59	0.21	0.28
4	225	0.15	0.7	45	0.18	0.16	0.24
5	350	0.12	0.3	40	0.80	0.18	0.14
6	350	0.13	0.1	45	0.61	0.09	0.16
7	350	0.14	0.7	30	0.33	0.23	0.25
8	350	0.15	0.5	35	0.25	0.13	0.36
9	500	0.12	0.5	45	0.63	0.66	0.81
10	500	0.13	0.7	40	0.63	0.12	0.56
11	500	0.14	0.1	35	0.19	0.15	0.28
12	500	0.15	0.3	30	0.19	0.16	0.21
13	800	0.12	0.7	35	0.97	0.87	1.19
14	800	0.13	0.5	30	0.20	0.63	0.20
15	800	0.14	0.3	45	0.44	0.36	0.72
16	800	0.15	0.1	40	0.14	0.15	0.23

3.8.3.6. ANNOVA for 100-150 mm

Performing the ANNOVA methodology for the earlier presented tool element (100-150 mm), the main effect plot for the three components of tool vibrations and the S-N diagram are developed as given below in fig 3.33 and fig 3.34 respectively.

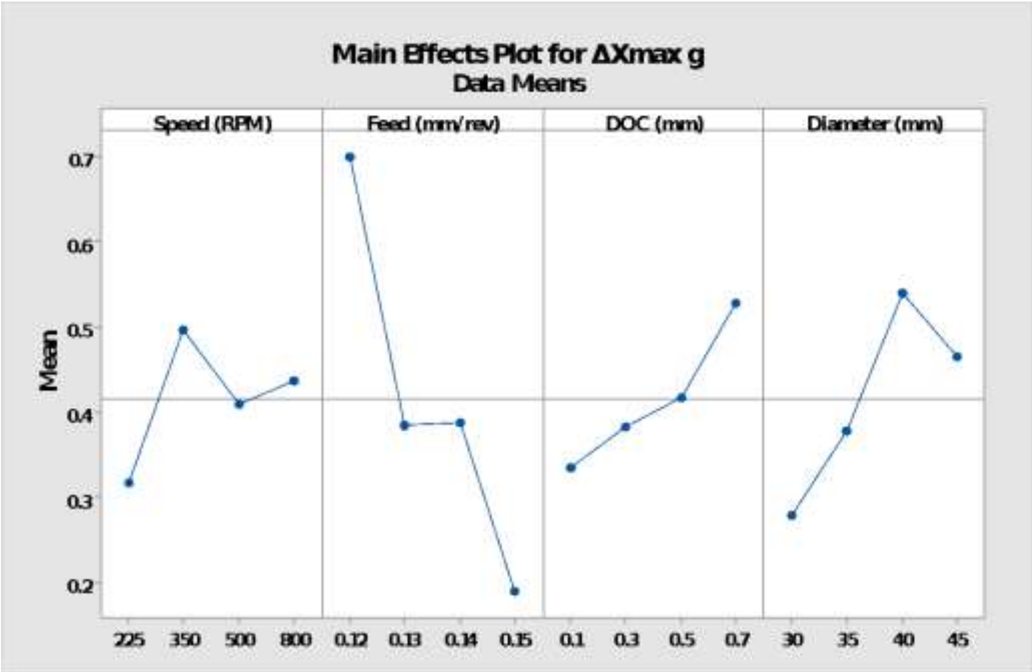

(a)

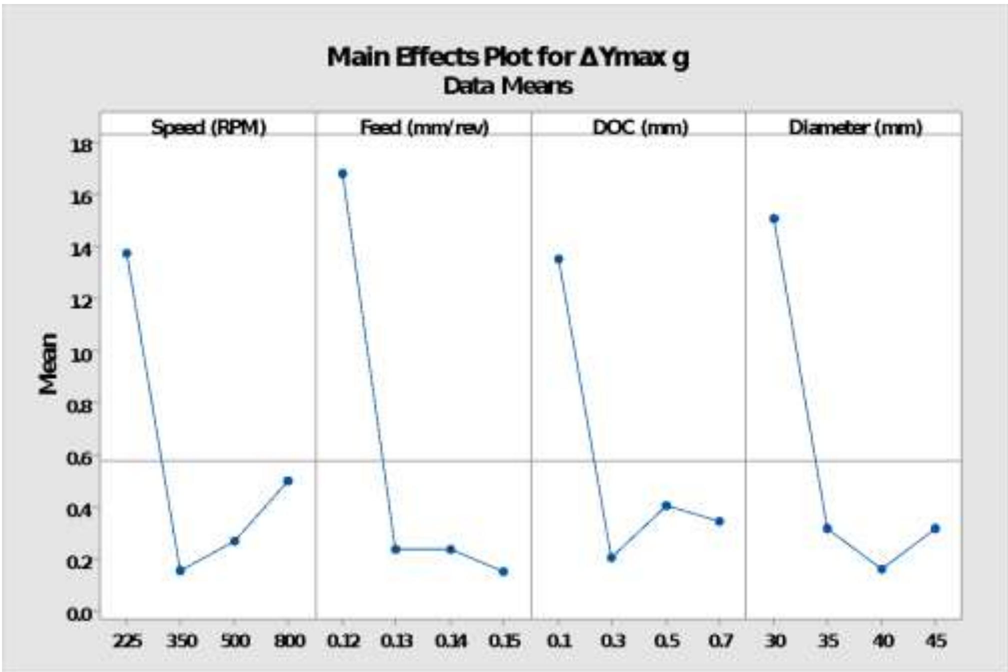

(b)

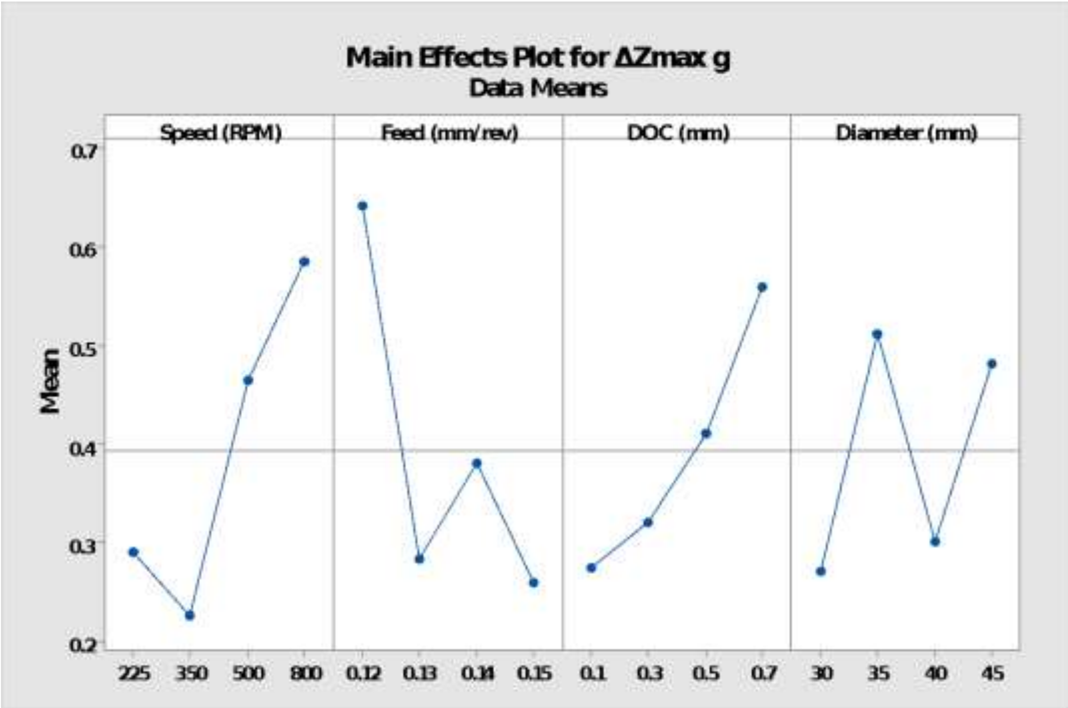

(c)

Fig.3.33 Main effect plot (100-150 mm size from the free end) for (a) ΔX_{maxg}, (b) ΔY_{maxg} and (c) ΔZ_{maxg}

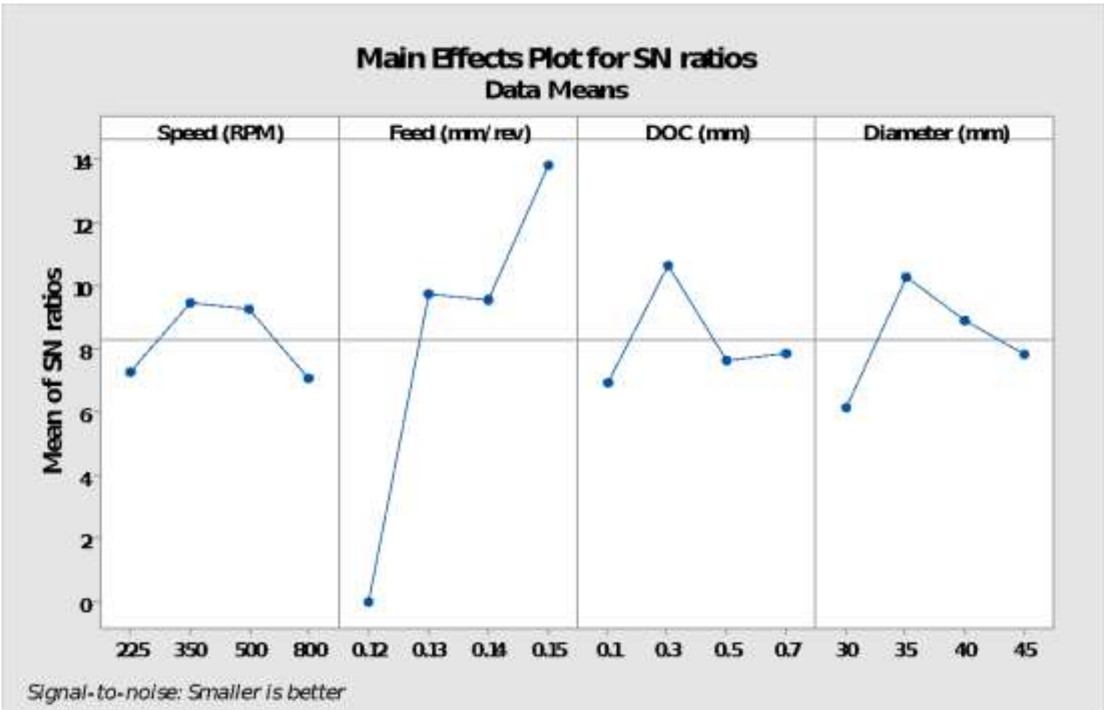

Fig.3.34 S-N ratio (100-150 mm from the free end)

3.8.3.7. Response table for 150-200 mm

The response vibration components derived for the element of 150-200 mm from the free end with respect to L16 set of the independent parameters are as given in Table 3.14.

Table 3.14 DOE parameters for 150-200 mm size from the free end

Sr. no.	**Speed (*N*) (*RPM*)**	**Feed rate (*f*) (*mm/rev*)**	**Depth of cut (d_c) (*mm*)**	**Diameter (*D*) (*mm*)**	$\Delta X_{max\ g}$	$\Delta Y_{max\ g}$	$\Delta Z_{max\ g}$
1	225	0.12	0.1	30	0.58	5.03	0.41
2	225	0.13	0.3	35	0.10	0.09	0.41
3	225	0.14	0.5	40	0.14	0.14	0.46
4	225	0.15	0.7	45	0.31	0.15	0.20
5	350	0.12	0.3	40	0.21	0.15	0.15
6	350	0.13	0.1	45	0.09	0.09	0.14
7	350	0.14	0.7	30	0.47	0.16	0.31
8	350	0.15	0.5	35	0.24	0.10	0.20
9	500	0.12	0.5	45	0.15	0.69	1.52
10	500	0.13	0.7	40	0.11	0.15	0.25
11	500	0.14	0.1	35	0.17	0.18	0.24
12	500	0.15	0.3	30	0.17	0.12	0.15
13	800	0.12	0.7	35	1.14	1.21	1.06
14	800	0.13	0.5	30	0.06	0.30	0.21
15	800	0.14	0.3	45	0.29	0.31	0.50
16	800	0.15	0.1	40	0.10	0.09	0.17

3.8.3.8. ANOVA for 150-200 mm

Performing the ANOVA methodology for the earlier presented tool element (150-200 mm), the main effect plot for the three components of tool vibrations and the S-N diagram is developed as given in fig 3.35 and fig 3.36 respectively.

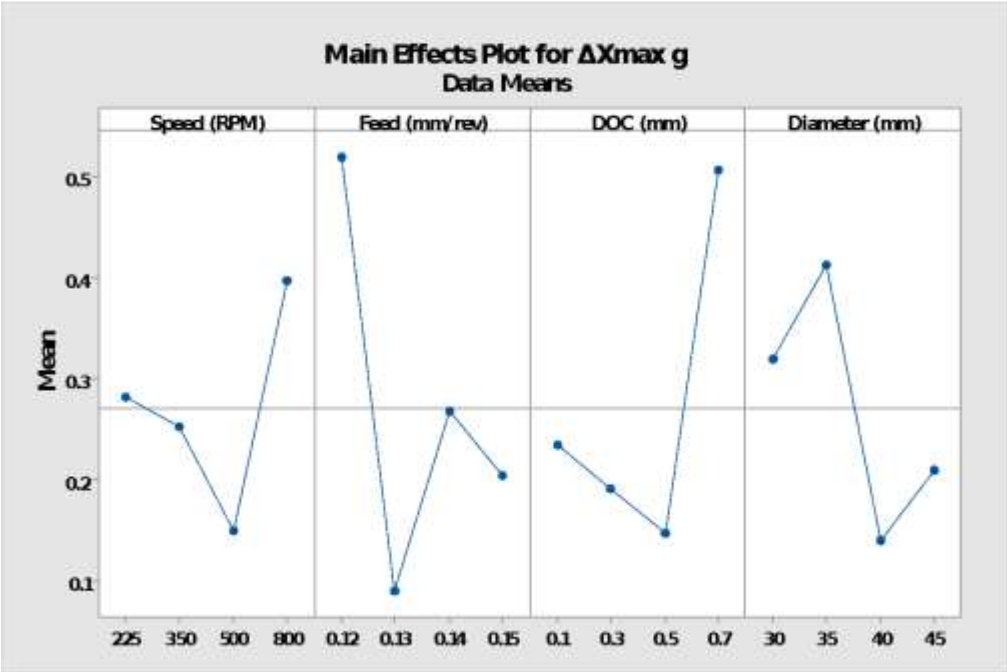

(a)

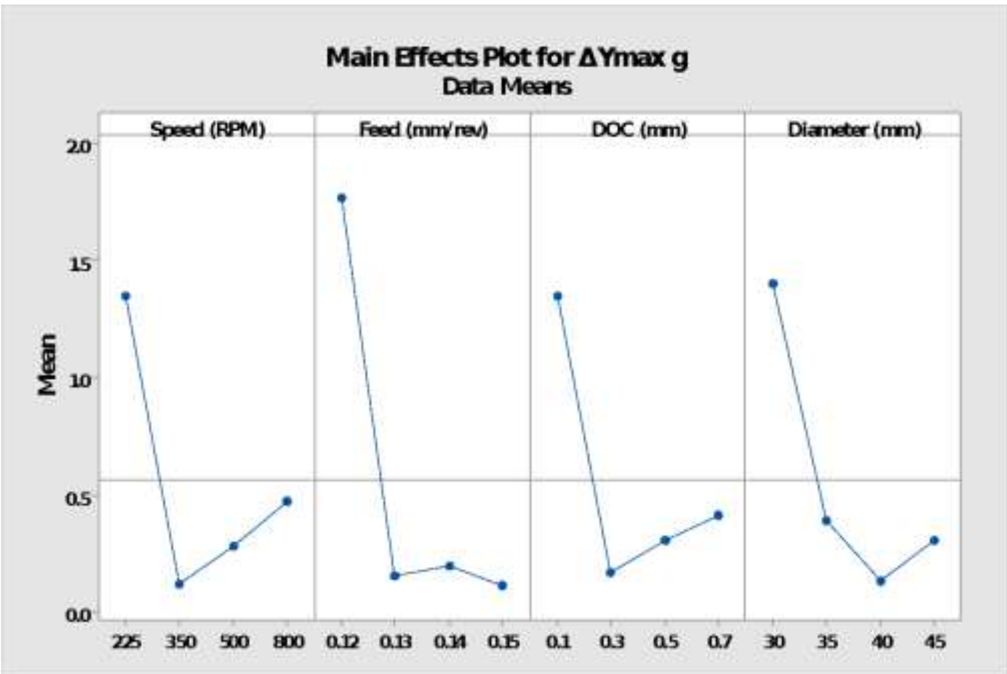

(b)

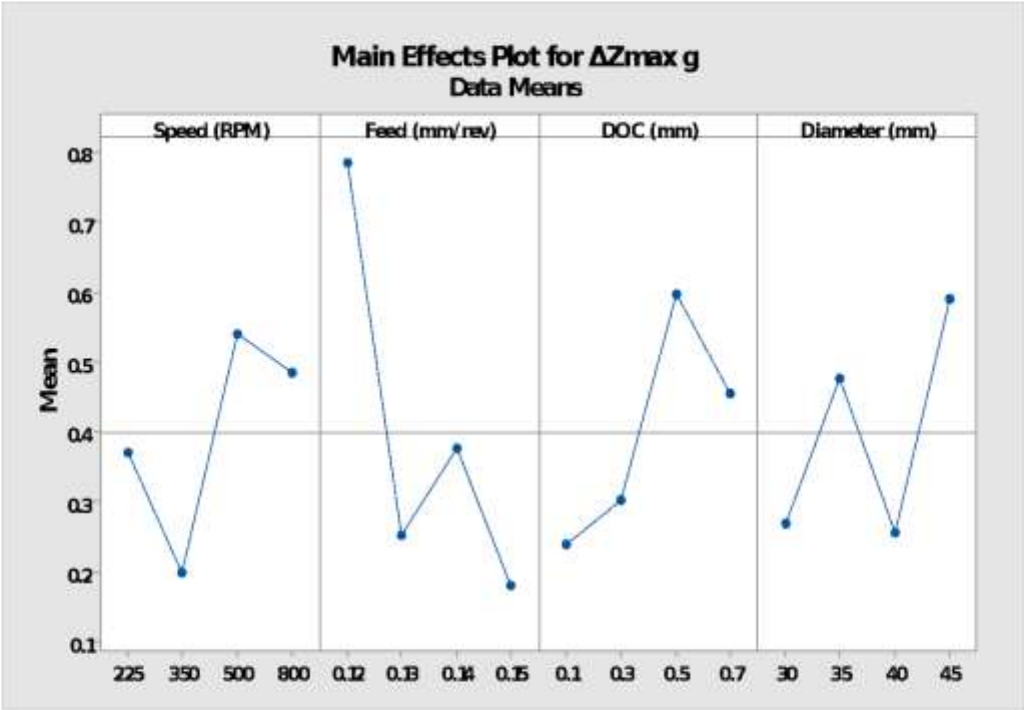

(c)

Fig.3.35 Main effect plot (150-200 mm size from the free end) for (a) ΔX_{maxg}, (b) ΔY_{maxg}, and (c) ΔZ_{maxg}

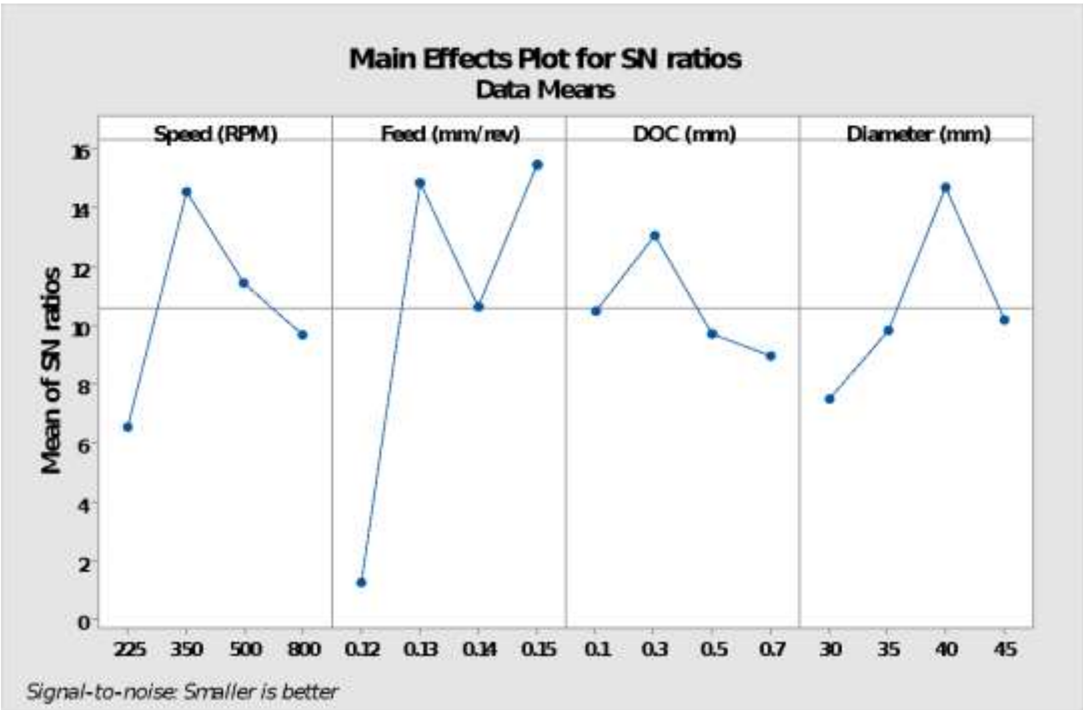

Fig.3.36 S-N ratio (150-200 mm from the free end)

3.8.3.9. Response table for 0-200 mm

The response vibration components derived for the element of 0-200 mm from the free end with respect to L16 set of the independent parameters are as given in Table 3.15.

Table 3.15 DOE parameters for 0-200 mm size from the free end

Sr. no.	Speed (*N*) (*RPM*)	Feed rate (*f*) (*mm/rev*)	Depth of cut (d_c) (*mm*)	Diameter (*D*) (*mm*)	$\Delta X_{max\ g}$	$\Delta Y_{max\ g}$	$\Delta Z_{max\ g}$
1	225	0.12	0.1	30	0.58	5.03	3.47
2	225	0.13	0.3	35	0.22	0.12	0.41
3	225	0.14	0.5	40	1.18	0.21	0.46
4	225	0.15	0.7	45	0.97	0.24	0.31
5	350	0.12	0.3	40	0.80	0.18	0.33
6	350	0.13	0.1	45	0.65	0.10	0.16
7	350	0.14	0.7	30	0.81	0.23	0.31
8	350	0.15	0.5	35	0.25	0.16	0.37
9	500	0.12	0.5	45	1.31	0.69	1.58
10	500	0.13	0.7	40	0.63	0.69	0.56
11	500	0.14	0.1	35	1.12	0.21	0.36
12	500	0.15	0.3	30	0.19	0.17	0.25
13	800	0.12	0.7	35	1.51	1.21	1.65
14	800	0.13	0.5	30	0.55	0.66	0.51
15	800	0.14	0.3	45	0.60	0.36	0.88
16	800	0.15	0.1	40	0.18	0.15	0.23

3.8.3.10. ANOVA for 0-200 mm

Performing the ANOVA methodology for the earlier presented tool element (0-200 mm), the main effect plot for the three components of tool vibrations and the S-N diagram is developed as given below in fig 3.37 and fig 3.38 respectively.

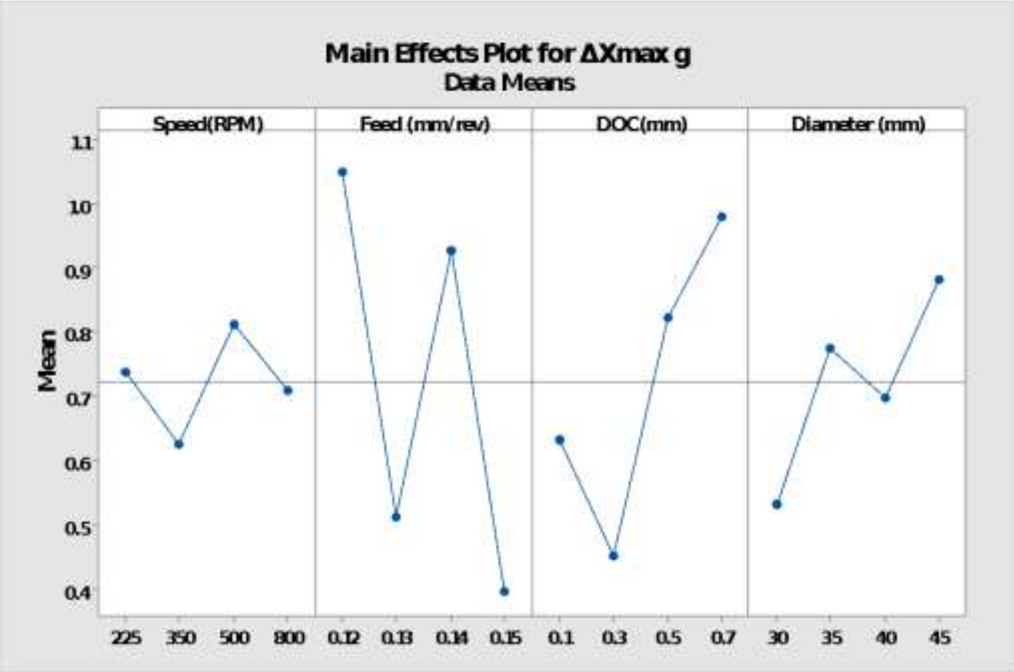

(a)

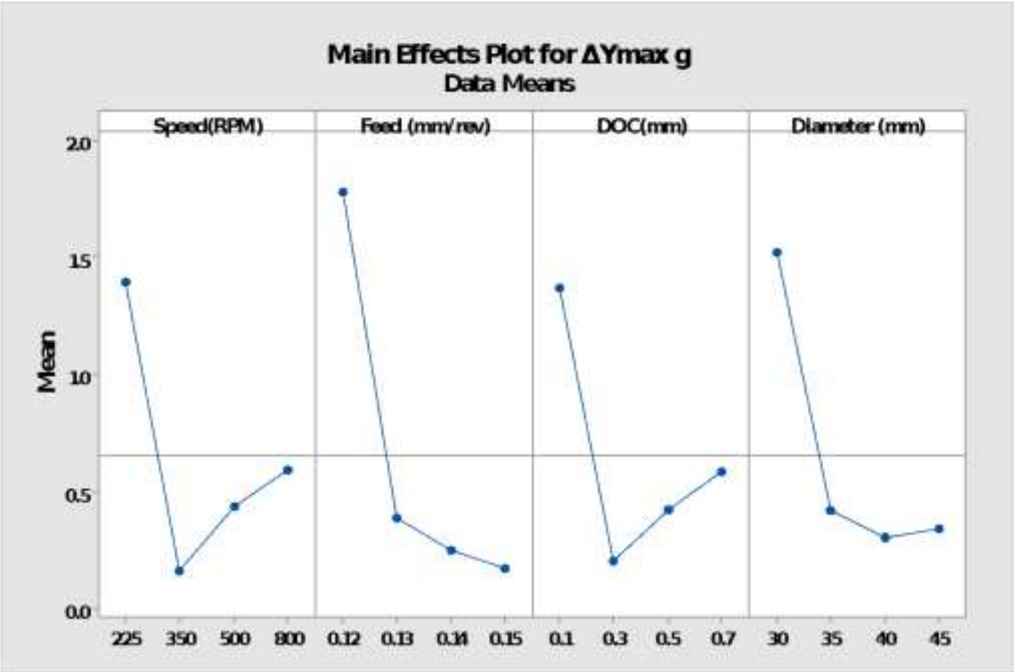

(b)

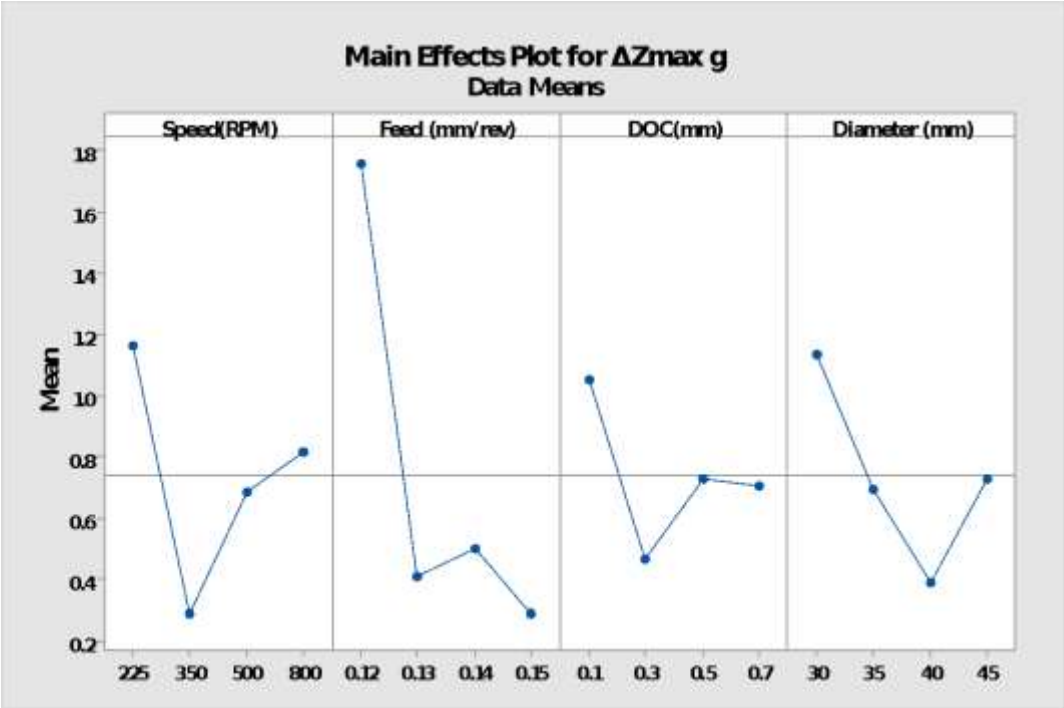

(c)

Fig.3.37 Main effect plot (0-200 mm size from the free end) for (a) ΔX_{maxg}, (b) ΔY_{maxg}, and (c) ΔZ_{maxg}

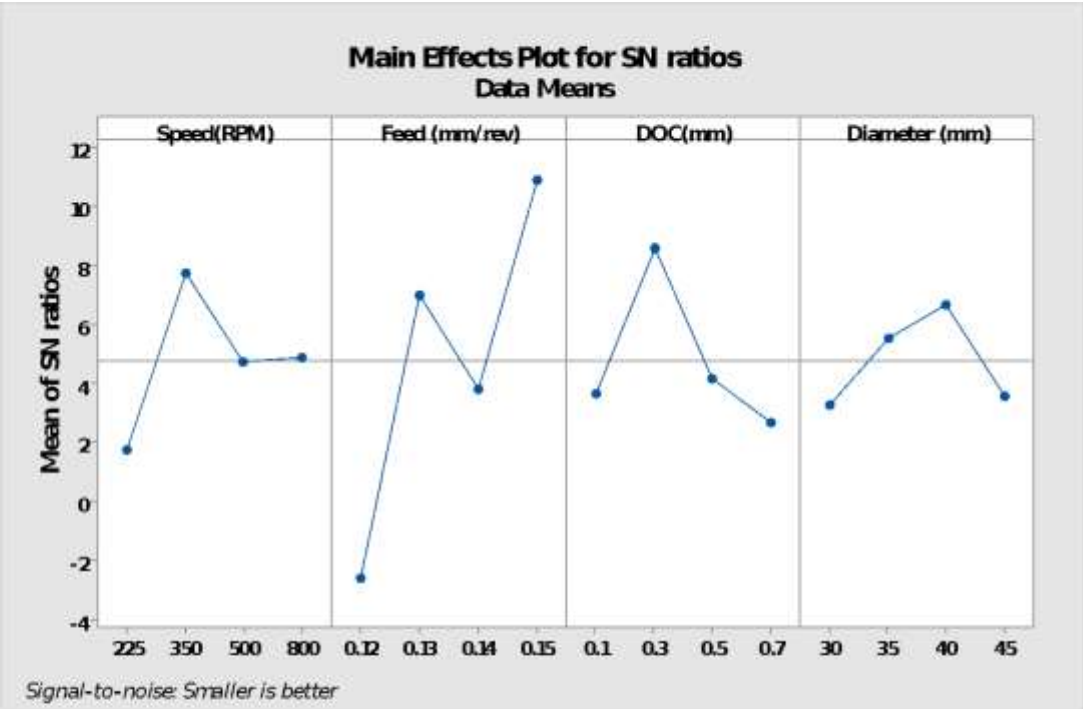

Fig.3.38 S-N ratio (0-200 mm size from the free end)

The optimum values of the four independent parameters derived from the investigated five sets of analysis are given in table 3.16.

Table 3.16 Optimum parameter values for different sets of analysis based on the distance from the free end

Set of Analysis	Optimum parameters
0-50	N = 350 rpm f = 0.13 mm/rev d_c = 0.3 mm D = 40 mm
50-100	N = 350 rpm f = 0.15 mm/rev d_c = 0.3 mm D = 40 mm
100-150	N = 350 rpm f = 0.15 mm/rev d_c = 0.3 mm D = 35 mm
150-200	N = 350 rpm f = 0.15 mm/rev d_c = 0.3 mm D = 40 mm
0-200	N = 350 rpm f = 0.15 mm/rev d_c = 0.3 mm D = 40 mm

3.8.4. Percentage Contribution of Parameter for Tool Vibration

The percentage amount of the contribution of each one of the four parameters on the overall vibration is computed for the five-set of tool element investigation; and presented in a tabular and graphical manner in table 3.17 and fig 3.39 respectively.

Table 3.17 Percentage contribution of parameter for tool vibration

Size in mm from the free end	Direction	Speed (*N*) (%)	Feed rate (*f*) (%)	Depth of cut (d_c) (%)	Diameter (*D*) (%)
0-50	*X*	16.32	22.53	28.68	22.12
	Y	23.17	11.47	38.17	16.09
	Z	12.41	54.06	6.38	11.93
50-100	*X*	5.05	26.15	19.52	23.31
	Y	26.07	28.97	27.09	3.17
	Z	14.46	43.75	7.37	16.10
100-150	*X*	6.53	51.83	7.81	14.65
	Y	16.73	29.90	15.03	21.50
	Z	25.18	29.08	14.95	14.27
150-200	*X*	11.20	35.69	28.32	15.59
	Y	15.92	34.60	15.18	17.38
	Z	12.77	41.26	14.53	14.95
0-200	*X*	2.70	47.08	24.77	10.24
	Y	15.42	31.43	14.09	18.69
	Z	14.17	51.32	6.38	10.12

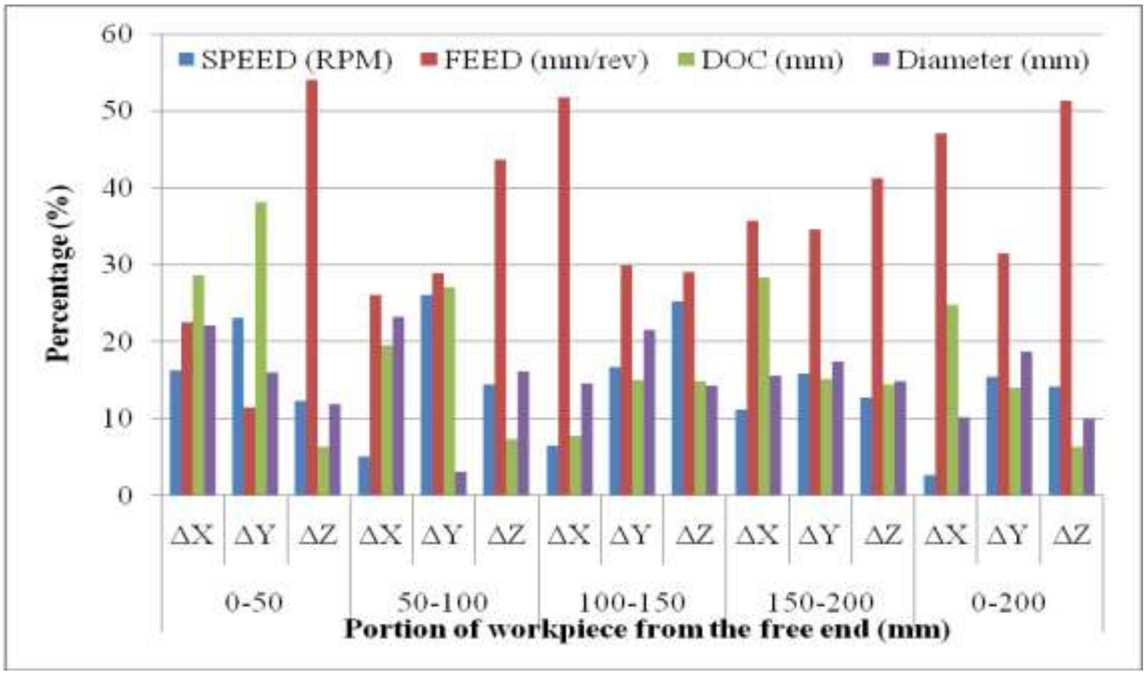

Fig.3.39 Percentage contribution of parameter for tool vibration

Fig. 3.39 is the graphical representation of the percentage contribution of parameter for tool vibration for each portion along with full workpiece length. The X-axis represents the length of the workpiece from the free end of the cantilever (i.e. another side of chuck holding the workpiece)

3.8.5. Root Mean Square (RMS)

The Root Mean Squared (RMS) is a measure of the error in data sets[59,60]. The amplitudes are averaged in a way only the magnitude of positive and negative points are considered[61,62]. This is done by squaring every point. This indicator is often used once the signal has been filtered to the frequency of interest[63,64].The RMS is a standard way to measure the error of a model in predicting quantitative data[65]. The standard equation for the RMS value can be given as[66],

$$RMS = \sqrt{\frac{1}{n}\sum_i x_i^2} \qquad \textbf{(24)}$$

In the present study, the RMS would provide the resultant vibration by means of combining the effects of vibration components in X, Y, and Z directions. The RMS value for the present application of vibration components can be evaluated using the following expression.

$$RMS = \sqrt{\frac{1}{3}((\Delta x g_{\max})^2 + (\Delta y g_{\max})^2 + (\Delta z g_{\max})^2)} \qquad \textbf{(25)}$$

3.8.6. Regression Analysis

In statistics, it’s hard to stare at a set of random numbers in a table and try to make any sense of it[67,68]. One can make a better guess, by using regression[69].Regression analysis is a way of mathematically sorting out which of those variables does indeed have an impact[70–72]. Regression analysis is a set of statistical methods used for the estimation of relationships between a dependent variable and one or more independent variables[73–75]. It can be utilized to assess the strength of the relationship between variables and for modeling the future relationship between them[76,77].

Regression analysis includes several variations, such as linear, multiple linear, and nonlinear[78]. The most common models are simple linear and multiple linear[79]. Nonlinear regression analysis is commonly used for more complicated data sets in which the dependent and independent variables show a nonlinear relationship[80,81]. Regression analysis offers numerous applications in various disciplines, including finance[82].

Regression examination is utilized to gauge the connection between a reliant variable and at least one free factor [83]. This strategy is generally applied to anticipate the yields, estimating the information, dissecting the time arrangement, and tracking down the causal impact conditions between the variables[84,85]. There are a few sorts of relapse methods close by dependent on the quantity of autonomous factors, the dimensionality of the relapse line, and the kind of ward variable [86]. Out of these, the two most famous relapse methods are straight relapse and calculated relapse [87].

Scientists use relapse to show the strength of the effect of numerous free factors on a reliant variable on various scales [88]. Relapse has various applications [89,90]. For instance, consider an informational collection comprising of climate data recorded in the course of the last not many decades[91]. Utilizing that information, we could conjecture climate for a few years[92]. Relapse is likewise generally utilized in associations and organizations to survey hazard and development dependent on recently recorded data[93].

The polynomial regression is a form of regression analysis in which the relationship between the independent variable x and the dependent variable y is modeled as an nth degree polynomial in x[94]. Polynomial regression fits a nonlinear relationship between the value of *x* and the corresponding conditional mean of *y*[95]. Although polynomial regression fits a nonlinear model to the data, as a statistical estimation problem it is linear, in the sense that the regression function is linear in the unknown parameters that are estimated from the data[96–98]. For this reason, polynomial regression is considered to be a special case of multiple linear regressions[99].

Although polynomial regression is technically a special case of multiple linear regressions, the interpretation of a fitted polynomial regression model requires a somewhat different perspective[100]. It is often difficult to interpret the individual coefficients in a polynomial regression fit since the underlying monomials can be highly correlated[101]. Although the correlation can be reduced by using orthogonal polynomials, it is generally more informative to consider the fitted regression function as a whole[102]. Point-wise or simultaneous confidence bands can then be used to provide a sense of the uncertainty in the estimate of the regression function[103].

Polynomial provides the best approximation of the relationship between the dependent and independent variable[104]. A broad range of functions can be fit under it. Polynomial fits a wide range of curvature[105]. Hence, the polynomial regression of different order is a preferable method for the present study for the identification of the expression of the dependent parameter (i.e. vibration components) with respect to independent parameters (i.e. N, f, $d_{c,}$ and D).

In order to develop an empirical relation among the independent and dependent parameters, the regression analysis has been performed using different polynomial orders as elaborated below. Moreover, the limits used for the regression analysis are as listed below.

- N = 0 to 1000 rpm
- f = 0.1 to .0.2 mm/rev

- d_c = 0 to 1 mm
- D = 25 to 50 mm
- Work Material = EN 8
- Work-piece condition: Cantilever

3.8.6.1. Polynomial relation of order 2

Regression equations for assuming Polynomial relation of order 2 can be given as follows:

$$\Delta Xg = 1.455 + 20.49f + 18.75f^2 - 98.12d_c + 2.10d_c^2 + 0.006D \quad \textbf{(26)}$$

$$\Delta Y_g = 88.92 - 0.01N - 93.52f + 3281.25f^2 - 7.696d_c + 8.297d_c - 0.926D + 0.014D^2 \quad \textbf{(27)}$$

$$\Delta Z_g = 71.65 - 0.006N - 809.2f + 2837.5f^2 - 3.215d_c + 3.531d_c^2 - 0.611D + 0.008D^2 \quad \textbf{(28)}$$

$$RMS = 60.31 - 0.006N + 642.5f - 2233.7f^2 - 4.883d_c + 5.544d_c^2 - 0.587D + 0.007D^2 \quad \textbf{(29)}$$

$$RMS_N = -0.006N \quad \textbf{(30)}$$

$$RMS_f = 642.5f - 2233.7f^2 \quad \textbf{(31)}$$

$$RMS_{dc} = -4.883d_c + 5.544d_c^2 \quad \textbf{(32)}$$

$$RMS_D = -0.587D + 0.007D^2 \quad \textbf{(33)}$$

Table 3.18 Statistics of regression fit (polynomial order 2) for ΔX_{maxg}

ΔX_{maxg}	**Value**	**Std. Error**	
a_0	1.45E+00	1.48E+01	
a_1	5.11E-04	2.32E-03	No. Points = 16
a_2	-4.56E-07	2.18E-06	RMS = 3.1095E-01
a_3	-2.05E+01	2.10E+02	Bias = 9.7578E-19
a_4	1.88E+01	7.77E+02	R^2 = 46.71%
a_5	-9.81E-01	1.59E+00	
a_6	2.11E+00	1.94E+00	

a_7	6.26E-02	2.34E-01	
a_8	-5.75E-04	3.11E-03	

Table 3.19 Statistics of regression fit (polynomial order 2) for ΔY_{maxg}

ΔY_{maxg}	Value	Std. Error	
a_0	8.89E+01	3.19E+01	
a_1	-1.07E-02	5.01E-03	
a_2	9.45E-06	4.73E-06	No. Points = 16
a_3	-9.35E+02	4.55E+02	RMS = 6.7321E-01
a_4	3.28E+03	1.68E+03	Bias = 2.73E-19
a_5	-7.70E+00	3.45E+00	R^2 = 70.95%
a_6	8.30E+00	4.21E+00	
a_7	-9.26E-01	5.06E-01	
a_8	1.14E-02	6.73E-03	

Table 3.20 Statistics of regression fit (polynomial order 2) for ΔZ_{maxg}

ΔZ_{maxg}	Value	Std. Error	
a_0	7.17E+01	2.44E+01	
a_1	-6.36E-03	3.83E-03	
a_2	5.94E-06	3.61E-06	No. Points = 16
a_3	-8.09E+02	3.47E+02	RMS = 5.144E-01
a_4	2.84E+03	1.29E+03	Bias = 2.0061E-19
a_5	-3.22E+00	2.64E+00	R^2 = 66.12%
a_6	3.53E+00	3.22E+00	
a_7	-6.11E-01	3.87E-01	
a_8	7.75E-03	5.14E-03	

Table 3.21 Statistics of regression fit (polynomial order 2) for *RMS*

RMS	**Value**	**Std. Error**	
a_0	6.03E+01	2.22E+01	
a_1	-6.74E-03	3.48E-03	
a_2	5.89E-06	3.29E-06	No. Points = 16
a_3	-6.43E+02	3.16E+02	RMS = 4.6785E-01
a_4	2.23E+03	1.17E+03	Bias = 2.1386E-16
a_5	-4.88E+00	2.40E+00	R^2 = 69.16%
a_6	5.54E+00	2.92E+00	
a_7	-5.87E-01	3.52E-01	
a_8	7.40E-03	4.68E-03	

3.8.6.2. Polynomial relation of order 3

Regression equations for assuming Polynomial relation of order 3 can be given as follows.

$$\Delta Xg = 733.5 - 0.01N - 1724.6f + 128.1f^2 - 31635f^3 - 7.304d_c + 21.17d_c^2 - 15.88d_c^3 + 3.299D - 0.008D^2 \quad \textbf{(34)}$$

$$\Delta Y_g = 629.9 - 0.006N - 11625f + 82762f^2 - 196250f^3 - 19.7d_c + 44.48d_c^2 - 30.16d_c^3 - 5.496D + 0.135D^2 - 0.001D^3 \quad \textbf{(35)}$$

$$\Delta Z_g = 751.7 - 0.0523N - 16650f + 120625f^2 - 233890f^3 - 12.63d_c + 31.91d_c^2 - 23.65d_c^3 + 2.194D - 0.068D^2 \quad \textbf{(36)}$$

$$RMS = 844.8 + 4.794N - 18054f + 13169f^2 - 319666f^3 - 15.65d_c + 37.99d_c^2 - 27.04d_c^3 - 0.632D + 0.009D^2 \quad \textbf{(37)}$$

$$RMS_N = 4.794N \quad \textbf{(38)}$$

$$RMS_f = -18054f + 13169f^2 - 319666f^3 \quad \textbf{(39)}$$

$$RMS_{dc} = -15.65d_c + 37.99d_c^2 - 27.04d_c^3 \quad \textbf{(40)}$$

$$RMS_D = -0.632D + 0.009D^2 \quad \textbf{(41)}$$

Table 3.22 Statistics of regression fit (polynomial order 3) for ΔX_g

ΔX_g	Value	Std. Error	No. Points = 16
a_0	7.34E+02	1.53E+02	RMS = 1.6572E-01
a_1	-1.24E-02	8.50E-03	Bias = -6.9588E-16
a_2	2.86E-05	1.89E-05	R^2 = 84.86%
a_3	-1.95E-08	1.26E-08	
a_4	-1.72E+04	3.37E+03	
a_5	1.28E+05	2.50E+04	
a_6	-3.16E+05	6.18E+04	
a_7	-7.30E+00	3.19E+00	
a_8	2.12E+01	9.32E+00	

Table 3.23 Statistics of regression fit (polynomial order 3) for ΔY_{maxg}

ΔY_{maxg}	Value	Std. Error	No. Points = 16
a_0	6.30E+02	5.19E+02	RMS = 5.6350E-01
a_1	-6.32E-02	2.89E-02	Bias = -3.2594E-16
a_2	1.27E-04	6.44E-05	R^2 = 79.65%
a_3	-7.89E-08	4.30E-08	
a_4	-1.16E+04	1.14E+04	
a_5	8.28E+04	8.51E+04	
a_6	-1.96E+05	2.10E+05	
a_7	-1.97E+01	1.08E+01	
a_8	4.45E+01	3.17E+01	

Table 3.24 Statistics of regression fit (polynomial order 2) for ΔZ_{maxg}

ΔZ_{maxg}	Value	Std. Error	No. Points = 16
a_0	7.52E+02	3.45E+02	RMS = 3.74472E-01
a_1	-5.24E-02	1.92E-02	Bias = -4.5731E-16
a_2	1.09E-04	4.28E-05	R^2 = 82.02%
a_3	-6.92E-08	2.86E-08	
a_4	-1.67E+04	7.61E+03	
a_5	1.21E+05	5.66E+04	
a_6	-2.91E+05	1.40E+05	
a_7	-1.26E+01	7.21E+00	
a_8	3.19E+01	2.11E+01	

Table 3.25 Statistics of regression fit (polynomial order 2) for *RMS*

RMS	Value	Std. Error	No. Points = 16
a_0	8.45E+02	2.84E+02	RMS = 3.0853E-01
a_1	-4.79E-02	1.58E-02	Bias = -5.1598E-16
a_2	9.84E-05	3.52E-05	R^2 = 86.59%
a_3	-6.20E-08	2.35E-08	
a_4	-1.81E+04	6.27E+03	
a_5	1.32E+05	4.66E+04	
a_6	-3.20E+05	1.15E+05	
a_7	-1.56E+01	5.93E+00	
a_8	3.80E+01	1.74E+01	

3.8.6.3. Polynomial relation of order 2 with cross-terms

Regression equations for assuming Polynomial relation of order 2 including cross-terms can be given as follows.

$$\Delta Xg = 1.09 + 0.037N + 144.9f - 173.6f^2 + 8.193d_c + 1.987d_c^2 - 0.244D + 0.002D^2 - 0.089Nf - 0.001Nd_c - 58.50fd_c + 0.196fD + 0.038d_cD \quad (42)$$

$$\Delta Y_g = 38.79 - 0.0423N - 287.4f + 1176.2f^2 - 57.54d_c + 11.48d_c^2 + 0.144D + 0.003D^2 + 0.138Nf + 0.001Nd_c + 207.7fd_c - 5.101fD + 0.421d_cD \quad (43)$$

$$\Delta Z_g = 29.51 - 0.014N - 23.08f + 1321.6f^2 - 25.65d_c + 6.021d_c^2 - 0.172D - 0.005D^2 - 0.007Nf + 0.003Nd_c + 56.76fd_c - 3.98fD + 0.303d_cD \quad (44)$$

$$RMS = 21.01 - 0.007N - 124.2f + 789.6f^2 - 30.1d_c + 7.593d_c^2 - 0.109D + 0.003D^2 - 0.08Nf + 89.75fd_c - 3.28fD + 0.288d_cD \quad (45)$$

$$RMS_N = -0.007N - 0.08Nf \quad (46)$$

$$RMS_f = -124.2f - 0.08Nf + 89.75fd_c - 3.28fD \quad (47)$$

$$RMS_{dc} = -30.1d_c + 7.593d_c^2 + 89.75fd_c + 0.288d_cD \quad (48)$$

$$RMS_D = -0.109D + 0.003D^2 - 3.28fD + 0.288d_cD \quad (49)$$

Table 3.26 Statistics of regression fit (polynomial order 2 with cross-terms) for ΔX_{maxg}

ΔX_{maxg}	Value	Std. Error	No. Points = 16
a_0	-1.10E+01	7.17E+07	RMS = 1.5668E-01
a_1	3.66E-02	1.18E+04	Bias = -1.2324E-18
a_2	1.72E-08	1.33E+01	R^2 = 86.47%
a_3	1.45E+02	6.18E+08	
a_4	-1.74E+02	9.41E+08	
a_5	8.19E+00	4.03E+07	
a_6	1.99E+00	7.41E+06	
a_7	-2.44E-01	2.13E+06	
a_8	1.77E-03	8.10E+03	

Table 3.27 Statistics of regression fit (polynomial order 2 with cross-terms) for ΔY_{maxg}

ΔY_{maxg}	Value	Std. Error	No. Points = 16
a_0	3.88E+01	1.64E+08	RMS = 3.5788E-01
a_1	-4.23E-02	2.69E+04	Bias = 9.2327E-19
a_2	1.22E-05	3.05E+01	R^2 = 91.79%
a_3	-2.87E+02	1.41E+09	
a_4	1.18E+03	2.15E+09	
a_5	-5.75E+01	9.21E+07	
a_6	1.15E+01	1.69E+07	
a_7	1.45E-01	4.87E+06	
a_8	3.07E-03	1.85E+04	

Table 3.28 Statistics of regression fit (polynomial order 2 with cross-terms) for ΔZ_{maxg}

ΔZ_{maxg}	Value	Std. Error	No. Points = 16
a_0	2.95E+01	1.18E+08	RMS = 2.5879E-01
a_1	-1.40E-02	1.95E+04	Bias = 1.2777E-18
a_2	9.79E-06	2.20E+01	R^2 = 91.43%
a_3	-2.31E+02	1.02E+09	
a_4	1.32E+03	1.55E+09	
a_5	-2.57E+01	6.66E+07	
a_6	6.02E+00	1.22E+07	
a_7	-1.72E-01	3.52E+06	
a_8	5.48E-03	1.34E+04	

Table 3.29 Statistics of regression fit (polynomial order 2 with cross-terms) for *RMS*

RMS	**Value**	**Std. Error**	
a_0	2.10E+01	1.29E+08	No. Points = 16 RMS = 2.8196E-01 Bias = -5.9148E-18 R^2 = 88.80%
a_1	-6.90E-03	2.12E+04	
a_2	8.28E-06	2.40E+01	
a_3	-1.24E+02	1.11E+09	
a_4	7.90E+02	1.69E+09	
a_5	-3.01E+01	7.25E+07	
a_6	7.59E+00	1.33E+07	
a_7	-1.09E-01	3.84E+06	
a_8	3.81E-03	1.46E+04	

3.8.6.4. Overall outcome of regression analysis

R-squared is an integrity of-fit measure for direct relapse models. R-squared measures the strength of the connection between your model and the dependent variable on an advantageous 0-100% scale. The R-Square values for each of the three dependent variables for all three considered polynomial types are presented in Table 3.30 and the 2^{nd} order polynomial with cross-terms has been identified to be the most reliable one with the highest R-Square values of 86.47, 91.79, and 91.43 for three dependent parameters.

Further, the parametric impact of the independent parameters (i.e. N, f, d_c, and D) on X, Y, and Z components of tool vibration and the corresponding RMS values is also studied, in order to investigate the impact of individual parameters on tool vibration.

Table 3.30 R-Square values for the considered three regression fits

Polynomial Order	Direction	R-Square (%)
2	X	46.71
	Y	70.95
	Z	66.12
3	X	84.86
	Y	79.65
	Z	82.02
2 (Cross Term)	X	86.47
	Y	91.79
	Z	91.43

Furthermore, the parametric variations of the vibration components (X, Y, and Z) with respect to the four independent parameters (i.e. D, d_C, f, and N) are illustrated in the following depictions (fig 3.40 to fig 3.43). The observations indicate that the variation curve of the Y and Z components of the vibration follows more or less a similar trend; whereas the X component shows a contradictory trend in the case of *D* and the same trend with higher magnitude for the rest of the three cases. The overall RMS value mostly overlaps or follows the same trend as the Z component of the tool vibration.

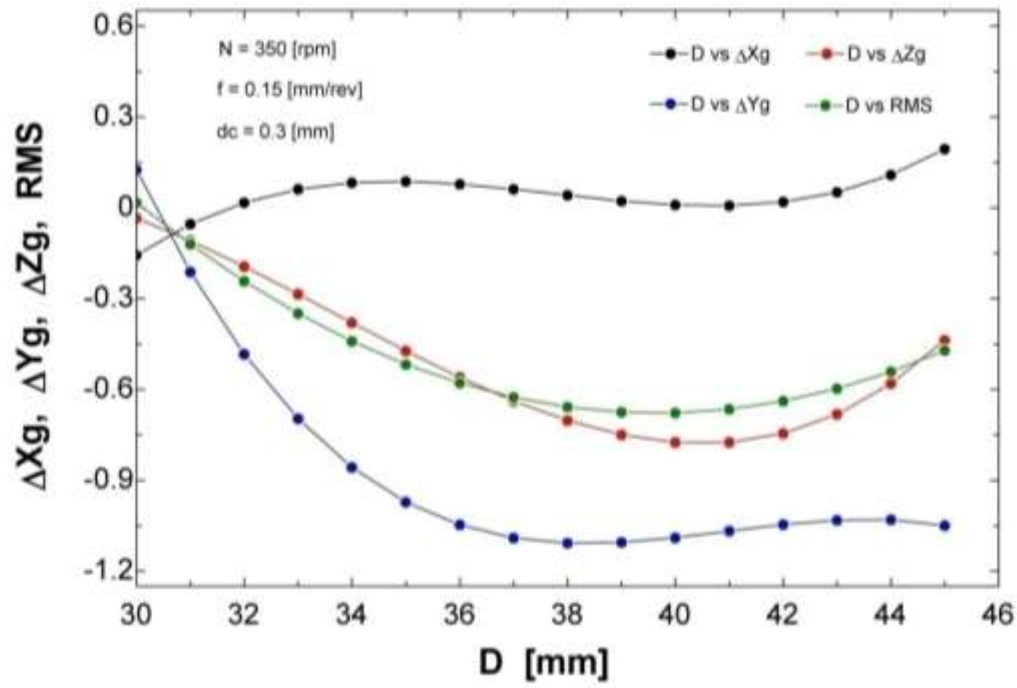

Fig.3.40 Effect of work-piece diameter variation on vibration

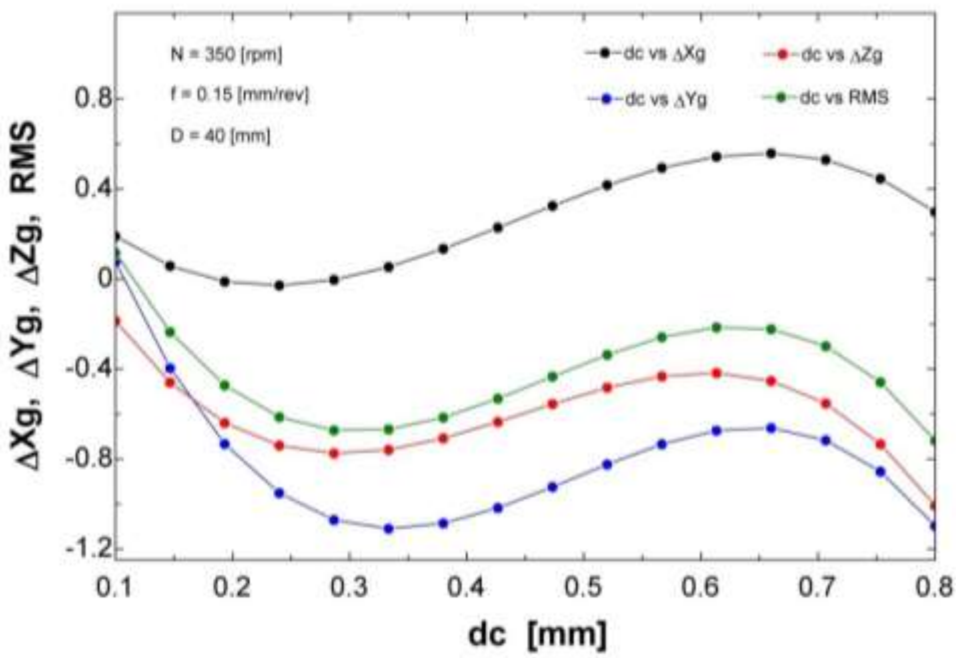

Fig.3.41 Effect of depth of cut variation on vibration

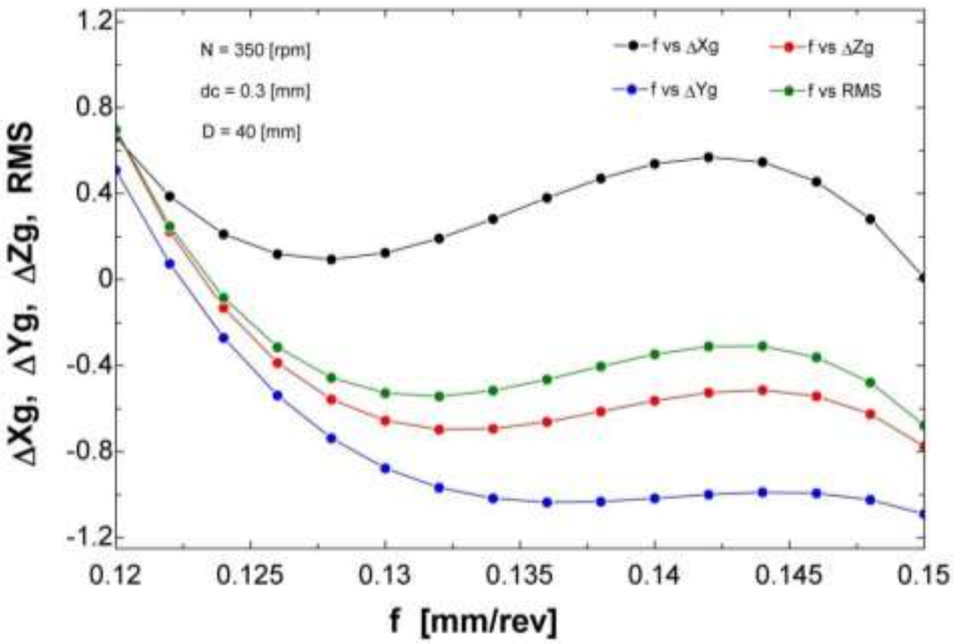

Fig.3.42 Effect of feed variation on vibration

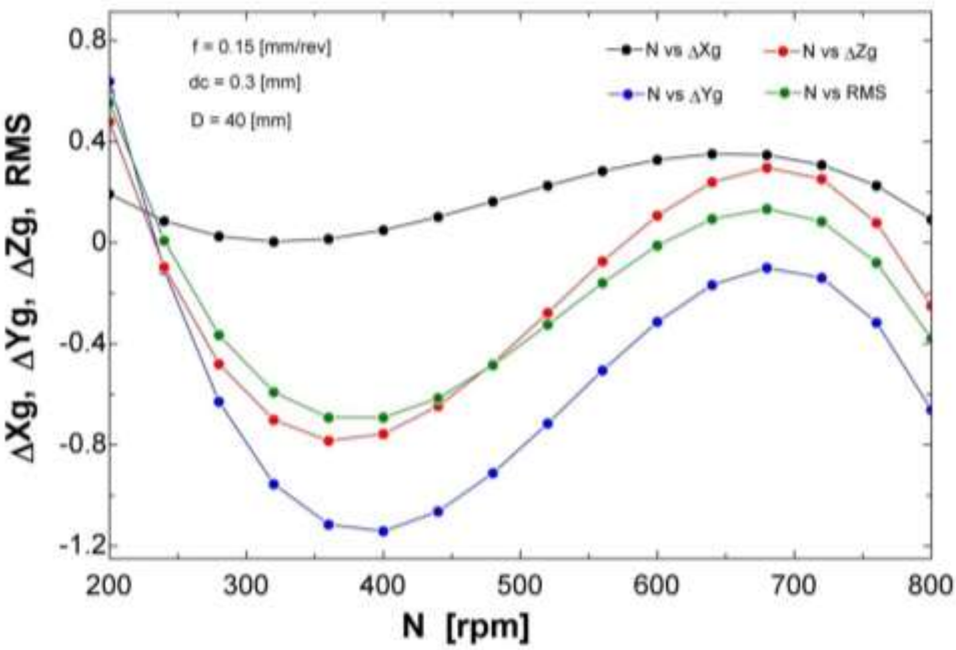

Fig.3.43 Effect of speed variation on vibration

3.9. Summary

In the present study, the performance of the cutting tool subjected to vibration has been investigated which depends upon the operational parameters of the systems. As experimentation is the most reliable means of investigating the vibration behavior of the cutting tool during the turning operation on the work-piece; and the empirical expressions developed based on the well-designed experimental observations give many reliable predictions. The core contribution of the present study is the application of the DOE approach with Taguchi and ANOVA techniques on the vibration study of cutting tool considering the four key variables: rotational speed (N) of the spindle i.e. work-piece, feed rate (f), depth of cut (DOC) (d_C) and the work-piece diameter (D). Based on the observations, the optimum parameter values identified are: N = 350 RPM, f = 0.15mm/rev, d_C = 0.3 mm and D = 40 mm. Moreover, the second-order polynomial equation with cross-terms has been identified as the more suitable regression expression than the second and third-order polynomial. The present study will benefit future researchers in defining the regression equations and using the same for different input conditions which will reduce the experimental cost requirements and will provide reliable predictions. These satisfy the condition of third objective of the research work.

4. ADAPTIVE CONTROL IMPLEMENTATION

4.1. Preamble

The Chapter includes the adaptive control methodology implemented for the present study. It will be helpful in modification, identification of problems in existing systems and to see how it behaves when certain parameters change. This chapter presents the implementation of adaptive control for the machining process. It is another step towards automation; wherein decision-making the elements are added [106]. When a component is being manufactured, the important variables are measured, and then if needed, the certain variables are altered with programmed limits, to get as accurate a finished part as possible [107,108]. The constraint of the adaptive control in the present study is tool vibration. Adaptive Control Constraint is used to constrain the tool vibration and find the affected parameter [109]. The outcomes of the regression analysis are validated concerning the experimental observations [110]. This study can further be used for the optimization of the affected parameter and can be fed into the system for reconsideration [111].

4.2. Introduction

The control system implies by which a variable amount or set of variable amounts is made to adjust to a recommended standard [17]. It either holds the upsides of the controlled amounts steady or makes them shift in an endorsed way [43]. A control framework might be worked by power, by mechanical methods, by a liquid pressing factor (fluid or gas), or by a mix of means [21]. At the point when a computer is engaged with the control circuit, it is normally more advantageous to work the entirety of the control frameworks electrically, in spite of the fact that intermixtures are genuinely normal [112].

There are several studies conducted on the application of optimization techniques and adaptive control mechanisms along with several other methodologies by a number of researchers [18]. Adaptive control is a step towards automation, wherein decision-making elements are added [6]. When a component is being manufactured, the important variables are measured, and then if needed be, certain variables are altered with programmed limits, to get as accurate as possible [7].

Adaptive control is the ability of the framework to alter its own activity to accomplish the most ideal method of activity [8]. The overall meaning of versatile control suggests that a versatile framework should be fit for playing out the accompanying capacities: giving nonstop data about the current situation with the framework or recognizing the cycle; contrasting present framework execution with the ideal or ideal exhibition and settling on a choice to change the framework to accomplish the characterized ideal presentation, and starting an appropriate adjustment to drive the control framework to the ideal [9].

In factual displaying, regression examination is a lot of quantifiable cycles for evaluating the associations between a dependent variable (as often as possible called the 'result variable') and at any rate one free factor (routinely called 'markers', 'covariates', or 'includes') [19]. The most generally perceived kind of backslide examination is immediate backslide, in which one finds the line (or a more unpredictable straight blend) that most eagerly fits the data according to a specific mathematical measure [30]. For example, the system for standard least-squares calculates the exceptional line (or hyperplane) that restricts the quantity of squared differences between the veritable data and that line (or hyperplane) [20]. For unequivocal mathematical reasons (see direct backslide), this allows the researcher to assess the prohibitive supposition (or people's ordinary worth) of the dependent variable when the free factors take on a given plan of characteristics [34]. More uncommon types of relapse utilize somewhat various systems to gauge elective area boundaries (e.g., quintile relapse or Necessary Condition Analysis) or gauge the restrictive assumption across a more extensive assortment of non-straight models (e.g., nonparametric regression).

With the aim of implementing adaptive control methods to the machine tool vibration problem, the present study has been conducted.

4.3. Adaptive Control Constraints

Adaptive control constraint (ACC) is one of the machining cycle control types [6]. The huge ACC of the systems can be considered ward on the analysis control, limit versatile control/self-tuning control, model reference versatile control, variable development control/sliding mode control, neural organization control, and feathery control [10]. ACC is one of the powerful strategies for tackling the above issues of cutting device vibration [11]. ACC controls the machining boundaries to keep up the greatest working conditions during the time-changing machining measure [49]. The early forms of boundary versatile control-based ACC frameworks were created utilizing a basic online assessor for the interaction acquire and an incorporated technique to change the addition of a necessary regulator. The imperfections of this system are that the elements of the cutting cycle were ignored and no hypothetical versatile plan procedure was utilized. The versatile regulator comprises two capacities: (a) Online assessment of the boundaries of the cutting interaction and (b) Real-time control.

The ACC boosts the feed rate under the condition that few estimated or assessed factors of the cutting cycle are kept underneath or at particular limitation limit esteems are preferably easier to develop the frameworks over the rest. Versatile control limitation has just been applied for functional frameworks [11]. The versatile control program creates the ideal feed rate as indicated by the difference in the cutting cycle.

4.4. Adaptive Control Constraints (ACC) Algorithm

First, the experimentation was performed and the corresponding regression equations were formulated for four dependent and three independent parameters using three different types of polynomials. Later on, the concept of the adaptive control parameters was applied and the corresponding corrective action process was performed. The experimental observations are compared to the regression findings for the validation purpose.

The flowchart of the ACC methodology implementation is depicted in Fig. 4.1 and the step by step procedure is presented below.

Step 1: In the starting, the system constraints are studied and the target constraint is defined, which is tool vibration in the present study; and the limit values of the constraint parameter i.e. tool vibration components are fixed.

Step 2: Specification of Input parameters i.e. rotational speed (*N*) of the spindle i.e. work-piece, feed rate (*f*), depth of cut (DOC) (d_C), and the work-piece diameter (*D*).

Step 3: Computation of the X, Y, and Z components of the tool vibration

Step 4: Calculation of the corresponding RMS values of the parameters taken in Step 2 from the regression equations formulated based on the experimental observations

Step 5: Computation of overall RMS values by using RMS regression equation.

Step 6: Checking if the obtained RMS value is within the predefined limit or not.

Step 7: If the answer is Yes in Step 6, the algorithm moves forward with the turning operation. If the answer to Step 6 is No, the algorithm optimizes the input parameters in such a way that the RMS value remains below the set limit.

The depiction of the adaptive in terms of the control system the system components are given in Fig 4.2 As the illustration shows, the adaptive control mechanism takes direct inputs i.e. constraints, strategies, and performance index; and processes inputs from the sensors which receive its signals from the machine tool. The adaptive control system processes the data as explained earlier and feeds the signal to the machining operation which provides enhanced performance due to the influence of adaptive control methodology. The process of optimizing the RMS values by means of ACC corrective action methodology is presented in Fig. 4.3 along with the intermediate results of the RMS values with reference to the key governing parameters i.e.d_c, f, and N. These intermediate results of variation in RMS values with variable input parameters are presented in Fig. 4.4, Fig. 4.5 and Fig. 4.6 for depth of cut, feed rate and the rotation speed respectively.

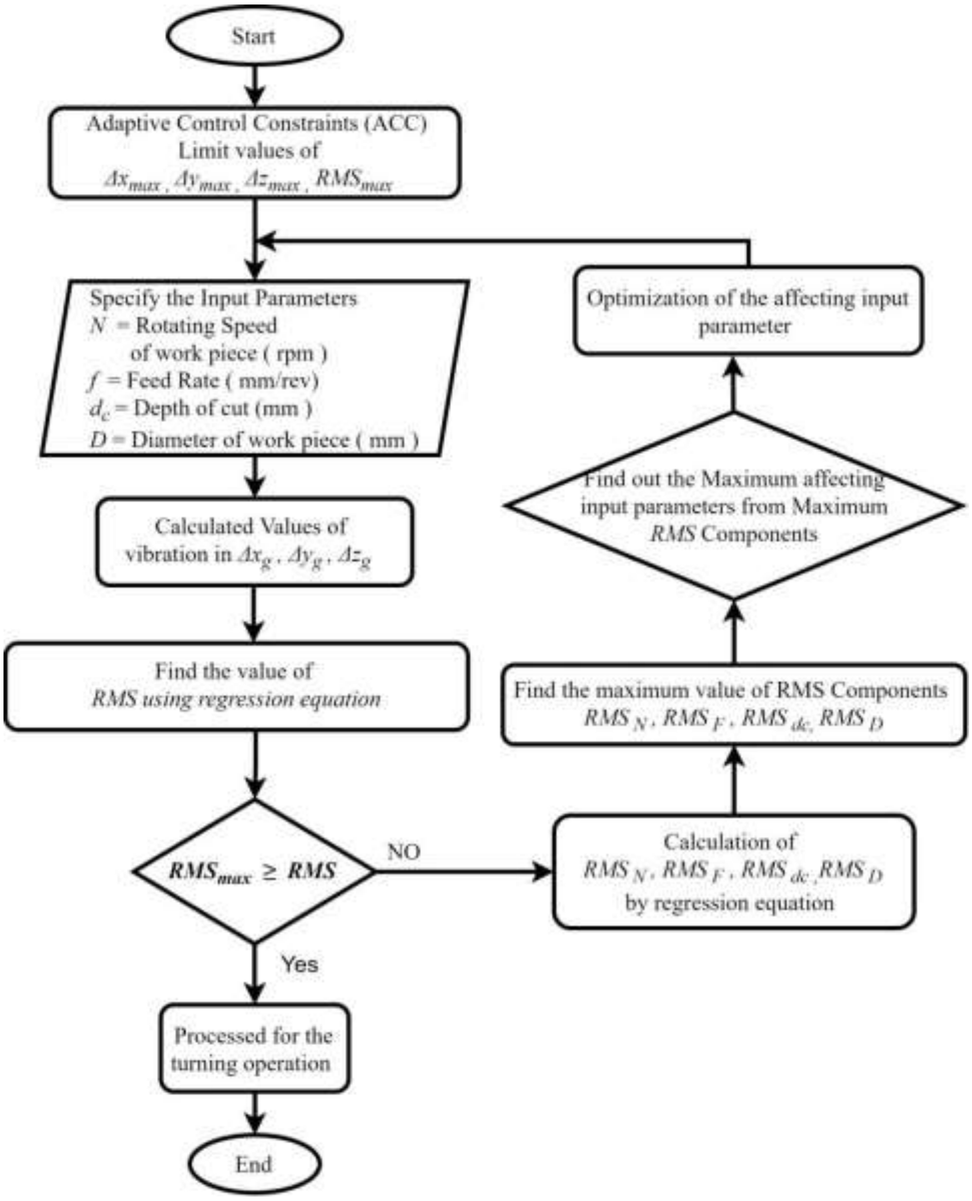

Fig.4.1 Flowchart of ACC methodology

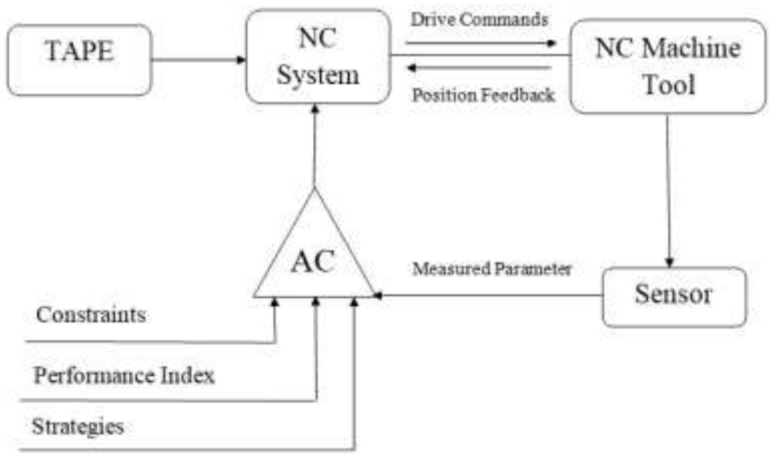

Fig.4.2 Block diagram of adaptive control system

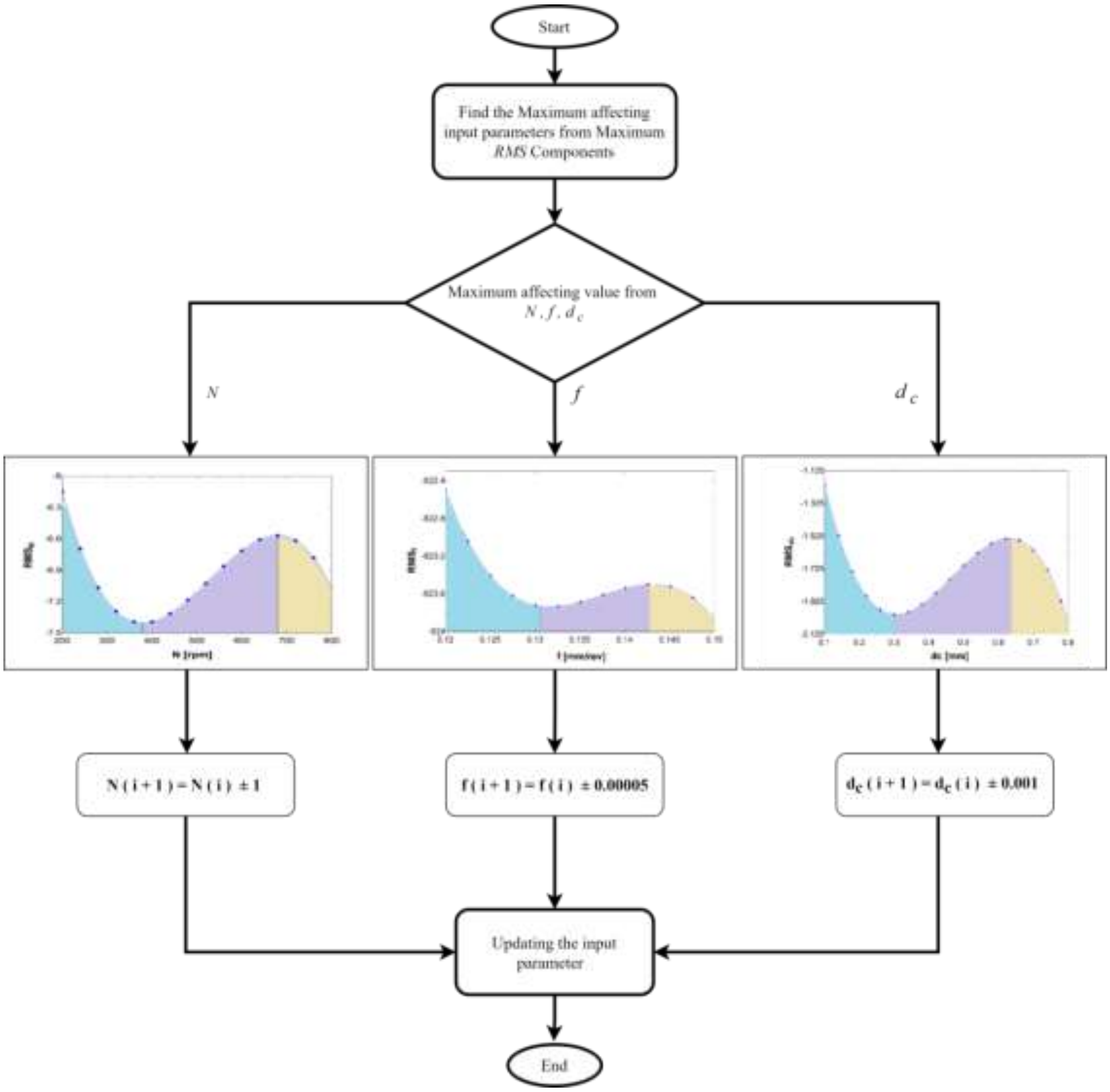

Fig.4.3 Flowchart of ACC corrective action

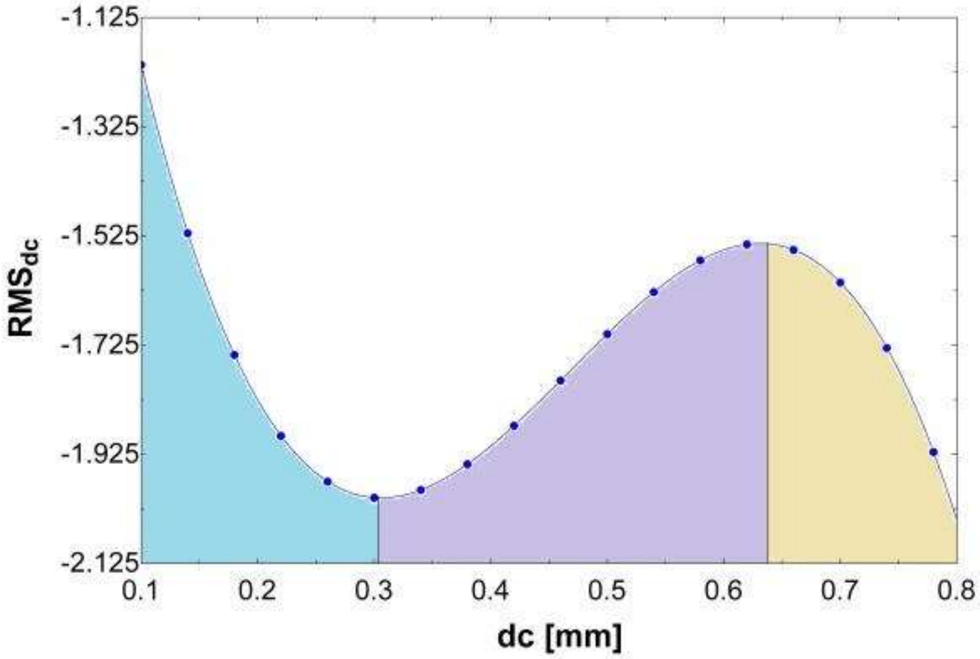

Fig.4.4 RMS values for variable depth of cut

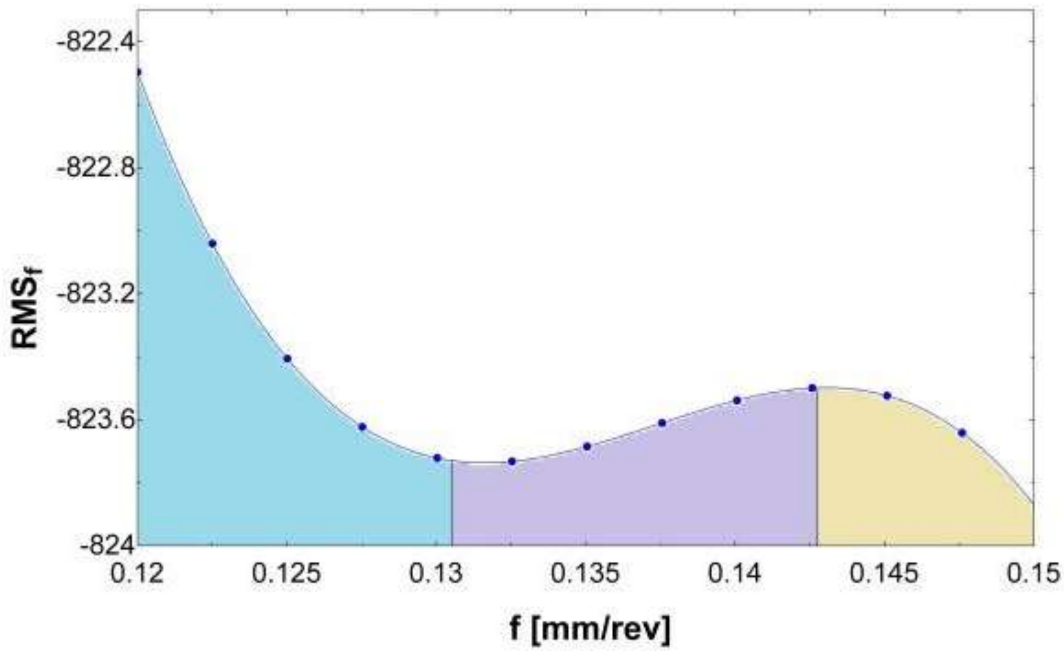

Fig.4.5 RMS values for variable feed rate

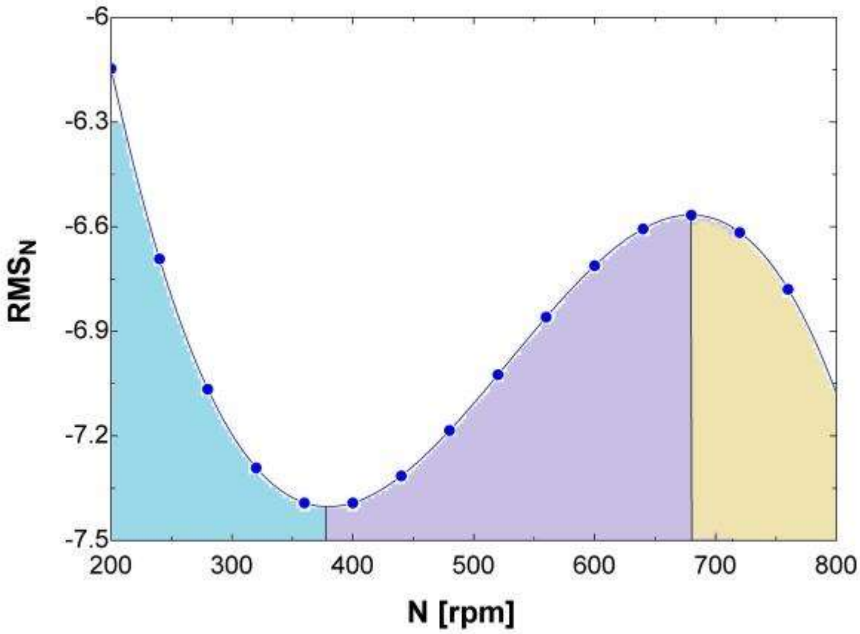

Fig.4.6 RMS values for variable rotation speed

4.4.1. Constraints

The typical adaptive control constraints (ACC) are: tool vibration, tool force, chip load, spindle power, and chip tool interface temperature. The constraint used for the present study is tool vibration.

4.4.2. Strategies and selection of input parameters

The strategies used for the implementation of the Adaptive control methodology the present application of tool vibration are:

- RMS Component Calculation by the regression equation.
- Compare the RMS Value with Constraints value.
- Find the responsible parameters for Tool Vibration.
- Generate signal for altering the responsible parameter.

Moreover, these strategies can be elaborated step-wise as follows. First, according to the application of the machining component, the roughness limit has been selected. Later, the feed rate for the tool has been calculated using the expression of surface roughness. The corner radius for the present study is taken as 0.8 mm. Later on, the selection of the maximum values of work-piece speed (N) and depth of cut (d_C) are defined. The next step is to find out the maximum value of vibration $\Delta X_{max\ g}$, $\Delta Y_{max\ g}$, $\Delta Z_{max\ g}$, and $RMS_{max\ g}$ from the regression equation developed in the earlier chapter using the 2nd order polynomial with cross-terms methodology. These values are used as the limiting values for adaptive control.

An agitator shaft is taken for the limit value of vibration calculation as an example.

Work-piece Speed (N): 200 to 800 rpm

Feed Rate (f): 0.12 to 0.15 mm/rev

Depth of Cut (dc): 0.1 to 0.8 mm

Surface roughness is required for agitator shaft: less than 3 µm

From the expression of surface roughness,

$$3 = \frac{f^2}{8 \times 0.8} \times 1000$$

f = 0.138 mm /rev

N = 800 rpm (Max value of bound)

d_C = 0.8 mm (Max value of bound)

Regression Equation for polynomial of order 3:

ΔX_{glimit}= 0.6770

ΔY_{glimit} = 0.6020

ΔZ_{glimit} = 0.4197

RMS_{glimit} = 0.5472

Predefined ranges of the study parameters i.e.feed, speed, depth of cut and diameter are as listed below.

- N = 0 to 1000 rpm
- f = 0.1 to .0.2 mm/rev

- d_c = 0 to 1 mm
- D = 25 to 50 mm

The observation of the vibration components and the respective overall RMS values for the defined L16 experimental sets have been tabulated below.

Table 4.1 RMS values for the corresponding input parameters and vibration components

Sr. No	Speed (*N*) (*RPM*)	Feed rate (*f*) (*mm/rev*)	Depth of cut (d_c) (*mm*)	Diameter (*D*) (*mm*)	ΔX_{max} *g*	ΔY_{max} *g*	ΔZ_{max} *g*	RMS
1	225	0.12	0.1	30	0.58	5.03	3.47	1.862794
2	225	0.13	0.3	35	0.22	0.12	0.41	0.640312
3	225	0.14	0.5	40	1.18	0.21	0.46	0.678233
4	225	0.15	0.7	45	0.97	0.24	0.31	0.556776
5	350	0.12	0.3	40	0.80	0.18	0.33	0.574456
6	350	0.13	0.1	45	0.65	0.10	0.16	0.4
7	350	0.14	0.7	30	0.81	0.23	0.31	0.556776
8	350	0.15	0.5	35	0.25	0.16	0.37	0.608276
9	500	0.12	0.5	45	1.31	0.69	1.58	1.256981
10	500	0.13	0.7	40	0.63	0.69	0.56	0.748331
11	500	0.14	0.1	35	1.12	0.21	0.36	0.6
12	500	0.15	0.3	30	0.19	0.17	0.25	0.5
13	800	0.12	0.7	35	1.51	1.21	1.65	1.284523
14	800	0.13	0.5	30	0.55	0.66	0.51	0.714143
15	800	0.14	0.3	45	0.60	0.36	0.88	0.938083
16	800	0.15	0.1	40	0.18	0.15	0.23	0.479583

4.5. Results Validation

The experimental observation for the input parameters: rotational speed (*N*) of the spindle i.e. work-piece, feed rate (*f*), depth of cut (DOC) (d_C), and the work-piece diameter (*D*) are presented in Table 4.2.

The regression equation using three different types of polynomials, i.e. second-order polynomial, third order polynomial, and second-order cross-term polynomial, as presented in the earlier section. Moreover, the expressions for the RMS value for all three types of a polynomial equation and all four independent variables (both combined and separate expressions of RMS) are formulated.

Based on the regression analysis, the vibration components are developed as tabulated in Table 4.3 and the percentage difference between the components of the respective vibration are presented in Table 4.4 along with the RMS values. Fig. 4.4, Fig. 4.5, and Fig. 4.6 depict the impact of individual parameters namely for depth of cut, feed rate, and rotation speed (rpm) respectively on RMS values.

Table 4.2 Experimental recordings

Sr. No.	**Speed (*N*) (*RPM*)**	**Feed rate (*f*) (*mm/rev*)**	**Depth of cut (d_c) (*mm*)**	**Diameter (*D*) (*mm*)**	$\Delta X_{max\ g}$	$\Delta Y_{max\ g}$	$\Delta Z_{max\ g}$
1	225	0.12	0.2	32	0.72	2.49	2.3
2	225	0.13	0.4	37	0.48	0.42	0.42
3	225	0.14	0.6	42	1.31	0.61	0.76
4	350	0.12	0.2	32	0.61	1.43	1.31
5	350	0.13	0.4	37	0.37	0.89	0.41
6	350	0.14	0.6	42	1.17	0.6	0.19
7	500	0.12	0.2	32	0.81	1.74	1.92
8	500	0.13	0.4	37	0.5	0.62	0.03
9	500	0.14	0.6	42	1.28	0.28	0.24
10	800	0.12	0.2	32	0.79	1.92	1.85
11	800	0.13	0.4	37	0.42	0.45	0.11
12	800	0.14	0.6	42	1.06	0.14	0.35

Table 4.3 Regression findings

Sr. No.	$\Delta X_{max\ g}$	$\Delta Y_{max\ g}$	$\Delta Z_{max\ g}$
1	0.7531	2.665	2.26
2	0.4506	0.3829	0.448
3	1.182	0.6605	0.6952
4	0.6431	1.432	1.39
5	0.3406	0.8496	0.422
6	1.072	0.572	0.1748
7	0.8281	1.705	1.785
8	0.5256	0.5771	0.02705
9	1.257	0.2995	0.2202
10	0.7256	1.86	1.915
11	0.4231	0.4221	0.103
12	1.155	0.1445	0.3502

Table 4.4 Percentage difference between experimental and regression results

Sr. No.	$\Delta X_{max\ g}$	$\Delta Y_{max\ g}$	$\Delta Z_{max\ g}$
1	-4.60	-7.03	1.74
2	6.13	8.83	-6.67
3	9.77	-8.28	8.53
4	-5.43	-0.14	-6.11
5	7.95	4.54	-2.93
6	8.38	4.67	8.00
7	-2.23	2.01	7.03
8	-5.12	6.92	9.83

9	1.80	-6.96	8.25
10	8.15	3.12	-3.51
11	-0.74	6.20	6.36
12	-8.96	-3.21	-0.06

Table 4.5 Validation of regression outcomes with reference to the experimental observations

Sr. No	Speed (*N*) (*RPM*)	Feed rate (*f*) (*mm/rev*)	Depth of cut (d_c) (*mm*)	Diameter (*D*) (*mm*)	Experimental Result			Regression Results			Difference (%)		
					$\Delta X_{max\,g}$	$\Delta Y_{max\,g}$	$\Delta Z_{max\,g}$	$\Delta X_{max\,g}$	$\Delta Y_{max\,g}$	$\Delta Z_{max\,g}$	$\Delta X_{max\,g}$	$\Delta Y_{max\,g}$	$\Delta Z_{max\,g}$
1	225	0.12	0.2	32	0.72	2.49	2.3	0.7531	2.665	2.26	-4.60	-7.03	1.74
2	225	0.13	0.4	37	0.48	0.42	0.42	0.4506	0.3829	0.448	6.13	8.83	-6.67
3	225	0.14	0.6	42	1.31	0.61	0.76	1.182	0.6605	0.6952	9.77	-8.28	8.53
4	350	0.12	0.2	32	0.61	1.43	1.31	0.6431	1.432	1.39	-5.43	-0.14	-6.11
5	350	0.13	0.4	37	0.37	0.89	0.41	0.3406	0.8496	0.422	7.95	4.54	-2.93
6	350	0.14	0.6	42	1.17	0.6	0.19	1.072	0.572	0.1748	8.38	4.67	8.00
7	500	0.12	0.2	32	0.81	1.74	1.92	0.8281	1.705	1.785	-2.23	2.01	7.03
8	500	0.13	0.4	37	0.5	0.62	0.03	0.5256	0.5771	0.0270	-5.12	6.92	9.83
9	500	0.14	0.6	42	1.28	0.28	0.24	1.257	0.2995	0.2202	1.80	-6.96	8.25
10	800	0.12	0.2	32	0.79	1.92	1.85	0.7256	1.86	1.915	8.15	3.12	-3.51
11	800	0.13	0.4	37	0.42	0.45	0.11	0.4231	0.4221	0.103	-0.74	6.20	6.36
12	800	0.14	0.6	42	1.06	0.14	0.35	1.155	0.1445	0.3502	-8.96	-3.21	-0.06

4.6. Summary

The aim of the present study was to perform the adaptive control methods to the machining tool application and validate the results with the regression formulations which compile the fourth objective of the work. The outcome of the study indicates that the percentage difference between the regression and experimental observations is found to be less than 10%. Hence, the proposed methodology is validated for the present application and can be used with decent reliability. The present study will benefit future researchers in defining the regression equations and using the same for different input conditions which will reduce the experimental cost requirements and will provide reliable predictions.

5. CONCLUSION

In the present study, the performance of the cutting tool subjected to vibration has been investigated which depends upon the operational parameters of the systems. Experiments are the most reliable means of investigating the vibration behavior of the cutting tool during the turning operation on the work-piece, and the empirical expressions developed based on the well-designed experimental observations give many reliable predictions. The core contribution of the present study is the application of the DOE approach with Taguchi and ANOVA techniques on the vibration study of cutting tool considering the four key variables: rotational speed (N) of the spindle i.e. work-piece, feed rate (f), depth of cut (DOC) (d_C) and the work-piece diameter (D). Based on the observations, the optimum parameter values identified are: N = 350 RPM, f = 0.15mm/rev, d_C = 0.3 mm and D = 40 mm. Moreover, the second-order polynomial equation with cross-terms has been identified as the more suitable regression expression than the second and third-order polynomial. The present study will benefit future researchers in defining the regression equations and using the same for different input conditions which will reduce the experimental cost requirements and will provide reliable predictions.

Moreover, the key findings of the present study are as listed below.

- Effect of feed rate on vibration is very high compared to other affecting parameters like speed, depth of cut, and diameter.
- Regression pattern studies show the effect of all 4 parameters on vibration with its pattern.
- DOE is a very important tool for experimental work and gives the effect of 64 experiments in 16 experiments.

- Seeing as vibration occurs in all three directions, the effect of three-dimensional vibration data is difficult to incorporate into the study adaptive control method. As a result, the RMS term aids in providing the vibration effect with a single term.
- Adaptive Control Constraint used to constraints the tool vibration and finding the affected parameter.
- By regression, the calculated component RMS value is useful to determine the effect of the affected parameter.
- By using this study further the affected parameter can be optimized using adaptive control techniques and fed into the system for reconsideration through experimentation or regression formulations.

5.1. FUTURE SCOPE

As the future work of the present study, the following research can be performed.

- Implementation of the adaptive control system by the same concept in current CNC machining operation for making them more vibration efficient.
    - For particular parameter sets of the available machine tool can be applied to the same algorithm to optimize the parameters.
- Investigation of the means of controlling tool vibration without changing the cutting parameters.
    - The affected tool vibration can be minimized by using a piezoelectric actuator as a secondary mass on the cutting tool to minimize tool vibration of the primary mass.
- The performance analysis of the implemented adaptive control system can be conducted for obtaining reliable results.

RESEARCH PUBLICATIONS

International Journal:

- "Performance assessment of cutting tools - a review", International Journal of Advanced Research in Engineering and Technology (IJARET), Vol:11, Issue:12,Pg.3202-3209, IAEME Publication - Scopus Indexed.
  Link: https://iaeme.com/Home/article_id/IJARET_11_12_302

  - "Cantilever Beam Analogy for the Performance Assessment of Cutting Tools", International Journal for Research in Engineering Application & Management (IJREAM), Vol:7, Issue:1,
  Link: https://www.ijream.org/IJREAM_V07I01.html
- "An experimental investigation on the performance of cutting tool under vibration behavior with variable system parameters", International journal of creative research thoughts, Vol:9, Issue:5.
  Link: http://www.ijcrt.org/papers/IJCRT2105528
- "Implementation of Adaptive Control for Cutting Tool Vibration Minimization", International Journal for Research in Engineering Application & Management (IJREAM), May 2021, Vol: 07 , Issue: 02.
  Link: https://www.ijream.org/IJREAM_V07I02.html

International Conference:

- "A Review on development of adaptive control system for tool vibration minimization and feed optimization for turning center", International Conference on Research and Innovations in Science, Engineering & Technology (ICRISET-2017), Vidhyanagar.

REFERENCES

[1] Cutting Tool Examples, Classification, Materials and geometric features (n.d.). http://www.minaprem.com/machining/cutter/introduction/what-is-a-cutting-tool-examples-classification-and-materials/ (accessed April 30, 2021).

[2] H. El-Hofy, Advanced Machining Processes: Nontraditional and Hybrid Machining Processes, McGraw-Hill, 2005. https://doi.org/10.1036/0071466940.

[3] H.N. Gupta, R.C. Gupta, A. Mittal, Manufacturing Processes, Second Edi, New Age Publishers, 2009.

[4] A. Kumar, Single Point Cutting Tool-Definition, Geometry, Nomenclature, Angle., Learn Eng. (n.d.). https://learnmechanical.com/single-point-cutting-tool/ (accessed May 31, 2021).

[5] CNC Cook Book, Chatter in Machining: Milling & Lathe Vibration [Easy Guide], (n.d.). https://www.cnccookbook.com/chatter-in-machining-milling-lathe-vibration/ (accessed May 31, 2021).

[6] V. Georgiev, I. Chetrokov, RaDMI 2005 04 - 07., in: 5th Int. Conf. ″Research, 2005: pp. 147–152.

[7] G.C. Balan, THE IMPROVEMENT OF MACHINE-TOOLS DYNAMIC BEHAVIOUR WITH ADAPTIVE FUZZY CONTROL SYSTEMS (8-th PART) base Inputs Scaling factors Fuzzification Inferenc e Defuzzificatio Process Outputs Scaling factors Transducers, (n.d.).

[8] S.N. Mahmoodi, M.J. Craft, S.C. Southward, M. Ahmadian, Active vibration control using optimized modified acceleration feedback with Adaptive Line Enhancer for frequency tracking, J. Sound Vib. 330 (2011) 1300–1311. https://doi.org/10.1016/j.jsv.2010.10.013.

[9] A. Un, Intelligent adaptive control and monitoring of band sawing using a neural-

fuzzy system, J. Mater. Process. Technol. 9 (2008) 2302–2313. https://doi.org/10.1016/j.jmatprotec.2008.05.031.

[10] Y. Liu, T. Cheng, L. Zuo, Adaptive control constraint of machining processes, Int. J. Adv. Manuf. Technol. 17 (2001) 720–726. https://doi.org/10.1007/s001700170117.

[11] T. Watanabe, S. Iwai, Design of an Adaptive Control Constraint System of a Milling Machine Tool., IFAC Proc. Vol. 16 (1983) 553–564. https://doi.org/10.1016/s1474-6670(17)61737-3.

[12] A. Holovatyy, V. Teslyuk, M. Iwaniec, M. Mashevska, Development of a system for monitoring vibration accelerations based on the Raspberry Pi microcomputer and the ADXL345 accelerometer, Eastern-European J. Enterp. Technol. 6 (2017) 52–62. https://doi.org/10.15587/1729-4061.2017.116082.

[13] F. Aswin, I. Dwisaputra, R. Afriansyah, Online vibration monitoring system for rotating machinery based on 3-axis MEMS accelerometer, J. Phys. Conf. Ser. 1450 (2020). https://doi.org/10.1088/1742-6596/1450/1/012109.

[14] A. Hjort, Department of Physics and Astronomy Measuring mechanical vibrations using an Arduino as a slave I / O to an EPICS control system as a slave I / O to an EPICS control system, Dep. Phys. Astron. Uppsala Univ. 4 (2015).

[15] A.S.R. Murty, K. Teja, S. Naveen, Lathe performance monitoring using iot, Int. J. Mech. Eng. Technol. 9 (2018) 494–501.

[16] L. Abraham, P. Trivandrum, Vibration Monitoring Using MEMS Digital Accelerometer with ATmega and LabVIEW Interface for Space Application, IJISET-International J. Innov. Sci. Eng. Technol. 1 (2014) 3–7.

[17] N. Fang, P.S. Pai, S. Mosquea, Effect of tool edge wear on the cutting forces and vibrations in high-speed finish machining of Inconel 718: An experimental study

and wavelet transform analysis, Int. J. Adv. Manuf. Technol. 52 (2011) 65–77. https://doi.org/10.1007/s00170-010-2703-6.

[18] N. Mandal, B. Doloi, B. Mondal, R. Das, Optimization of flank wear using Zirconia Toughened Alumina (ZTA) cutting tool: Taguchi method and Regression analysis, Meas. J. Int. Meas. Confed. 44 (2011) 2149–2155. https://doi.org/10.1016/j.measurement.2011.07.022.

[19] A. Epureanu, V. Teodor, On-Line Geometrical Identification of Reconfigurable Machine Tool using Virtual Machining, World Acad. Sci. Eng. Technol. 15 (2006) 14–18.

[20] K.J. Kalinski, M.A. Galewski, Chatter vibration surveillance by the optimal-linear spindle speed control, Mech. Syst. Signal Process. 25 (2011) 383–399. https://doi.org/10.1016/j.ymssp.2010.09.005.

[21] A. Al-shayea, F.M. Abdullah, M.A. Noman, H. Kaid, E.A. Nasr, Studying and Optimizing the Effect of Process Parameters on Machining Vibration in Turning Process of AISI 1040 Steel, Adv. Mater. Sci. Eng. (2020).

[22] A. Siddhpura, R. Paurobally, A review of flank wear prediction methods for tool condition monitoring in a turning process, Int. J. Adv. Manuf. Technol. 65 (2013) 371–393. https://doi.org/10.1007/s00170-012-4177-1.

[23] M. Wiercigroch, E. Budak, Sources of nonlinearities, chatter generation and suppression in metal cutting, Philos. Trans. R. Soc. A Math. Phys. Eng. Sci. 359 (2001) 663–693. https://doi.org/10.1098/rsta.2000.0750.

[24] M.N. Hamdan, A.E. Bayoumi, An approach to study the effects of tool geometry on the primary chatter vibration in orthogonal cutting, J. Sound Vib. 128 (1989) 451–469. https://doi.org/10.1016/0022-460X(89)90785-2.

[25] E. Bagci, Monitoring and analysis of MRR-based feedrate optimization approach

and effects of cutting conditions using acoustic sound pressure level in free-form surface milling, Sci. Res. Essays. 6 (2011) 256–277.

[26] S.J. Zhang, S. To, G.Q. Zhang, Z.W. Zhu, A review of machine-tool vibration and its influence upon surface generation in ultra-precision machining, Int. J. Mach. Tools Manuf. 91 (2015) 34–42. https://doi.org/10.1016/j.ijmachtools.2015.01.005.

[27] K.H. Hajikolaei, H. Moradi, G. Vossoughi, M.R. Movahhedy, Spindle speed variation and adaptive force regulation to suppress regenerative chatter in the turning process, J. Manuf. Process. 12 (2010) 106–115. https://doi.org/10.1016/j.jmapro.2010.08.002.

[28] N.V.S. Shankar, A.G. Chand, K.H. Rao, K.P. Sai, Low Cost Vibration Measurement and Optimization During Turning Process, Adv. Mater. Res. 1148 (2018) 103–108. https://doi.org/10.4028/www.scientific.net/AMR.1148.103.

[29] N.V.S. Shankar, H.R. Shankar, N.P. Kumar, K. Saichandu, Process Parameter Optimization for Minimizing Vibrations and Surface Roughness During Turning EN19 Steel Using Coated Carbide Tool, Mater. Today Proc. 24 (2020) 788–797. https://doi.org/10.1016/j.matpr.2020.04.387.

[30] V. Sivaraman, L. Vijayaraghavan, S. Sankaran, Effect of Vibration on Surface Texture during Machining Multiphase Microalloyed Steel, Procedia Manuf. 10 (2017) 429–435. https://doi.org/10.1016/j.promfg.2017.07.019.

[31] P. Bansal, I.S.R. Vedaraj, Monitoring and Analysis of Vibration Signal in Machine Tool Structures, IJEDR. 2 (2014) 2310–2317.

[32] M. Girish Kumar, P. Vinod, P. V Shashikumar, Investigation and Analysis of Chatter Vibration in Centerless Bar Turning Machine, 2014.

[33] G. Quintana, J. Ciurana, Chatter in machining processes: A review, Int. J. Mach.

Tools Manuf. 51 (2011) 363–376. https://doi.org/10.1016/j.ijmachtools.2011.01.001.

[34] N. Hassan, Development of A Dynamic Model For Vibration During Turning Operation And Numerical Studies, 2014.

[35] I.B. Ã, L. Gallimard, S. Nikoukar, Optimal piezoelectric actuator and sensor location for active vibration control , using genetic algorithm, J. Sound Vib. 329 (2010) 1615–1635. https://doi.org/10.1016/j.jsv.2009.12.001.

[36] Y. Boz, O. Demir, I. Lazoglu, Model Based Feedrate Scheduling for Free-Form Surface Machining, Internaitonal J. Autom. Technol. 4 (2010) 3–4.

[37] N. Tsai, D. Chen, R. Lee, B. Wang, Milling Chatter Prevention by Adaptive Spindle Speed Tuning, World Acad. Sci. Eng. Technol. (2010) 597–602.

[38] L.N. Lo, I. Bediaga, J. Mun, International Journal of Machine Tools & Manufacture An automatic spindle speed selection strategy to obtain stability in high-speed milling, Int. J. Mach. Tools Manuf. 49 (2009) 384–394. https://doi.org/10.1016/j.ijmachtools.2008.12.003.

[39] F. Cus, U. Zuperl, E. Kiker, M. Milfelner, Adaptive self-learning controller design for feedrate maximisation of machining process, J. Achiev. Mater. Manuf. Eng. 31 (2008) 469–476.

[40] F. Cus, U. Zuperl, Model reference adaptive force and surface roughness control in milling, J. Achiev. Mater. Manuf. Eng. 26 (2008) 179–182.

[41] A. Turksoy, Y. Hames, A. Teke, M.B. Latran, A novel adaptive switching method to reduce DC-Link capacitor ripple in PV based grid-connected inverter, Sol. Energy. 173 (2018) 702–714. https://doi.org/10.1016/j.solener.2018.08.002.

[42] I. Mane, V.Ã. Gagnol, B.C. Bouzgarrou, P. Ray, Stability-based spindle speed control during flexible workpiece high-speed milling, Int. J. Mach. Tools Manuf.

48 (2008) 184–194. https://doi.org/10.1016/j.ijmachtools.2007.08.018.

[43] R.L. Hecker, G.M. Flores, Q. Xie, R. Haran, SERVOCONTROL OF MACHINE-TOOLS : A REVIEW, Letin Am. Appl. Res. 94 (2008) 85–94.

[44] R.P. Sharma, P.P. Tiwary, K. V. Modi, R.K. Singh, S. Sharma, V.R. Satsangi, Spatio-temporal evolution of magnetosonic wave in the laser plasma interaction, Phys. Plasmas. 22 (2015). https://doi.org/10.1063/1.4921132.

[45] J. V Abellan, F. Romero, H.R. Siller, A. Estruch, C. Vila, Adaptive Control Optimization of Cutting Parameters for High Quality Machining Operations based on Neural Networks and Search Algorithms, in: Adv. Robot. Autom. Control, 2008: pp. 1–20.

[46] K. Shirase, K. Nakamoto, E. Arai, T. Moriwaki, Real-Time Five-Axis Control Based on Digital Copy Milling Concept to Achieve Autonomous Milling, Int. J. Autom. Technol. 2 (2008) 2–3.

[47] S.Y. Kassab, Y.K. Khoshnaw, The Effect of Cutting Tool Vibration on Surface Roughness of Workpiece in Dry Turning Operation, Eng. Technol. 25 (2007) 879–889.

[48] Analog Devices, ADXL335 - Small, Low Power, 3-Axis ±3 g Accelerometer, (2010) 16. http://www.analog.com/media/en/technical-documentation/data-sheets/ADXL335.pdf.

[49] B.S. Prasad, D.S. Prasad, A. Sandeep, G. Veeraiah, Condition monitoring of CNC machining using adaptive control, Int. J. Autom. Comput. 10 (2013) 202–209. https://doi.org/10.1007/s11633-013-0713-1.

[50] PWE, Vibration - an age-old problem! - Plant & Works Engineering, 2014.

[51] S.A. TOBIAS, W. FISHWICK, Theory of regenerative machine tool chatter, 1958.

[52] T.G. Chuah, J. Gimbun, T.S.Y. Choong, A CFD study of the effect of cone dimensions on sampling aerocyclones performance and hydrodynamics, Powder Technol. 162 (2006) 126–132. https://doi.org/10.1016/j.powtec.2005.12.010.

[53] Farnell, Arduino Uno Datasheet, (2013) 1–4. https://www.farnell.com/datasheets/1682209.pdf.

[54] N. Balabhadra, S. Ugender, Effects of Cutting Variables on MRR and Tool Wear for EN8 Medium Carbon Steel with carbide insert, 2015. www.ijiset.com (accessed May 7, 2021).

[55] K. V. Modi, H.K. Jani, I.D. Gamit, Impact of orientation and water depth on productivity of single-basin dual-slope solar still with Al2O3 and CuO nanoparticles, J. Therm. Anal. Calorim. (2020). https://doi.org/10.1007/s10973-020-09351-1.

[56] H.K. Jani, K. V. Modi, Experimental performance evaluation of single basin dual slope solar still with circular and square cross-sectional hollow fins, Sol. Energy. 179 (2019) 186–194. https://doi.org/10.1016/j.solener.2018.12.054.

[57] R.P.N. Ayuthaya, P. Namprakai, W. Ampun, The thermal performance of an ethanol solar still with fin plate to increase productivity, Renew. Energy. 54 (2013) 227–234. https://doi.org/10.1016/j.renene.2012.08.004.

[58] K. Elsayed Khairy, C. Lacor, Optimization of the cyclone separator geometry for minimum pressure drop using mathematical models and CFD simulations, Chem. Eng. Sci. 65 (2010) 6048–6058. https://doi.org/10.1016/j.ces.2010.08.042.

[59] A. González-Laguna, J. Barreiro, A. Fernández-Abia, E. Alegre, V. González-Castro, Design of a TCM System Based on Vibration Signal for Metal Turning Processes, Procedia Eng. 132 (2015) 405–412. https://doi.org/10.1016/j.proeng.2015.12.512.

[60] W.P. Goss, R.G. Miller, Thermal properties of wood and wood products. In: Proceedings of thermal performance of the exterior envelopes of buildings, ASHRAE. (1992) 193–203. https://pdfs.semanticscholar.org/fc70/4903c8196894acfd4618fb48946d6927905b.pdf.

[61] F. Abdulhani, J. ALswede, Study Of Vibration For CNC Machine At Difference Feed, Int. J. Adv. Res. Technol. 3 (2014) 21–29.

[62] L. Kirkup, R. Frenkel, An introduction to uncertainty in measurement using the GUM (guide to the expression of uncertainty in measurement), 1st ed., Cambridge University Press, Cambridge, 2006.

[63] E.T. Pérez, Study of vibration severity assessment for Machine Tool spindles within Condition Monitoring, KTH - Vetenskap Och Konst, 2015.

[64] P.K. Chaviaropoulos, E.S. Politis, D.J. Lekou, R. Energy, S. Cres, Enhancing the Damping the DAMPBLADE Project, Renew. Energy. 5 (2006) 163–177. https://doi.org/10.1002/we.

[65] M. Lovric, International Encyclopedia of Statistical Science, Int. Encycl. Stat. Sci. (2010) 1653–54. https://doi.org/10.1007/978-3-642-04898-2.

[66] D. Mentis, Wind Energy Assessment in Africa A GIS-based approach, (2013) 76. https://www.diva-portal.org/smash/get/diva2:640338/FULLTEXT01.pdf.

[67] A. Sharafati, K. Khosravi, P. Khosravinia, K. Ahmed, S.A. Salman, Z.M. Yaseen, S. Shahid, The potential of novel data mining models for global solar radiation prediction, Int. J. Environ. Sci. Technol. 16 (2019) 7147–7164. https://doi.org/10.1007/s13762-019-02344-0.

[68] S. Abhishek, M. Mujumdar, A. Pandey, A. Jain, ISSN NO : 2394-8442 A Review paper on vibration analysis of Lath machine, 5 (2018) 836–838.

[69] A. Verhoef, A. Stoffelen, Validation of ASCAT 12.5 km winds, (2013) 1–11.

[70] L. Liberti, A. Carillo, G. Sannino, Wave energy resource assessment in the Mediterranean, the Italian perspective, Renew. Energy. 50 (2013) 938–949. https://doi.org/10.1016/j.renene.2012.08.023.

[71] A. Abilgaziyev, N. Nogerbek, L. Rojas-Solórzano, Mohammadjavad, A. Shahrabi, A. Abilgaziyev, N. Nogerbek, L. Rojas-Sol´orzano, Design Optimization of an Oil-Air Catch Can Separation System, J. Transp. Technol. 05 (2015) 247–262. https://doi.org/10.4236/jtts.2015.54023.

[72] G.K. Uyanık, N. Güler, A Study on Multiple Linear Regression Analysis, Procedia - Soc. Behav. Sci. 106 (2013) 234–240. https://doi.org/10.1016/j.sbspro.2013.12.027.

[73] F. Veronesi, S. Grassi, M. Raubal, Statistical learning approach for wind resource assessment, Renew. Sustain. Energy Rev. 56 (2016) 836–850. https://doi.org/10.1016/j.rser.2015.11.099.

[74] A.M. Foley, P.G. Leahy, A. Marvuglia, E.J. McKeogh, Current methods and advances in forecasting of wind power generation, Renew. Energy. 37 (2012) 1–8. https://doi.org/10.1016/j.renene.2011.05.033.

[75] K. Sørby, Development and Optimization of Vibration-Damped Tool Holders for High Length-to-Diameter Boring Operations, High Speed Mach. 2 (2017) 51–58. https://doi.org/10.1515/hsm-2016-0005.

[76] S. Mathew, Wind energy: Fundamentals, resource analysis and economics, Springer, 2007. https://doi.org/10.1007/3-540-30906-3.

[77] S.K. DASH, Multi Objective Optimization of Cutting Parameters in Turning Operation of Stainless Steel (Ss304) To Reduce Surface Roughness and Cutting Forces, Int. J. Mech. Eng. Technol. 6 (2012) 976–6340.

[78] S.V.V. Arun Kumar, G. Nagababu, R. Kumar, Comparative study of offshore winds and wind energy production derived from multiple scatterometers and met buoys, Energy. 185 (2019) 599–611. https://doi.org/10.1016/j.energy.2019.07.064.

[79] C.B. Hasager, M. Badger, A. Peña, X.G. Larsén, F. Bingöl, SAR-based wind resource statistics in the Baltic Sea, Remote Sens. 3 (2011) 117–144. https://doi.org/10.3390/rs3010117.

[80] R. Dev, H.N. Singh, G.N. Tiwari, Characteristic equation of double slope passive solar still, Desalination. 267 (2011) 261–266. https://doi.org/10.1016/j.desal.2010.09.037.

[81] R. Ibrahim, Vibration Assisted Machining : Modelling, Simulation, Optimization, Control and Applications, Uthm. (2010) 1–216.

[82] S.C. Pryor, J. Ledolter, Addendum to "Wind speed trends over the contiguous United States," J. Geophys. Res. Atmos. 115 (2010) 10103. https://doi.org/10.1029/2009JD013281.

[83] R.R. Moreno, A.M. Pérez, R.B. Pérez, Numerical optimization of a heat exchanger with slit fins and vortex generators using genetic algorithms, Int. J. Refrig. 119 (2020) 247–256. https://doi.org/10.1016/j.ijrefrig.2020.07.023.

[84] H.K. Ghritlahre, R.K. Prasad, Exergetic performance prediction of solar air heater using MLP, GRNN and RBF models of artificial neural network technique, J. Environ. Manage. 223 (2018) 566–575. https://doi.org/10.1016/j.jenvman.2018.06.033.

[85] Y. Pramudya, M. Islamiah, Vibration characteristics study on observatory using accelerometer ADXL345 sensor and Arduino, AIP Conf. Proc. 2169 (2019). https://doi.org/10.1063/1.5132658.

[86] B. Lin, Y. Chen, Impacts of policies on innovation in wind power technologies in China, Appl. Energy. 247 (2019) 682–691. https://doi.org/10.1016/j.apenergy.2019.04.044.

[87] X. Zhao, S. Li, S. Zhang, R. Yang, S. Liu, The effectiveness of China's wind power policy: An empirical analysis, Energy Policy. 95 (2016) 269–279. https://doi.org/10.1016/j.enpol.2016.04.050.

[88] G. Bekele, STUDY INTO THE POTENTIAL AND FEASIBILITY OF A STANDALONE SOLAR- WIND HYBRID ELECTRIC ENERGY SUPPLY For Application in Ethiopia, 2009.

[89] Y. Wang, Q. Hu, L. Li, A.M. Foley, D. Srinivasan, Approaches to wind power curve modeling: A review and discussion, Renew. Sustain. Energy Rev. 116 (2019) 109422. https://doi.org/10.1016/j.rser.2019.109422.

[90] V. Patel, M. Patel, Development of Smart Sensing Unit for Vibration Measurement by Embedding Accelerometer with the Arduino Microcontroller, Int. J. Instrum. Sci. 6 (2017) 1–7. https://doi.org/10.5923/j.instrument.20170601.01.

[91] A. Chakraborty, R. Kumar, A. Stoffelen, Validation of ocean surface winds from the OCEANSAT-2 scatterometer using triple collocation, Remote Sens. Lett. 4 (2013) 85–94. https://doi.org/10.1080/2150704X.2012.693967.

[92] M. Taki, A. Rohani, H. Yildizhan, R. Farhadi, Energy-exergy modeling of solar radiation with most influencing input parameters, Energy Sources, Part A Recover. Util. Environ. Eff. 41 (2019) 2128–2144. https://doi.org/10.1080/15567036.2018.1550126.

[93] T.V. Arjunan, H.Ş. Aybar, N. Nedunchezhian, Effect of sponge liner on the internal heat transfer coefficients in a simple solar still, Desalin. Water Treat. 29

(2011) 271–284. https://doi.org/10.5004/dwt.2011.1638.

[94] S. Liu, W. Huang, Z. Bao, T. Zeng, M. Qiao, J. Meng, Analysis, prediction and multi-objective optimization of helically coiled tube-in-tube heat exchanger with double cooling source using RSM, Int. J. Therm. Sci. 159 (2021) 106568. https://doi.org/10.1016/j.ijthermalsci.2020.106568.

[95] J. Jurasz, A. Beluco, F.A. Canales, The impact of complementarity on power supply reliability of small scale hybrid energy systems, Energy. 161 (2018) 737–743. https://doi.org/10.1016/j.energy.2018.07.182.

[96] A. Okninski, On use of hybrid rocket propulsion for suborbital vehicles, Acta Astronaut. 145 (2018) 1–10. https://doi.org/10.1016/j.actaastro.2018.01.027.

[97] S. Yafei, T. Yongjun, S. Jing, N. Dongjie, Effect of temperature and composition on thermal properties of carbon steel, 2009 Chinese Control Decis. Conf. CCDC 2009. (2009) 3756–3760. https://doi.org/10.1109/CCDC.2009.5191721.

[98] V. Glazar, A. Trp, K. Lenic, Optimization of air-water microchannel heat exchanger using response surface methodology, Int. J. Heat Mass Transf. 157 (2020) 119887. https://doi.org/10.1016/j.ijheatmasstransfer.2020.119887.

[99] P.K. Sharma, V. Warudkar, S. Ahmed, Application of lidar and measure correlate predict method in offshore wind resource assessments, J. Clean. Prod. 215 (2019) 534–543. https://doi.org/10.1016/j.jclepro.2018.12.267.

[100] S. Kulkarni, M.C. Deo, S. Ghosh, Changes in the design and operational wind due to climate change at the Indian offshore sites, Mar. Struct. 37 (2014) 33–53. https://doi.org/10.1016/j.marstruc.2014.02.005.

[101] F.J. Santos-Alamillos, D. Pozo-Vázquez, J.A. Ruiz-Arias, V. Lara-Fanego, J. Tovar-Pescador, Analysis of Spatiotemporal Balancing between Wind and Solar Energy Resources in the Southern Iberian Peninsula, J. Appl. Meteorol. Climatol.

51 (2012) 2005–2024. https://doi.org/10.1175/JAMC-D-11-0189.1.

[102] O. Charrouf, A. Betka, S. Abdeddaim, A. Ghamri, Artificial Neural Network power manager for hybrid PV-wind desalination system, Math. Comput. Simul. 167 (2020) 443–460. https://doi.org/10.1016/j.matcom.2019.09.005.

[103] R.B. Stull, An Introduction to Boundary Layer Meteorology, 1988. https://doi.org/10.1007/978-94-009-3027-8.

[104] J. Bosch, I. Staffell, A.D. Hawkes, Temporally explicit and spatially resolved global offshore wind energy potentials, Energy. 163 (2018) 766–781. https://doi.org/10.1016/j.energy.2018.08.153.

[105] M. Rezaei, A. Mostafaeipour, M. Qolipour, R. Tavakkoli-Moghaddam, Investigation of the optimal location design of a hybrid wind-solar plant: A case study, Int. J. Hydrogen Energy. 43 (2018) 100–114. https://doi.org/10.1016/j.ijhydene.2017.10.147.

[106] E.. Kussul, L.M. Kasatkina, D.A. Rachkovskij, D.C. Wunsch, Appliavation of Random Threshold Neural Networks for Diagnostics of Micro Machine Tool Condition, (1998) 241–244.

[107] G. Balan, The improvement of machine tools dynamic behaviour with adaptive fuzzy control systems (2nd Part), Ann. "Dunarea Jos" Univ. Galati. (1998).

[108] M. Liang, T. Yeap, A. Hermansyah, S. Rahmati, Fuzzy control of spindle torque for industrial CNC machining, Int. J. Mach. Tools Manuf. 43 (2003) 1497–1508. https://doi.org/10.1016/S0890-6955(03)00166-4.

[109] F. Cus, U. Zuperl, E. Kiker, M. Milfelner, Adaptive controller design for feedrate maximization of machining process, J. Achiev. Mater. Manuf. Eng. 17 (2006) 237–240.

[110] Y.S. Tarng, H.Y. Chuang, W.T. Hsu, Intelligent cross-coupled fuzzy feedrate

controller design for CNC machine tools based on genetic algorithms, Int. J. Mach. Tools Manuf. 39 (1999) 1673–1692.

[111] A.R. Kashani, J.W. Sutherland, Adaptive feedforward control for periodic diturbance rejection with application to machining processes, (n.d.).

[112] Y. Koren, Adaptive Control Systems for Machining, Manuf. Perspect. (1989).

APPENDIX A1: MATLAB CODE FOR ROTATING BEAM ANALYSIS

```
clc clear

L=input('Length of Test Speciman in m:    ');

Rho=input('Density of Test Speciman in kg/m3:    '); e=input('Young Modulus of
Test Speciman in GPa:    '); d=input('Diameter of Test Speciman in m:    ');

E=e*(10^9);
% Area Moment of Inertia, m4
I=pi*d*d*d*d/64; A=pi*d*d/4; % Cross-section area of bar, m2

fprintf('\n') fprintf('\n')


disp('Select your condition') disp('1 = Cantiliver Condition')
disp('2 = Clamped Clamped Condition') disp('3 = Clamped and
Supported Condition') disp('4 = Simply Supported Condition')

fprintf('\n') fprintf('\n') n = input('Enter a
number: ');

switch n     case
1
% Cantiliver Beam for i=1:4
X=[1.8573 4.6941 7.8548 10.9955];
B(i)=X(i)/L;

% Natural Frequency,rad/s
```

```
Wn(i)=B(i)*B(i)*[((E*I)/(Rho*A))^0.5];

% Natural Frequency,Hz
F(i)=Wn(i)/(2*pi);

% RPM
N(i)=F(i)*60; end


case 2
    % Clamped Clamped Condition for i=1:4
X=[4.7301 7.8532 10.99561 14.1372];
B(i)=X(i)/L;

% Natural Frequency, rad/s Wn(i)=B(i)*B(i)*[((E*I)/(Rho*A))^0.5];

% Natural Frequency,Hz
F(i)=Wn(i)/(2*pi);

% RPM
N(i)=F(i)*60; end


case 3
     % Clamped Supported Condition for i=1:4
X=[3.926602 7.068883 10.2103176 13.351768];
B(i)=X(i)/L;

% Natural Frequency,rad/s
```

```
Wn(i)=B(i)*B(i)*[((E*I)/(Rho*A))^0.5];

% Natural Frequency,Hz
F(i)=Wn(i)/(2*pi);

% RPM
N(i)=F(i)*60; end



case 4
% Simply Supported Condition for i=1:4
X=[pi 2*pi 3*pi 4*pi];
B(i)=X(i)/L;

% Natural Frequency,rad/s
Wn(i)=B(i)*B(i)*[((E*I)/(Rho*A))^0.5];

% Natural Frequency,Hz
F(i)=Wn(i)/(2*pi);

% RPM
N(i)=F(i)*60; end


otherwisefprintf('\n')   disp('Select Proper Value') end


fprintf('\n') fprintf('\n')


Wn
```

F

N

```
Mode=[1 2 3 4]; plot(Mode,Wn,'b-o')
```

APPENDIX A2: ARDINO UNO CODE

```
#include <math.h>

constintx_out = A1; /* connect x_out of module to A1 of UNO board */

constinty_out = A2; /* connect y_out of module to A2 of UNO board */

constintz_out = A3; /* connect z_out of module to A3 of UNO board */



void setup() {

  Serial.begin(9600);

}

void loop() {

  intx_adc_value, y_adc_value, z_adc_value;

  doublex_g_value, y_g_value, z_g_value;

  double roll, pitch, yaw;

  x_adc_value = analogRead(x_out); /* Digital value of voltage on x_out pin */

  y_adc_value = analogRead(y_out); /* Digital value of voltage on y_out pin */

  z_adc_value = analogRead(z_out); /* Digital value of voltage on z_out pin */

  Serial.print("x = ");

  Serial.print(x_adc_value);

  Serial.print("\t\t");

  Serial.print("y = ");

  Serial.print(y_adc_value);

  Serial.print("\t\t");

  Serial.print("z = ");

  Serial.print(z_adc_value);
```

```
  Serial.print("\t\t");
  //delay(100);


  x_g_value = ( ( ( (double)(x_adc_value * 5)/1024) - 1.65 ) / 0.330 );
  y_g_value = ( ( ( (double)(y_adc_value * 5)/1024) - 1.65 ) / 0.330 );
  z_g_value = ( ( ( (double)(z_adc_value * 5)/1024) - 1.80 ) / 0.330 );


  roll = ( ( (atan2(y_g_value,z_g_value) * 180) / 3.14 ) + 180 ); /* Formula for roll
*/
  pitch = ( ( (atan2(z_g_value,x_g_value) * 180) / 3.14 ) + 180 ); /* Formula for
pitch */
  //yaw = ( ( (atan2(x_g_value,y_g_value) * 180) / 3.14 ) + 180 ); /* Formula for
yaw */
  /* Not possible to measure yaw using accelerometer. Gyroscope must be used if
yaw is also required */
  Serial.print("Roll = ");
  Serial.print(roll);
  Serial.print("\t");
  Serial.print("Pitch = ");
  Serial.print(pitch);
  Serial.print("\n\n");
  delay(1000);
}
```

APPENDIX A3: MATLAB CODE FORADAPTIVECONTROL SYSTEM

❖ Coding

```
clc
clear
%Cantiliver Beam%
DeltaXg_Limit = 5;
DeltaYg_Limit = 5;
DeltaZg_Limit = 5;
RMS_Limit = 5;
fprintf('\n')
disp('<strong>Define the input parameters</strong>')
fprintf('\n')
N=input('Rotating Speed of Workpiece in rpm:    ');
f=input('Feed Rate in mm/rev:   ');
dc=input('Depth of Cut in mm:    ');
D=input('Diameter of Workpiece in mm:    ');
fprintf('\n')


disp('Calculation of Maximum Value of DeltaXg, DeltaYg, DeltaZg
and RMS by Regression Equation')
fprintf('\n')
disp('Regression Equation Calculation is based on Experimental
Result')
fprintf('\n')
%
disp('Regression Equation for Polynomial Order: 3')
```

```
DeltaXg=7.33530507E+02-1.24230500E-02*N+2.85956522E-05*N^2-
1.94519104E-08*N^3-1.72466250E+04*f+1.28100000E+05*f^2-
3.16250000E+05*f^3-7.30364583E+00*dc+2.11718750E+01*dc^2-
1.58854166E+01*dc^3+3.29933333E+00*D-8.79500000E-
02*D^2+7.76666667E-04*D^3;
DeltaYg=6.29908509E+02-6.31605051E-02*N+1.27244444E-04*N^2-
7.88686869E-08*N^3-1.16250000E+04*f+8.27625000E+04*f^2-
1.96250000E+05*f^3-1.96984375E+01*dc+4.44843750E+01*dc^2-
3.01562500E+01*dc^3-5.49633333E+00*D+1.34750000E-01*D^2-
1.09666666E-03*D^3;
DeltaZg=7.51744006E+02-5.23529293E-02*N+1.09244444E-04*N^2-
6.91717172E-08*N^3-1.66509167E+04*f+1.20625000E+05*f^2-
2.90833333E+05*f^3-1.26260416E+01*dc+3.19062500E+01*dc^2-
2.36458333E+01*dc^3+2.19466667E+00*D-6.80000000E-
02*D^2+6.73333333E-04*D^3;
RMS=8.44783170E+02-4.79379013E-02*N+9.84302805E-05*N^2-
6.19620452E-08*N^3-1.80547823E+04*f+1.31698731E+05*f^2-
3.19666661E+05*f^3-1.56464327E+01*dc+3.79947789E+01*dc^2-
2.70420760E+01*dc^3-6.32666246E-01*D+8.62136247E-03*D^2-
1.08656866E-05*D^3;

RMS_abs=abs(RMS);
fprintf('\n')

ifRMS_abs>RMS_Limit
    RMS
disp('<strong>Result: Vibration Value Exeeds the Limit</strong>')

disp('RMS Components')
RMS_N=-4.79379013E-02*N+9.84302805E-05*N^2-6.19620452E-08*N^3;
```

```
RMS_f=-1.80547823E+04*f+1.31698731E+05*f^2-3.19666661E+05*f^3;
RMS_dc=-1.56464327E+01*dc+3.79947789E+01*dc^2-2.70420760E+01*dc^3;
RMS_D=-6.32666246E-01*D+8.62136247E-03*D^2-1.08656866E-05*D^3;

disp('RMS Components Absolute Value')
RMS_N_abs=abs(RMS_N);
RMS_f_abs=abs(RMS_f);
RMS_dc_abs=abs(RMS_dc);
RMS_D_abs=abs(RMS_D);

RMS_Components = [RMS_N_absRMS_f_absRMS_dc_absRMS_D_abs];
RMS_Component_Max = max(RMS_Components);

[m,pos] = max(RMS_Components);

ifpos==1
disp('High Vibration because of Rotating Speed of Workpiece');
elseifpos==2
disp('High Vibration because of Feed Rate');
elseifpos==3
disp('High Vibration because of Depth of Cut');
elseifpos==4
disp('High Vibration because of Diameter of Workpiece')   ;
end
disp('Reduce the input value of affecting parameter')
else
disp(' <strong>Result: Vibration value is under limit</strong>')
DeltaXg
DeltaYg
DeltaZg
```

```
RMS

end
```

❖ Output cases

Result 1:

```
Define the input parameters

Rotating Speed of Workpiece in rpm:    225
Feed Rate in mm/rev:    0.12
Depth of Cut in mm:    0.1
Diameter of Workpiece in mm:    30

Calculation of Maximum Value of DeltaXg, DeltaYg, DeltaZg and RMS by Regression Equation

Regression Equation Calculation is based on Experimental Result

Regression Equation for Polynomial Order: 3

 Result: Vibration value is under limit

DeltaXg =

    0.7869


DeltaYg =

    4.1206


DeltaZg =

    2.8900


RMS =

    3.0524
```

Result 2:

```
Define the input parameters

Rotating Speed of Workpiece in rpm:    225
Feed Rate in mm/rev:    0.2
Depth of Cut in mm:    1
Diameter of Workpiece in mm:    30

Calculation of Maximum Value of DeltaXg, DeltaYg, DeltaZg and RMS by Regression Equation

Regression Equation Calculation is based on Experimental Result

Regression Equation for Polynomial Order: 3


RMS =

  -78.2740

Result: Vibration Value Exeeds the Limit
High Vibration because of Feed Rate
Reduce the input value of affecting parameter
```

Result 3:

```
Define the input parameters

Rotating Speed of Workpiece in rpm:    225
Feed Rate in mm/rev:    0.001
Depth of Cut in mm:    2
Diameter of Workpiece in mm:    25

Calculation of Maximum Value of DeltaXg, DeltaYg, DeltaZg and RMS by Regression Equation

Regression Equation Calculation is based on Experimental Result

Regression Equation for Polynomial Order: 3


RMS =

  714.1025

Result: Vibration Value Exeeds the Limit
High Vibration because of Depth of Cut
Reduce the input value of affecting parameter
```